



UNIVERSIDADE FEDERAL DE UBERLÂNDIA  
FACULDADE DE ENGENHARIA QUÍMICA  
PROGRAMA DE PÓS-GRADUAÇÃO EM ENGENHARIA QUÍMICA



# **Biodiesel production from oleic acid and ethanol using niobia based catalysts**

*Produção de biodiesel a partir de ácido oleico e etanol  
utilizando catalisadores a base de nióbio*

Letícia Leandro Rade

Uberlândia – MG

February-2018



UNIVERSIDADE FEDERAL DE UBERLÂNDIA  
FACULDADE DE ENGENHARIA QUÍMICA  
PROGRAMA DE PÓS-GRADUAÇÃO EM ENGENHARIA QUÍMICA



# **Biodiesel production from oleic acid and ethanol using niobia based catalysts**

*Produção de biodiesel a partir de ácido oleico e etanol  
utilizando catalisadores a base de nióbio*

Letícia Leandro Rade

Professor: Dr. Carla Eponina Hori

Work elaborated for defense examination submitted to the Graduate Program in Chemical Engineering of the Federal University of Uberlândia as part of the requirements necessary to obtain the PhD degree in Chemical Engineering.

Uberlândia – MG

February-2018

Dados Internacionais de Catalogação na Publicação (CIP)  
Sistema de Bibliotecas da UFU, MG, Brasil.

---

- R126p  
2018      Rade, Leticia Leandro, 1988-  
            Produção de biodiesel a partir de ácido oleico e etanol utilizando catalisadores a base de nióbio / Leticia Leandro Rade. - 2018.  
            120 f. : il.
- Orientadora: Carla Eponina Hori.  
            Tese (Doutorado) - Universidade Federal de Uberlândia, Programa de Pós-Graduação em Engenharia Química.  
            Disponível em: <http://dx.doi.org/10.14393/ufu.te.2018.763>  
            Inclui bibliografia.
1. Engenharia química - Teses. 2. Biodiesel - Teses. 3. Nióbio - Teses. 4. Catalisadores - Teses. I. Hori, Carla Eponina. II. Universidade Federal de Uberlândia. Programa de Pós-Graduação em Engenharia Química. III. Título.

---

CDU: 66.0

Maria Salete de Freitas Pinheiro – CRB6/1262

MEMBROS DA BANCA EXAMINADORA DA TESE DE DOUTORADO  
DE LETÍCIA LEANDRO RADE, APRESENTADA AO PROGRAMA DE  
PÓS-GRADUAÇÃO EM ENGENHARIA QUÍMICA DA UNIVERSIDADE  
FEDERAL DE UBERLÂNDIA EM 27 DE FEVEREIRO DE 2018.

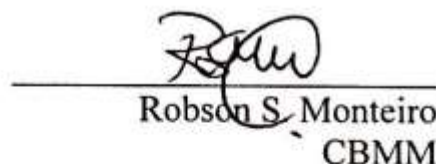
BANCA EXAMINADORA:



Carla Eponina Hori  
Orientadora/FEQUI-UFU



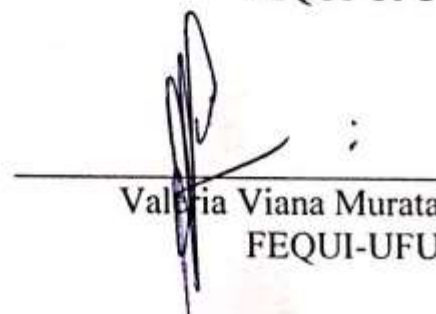
Lúcio Cardozo Filho  
DEQ-UEM



Robson S. Monteiro  
CBMM



Cláudio Roberto Duarte  
FEQUI-UFU



Valéria Viana Murata  
FEQUI-UFU

*“The scientist is not a person who gives the right answers, he is one who asks the right questions.”*

*Claude Lévi-Strauss*

## ACKNOWLEDGMENTS

I would like to express my sincere gratitude:

To God, for his protection and for giving me so many opportunities in my life.

To my parents, Domingos and Raquel, for being examples of persons and professionals and for supporting me spiritually throughout my life. You inspire me by your passionate attitude and hardworking. I am also grateful to my brother Arthur and all family members.

To my husband Arthur, for all the love, support and for always encouraging my professional life.

To my advisor, Professor Carla Eponina Hori, for the valuable guidance during my post-graduate studies. Thank you for your patience, knowledge and for providing me the tools that I needed for my professional growing.

To Professor Marcos Antônio de Souza Barrozo, for the encouragement and continuous support in the statistical analyses during my research.

To Professor Sérgio Mauro da Silva Neiro, for his patience, motivation and support in the simulation and economic assessment of this work. Thank you for your kindness.

To Professor Lúcio Cardozo Filho, for offering me opportunities to work and learn more on his laboratory, in UEM. Thank you for receiving me so kindly.

To my friend Caroline Ortega Terra Lemos, for her daily help, positive words and true friendship. I would also like to thank her mother, Marilda, for kindly hosting me for two months, in Maringá.

To Willyan Machado Giufrida, for all the support given in the phase equilibria experiments and for the good laughs and coffees.

To Rogério Ribas and Robson Monteiro, from CBMM, for the encouragement, valuable suggestions and for trusting in my work.

To my dear friends Dyovani, Karen, Lucas, Rafael, Sarah, Rondi and Kátia for sharing days, equipment, knowledge, coffees, laughs and good conversations with me.

To CBMM, for providing the catalysts used in my research and for the financial support.

## TABLE OF CONTENTS

<b>ABSTRACT .....</b>	<b>i</b>
<b>RESUMO .....</b>	<b>ii</b>
<b>1. INTRODUCTION .....</b>	<b>1</b>
<b>2. MANUSCRIPT PUBLISHED IN RENEWABLE ENERGY .....</b>	<b>11</b>
<b>3. MANUSCRIPT SUBMITTED IN RENEWABLE ENERGY .....</b>	<b>37</b>
<b>4. MANUSCRIPT THAT WILL BE SUBMITTED IN BIORESOURCE TECHNOLOGY .....</b>	<b>60</b>
<b>5. CONCLUSIONS AND PERSPECTIVES .....</b>	<b>81</b>
<b>5.1. Main conclusions .....</b>	<b>81</b>
<b>5.2. Perspectives .....</b>	<b>82</b>
<b>6. APPENDIX I .....</b>	<b>83</b>
<b>7. APPENDIX II.....</b>	<b>84</b>

## ABSTRACT

In this Doctorate research, niobia compounds were evaluated as solid acid catalysts in the continuous esterification reaction. Oleic acid was assumed as model component to represent the free fatty acids (FFA) and ethanol was selected as esterifying agent because is less toxic for humans, renewable, derived from agricultural products and widely available in Brazil. Samples of niobic acid and niobium phosphate were calcined at different temperatures (from 300 to 600 °C), characterized by nitrogen adsorption, thermogravimetric analysis (TGA-DSC), X-ray diffraction (XRD) and temperature-programmed desorption of ammonia (NH<sub>3</sub>-TPD) and, then, submitted to catalytic tests. For the samples which showed the highest catalytic activity, the experimental conditions of temperature, mass of catalyst and ethanol:oleic acid molar ratio were optimized using design of experiments (DOE) and canonical analysis. Results showed that calcination temperature affected the textural properties, structure and acidity of the materials. An increase on the calcination temperature promoted a decrease on the BET surface area, total acidity and, consequently, on the catalytic performance for the esterification reaction, for both catalysts. However, compared to niobic acid, niobium phosphate showed higher thermal stability, avoiding a more significant decline in the conversions obtained. This fact occurs because niobic acid changes from amorphous to crystalline when calcined at 500 °C and niobium phosphate changed its structure only at calcination temperatures up to 700°C. Besides that, all the parameters significantly affected the yield of esters. Yield of esters up to 70% could be obtained at optimized conditions, for niobic acid and niobium phosphate. In other step of this project, a plant of biodiesel production through hydroesterification process was simulated, using UniSim software and a preliminary economic analysis was performed. Conversions data obtained in laboratory for hydrolysis and esterification reactions were used as input data of the simulated reactors. The hydroesterification process simulated showed to be technologically feasible, producing biodiesel in a flowrate of 770 kg/h (6736 ton/year) with high purity (97%), however, based on the cash flow rate obtained, it was not economically reasonable.

**KEYWORDS:** biodiesel, niobia, continuous hydroesterification, heterogeneous catalyst, process design, economic analysis.



## RESUMO

No presente trabalho de doutorado, materiais a base de nióbio foram avaliados como catalisadores ácidos sólidos na reação de esterificação contínua. O ácido oleico foi utilizado como componente modelo para representar os ácidos graxos livres (AGL) e o etanol foi selecionado como agente esterificante, uma vez que não é tóxico, renovável, obtido a partir de produtos agrícolas e muito disponível no Brasil. Amostras de ácido nióbico e fosfato de nióbio foram calcinadas a diferentes temperaturas (de 300 a 600 °C), caracterizadas pelas técnicas de adsorção de nitrogênio, análise termogravimétrica (ATG), difração de raios X (DRX) e dessorção de amônia a temperatura programada (DTP-NH<sub>3</sub>) e, então, submetidas a testes catalíticos. Para as amostras que apresentaram melhores atividades catalíticas, as condições experimentais de temperatura, massa de catalisador e razão molar etanol:ácido oleico foram otimizadas, utilizando a técnica de planejamento de experimentos e análise canônica. Os resultados mostraram que a temperatura de calcinação afetou as propriedades texturais, a estrutura e a acidez dos materiais. O aumento na temperatura de calcinação provocou decréscimos na área superficial, na acidez total e, consequentemente, no desempenho catalítico para a reação de esterificação, em ambos os catalisadores. No entanto, se comparado ao ácido nióbico, o fosfato de nióbio apresentou maior estabilidade térmica, com diminuições não tão significativas nas conversões obtidas. Esse fato ocorreu, pois o ácido nióbico muda sua estrutura de amorfa para cristalina quando calcinado a 500 °C e o fosfato de nióbio somente sofre alterações em sua estrutura quando submetido a temperaturas de calcinação maiores que 700 °C. Todos os parâmetros afetaram significativamente o rendimento em ésteres. Rendimentos em ésteres de até 70% foram obtidos em condições operacionais otimizadas, para ácido nióbico e fosfato de nióbio. Em outra etapa deste projeto, o processo de hidroesterificação para a produção de biodiesel foi simulada, utilizando o software UniSim, e uma análise econômica preliminar foi realizada. Os dados de conversão obtidos em laboratório para as reações de hidrólise e esterificação foram utilizados como dados de entrada para os reatores simulados. O processo de hidroesterificação mostrou-se tecnicamente viável, produzindo biodiesel em uma vazão mássica de 770 kg/h (6736 toneladas/ano) com alta pureza (97%), no entanto, baseado no diagrama de fluxo de caixa obtido, o processo não se mostrou economicamente viável.

**PALAVRAS-CHAVE:** biodiesel, nióbio, hidroesterificação contínua, catalisador heterogêneo, simulação de processos, análise econômica.

---

## 1. INTRODUCTION

---

The transportation sector represents an important role to develop the economy of any country and the crucial point for this sector is the energy supply, which usually comes from fossil sources, such as gasoline and diesel fuel. However, the consumption of fossil fuels has a significant impact on the environment, since their combustion emits harmful pollutants into the atmosphere, such as carbon dioxide (CO<sub>2</sub>). The climate change is one of the most serious global environmental problems. If there is a slight increase on the average global temperature (around 2 °C), up to one million species could become extinct (Atabani et al., 2012).

In this context, there is a need to develop an alternative fuel to supply the energy demand of the world, which must be technologically feasible, economically competitive and environmentally friendly. Among them, biodiesel is very promising, since it is made from renewable resources, is biodegradable, nontoxic and has a higher flash point than normal diesel (Lotero et al., 2005). Besides that, biodiesel presents chemical characteristics similar to mineral diesel and, considering that it is free of aromatic and sulfur compounds, it can be used pure or mixed with diesel oil in diesel cycle engines with no modification (Guariero et al., 2011).

In Brazil, biodiesel was introduced to the energy matrix, aiming to partially or totally replace fossil fuels in internal combustion engines. The Decree-Law 11.097 (2005) established that a minimum percentage of biodiesel has to be added to mineral diesel sold. It is important to emphasize that these percentages changed, depending on installed production capacity, raw material production and demand behavior (De França, 2014). Thus, since the Decree-Law 11.097 was passed in Congress, the following schedule has been implanted: mixture of 2% (B2) biodiesel mandatory in 2008, mixture of 5% (B5) biodiesel obligatory in 2010 and mixture of 6 (B6) and 7% (B7) in 2014. Figure 1 presents the accumulated production for the periods B5 (until June, 2014), B6 (from July to October, 2014) and B7 (since November, 2014) (Boletim dos Biocombustíveis, 2017).

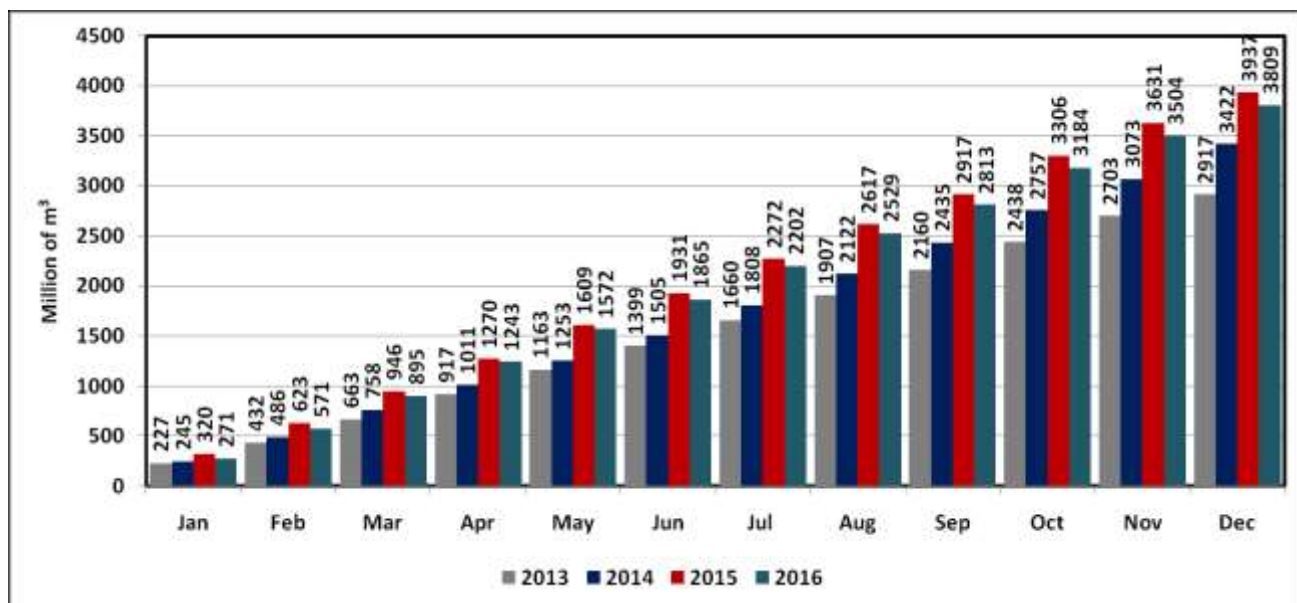


Figure 1- Biodiesel production in Brazil from 2013 to 2016 (Boletim dos Biocombustíveis, 2017).

In 2016, the nominal biodiesel production capacity in Brazil was approximately 7.4 million  $\text{m}^3$  (20.5 thousand  $\text{m}^3/\text{day}$ ). However, only 3.8 million  $\text{m}^3$  were actually produced, which corresponds to 51.3% of the total production capacity. In fact, the biodiesel production in 2016 was 3.5% lower than in 2015. The center-west region of Brazil remained as the largest biodiesel producer, accounting for 43.3% of the Brazilian production (1.6 million  $\text{m}^3$ ), followed by the south region, responding for 41% of the national production (1.5 million  $\text{m}^3$ ). Regarding to the production by different states, Rio Grande do Sul remained as the largest producer of biodiesel, with 28.3% of national production, followed by Mato Grosso, with 21.5% of the total biodiesel production (Anuário Estatístico, 2017).

There are currently 51 biodiesel production plants authorized by ANP (National Agency of Petroleum, Natural Gas and Biofuels) in operation in Brazil, which correspond to a total authorized capacity of 22066.81  $\text{m}^3/\text{day}$  (Figure 2). There are also two new biodiesel plants authorized for construction and two biodiesel plants authorized to expand capacity. With the construction and authorization of these plants, the total biodiesel production capacity could be increased to 2.225  $\text{m}^3/\text{day}$ , which represents an increase of 10.08% in the current capacity (Data for 2018, ANP).

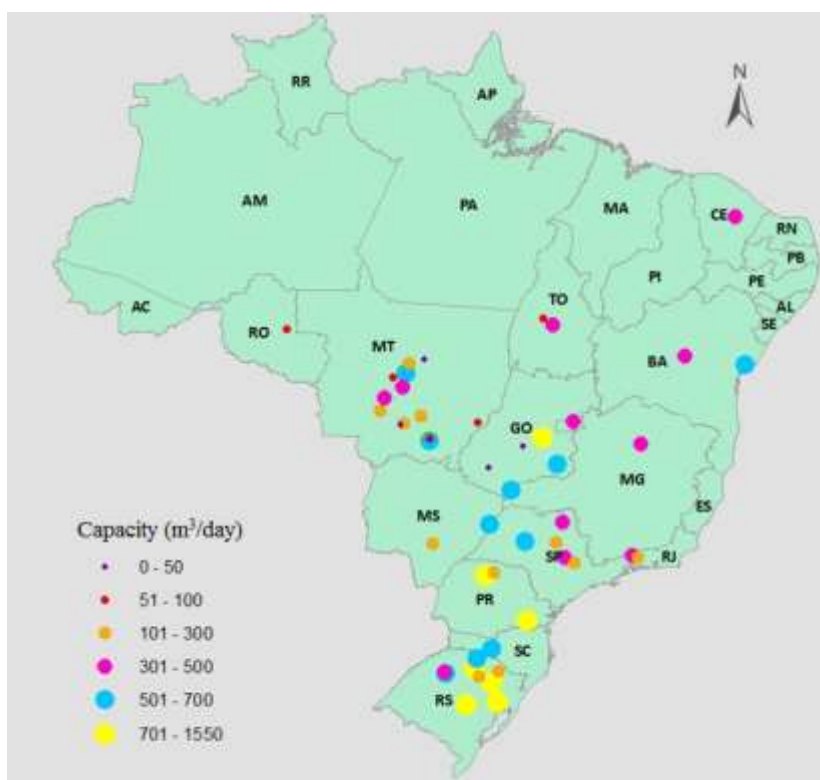


Figure 2- Operating plants for biodiesel production, in 2018 (ANP)

Table 1- Percentage of raw materials used in biodiesel production in 2018

Raw material	Southeast	South	Center-west	Northeast	North
Soybean oil	15.81%	71.47%	77.65%	35.20%	0.00%
Beef tallow	56.15%	17.11%	6.69%	35.49%	95.90%
Cotton oil	1.55%	0.67%	0.22%	0.21%	0.00%
Other fatty materials	14.43%	3.48%	12.2%	19.3%	0.00%
Waste cooking oil	9.16%	0.18%	0.78%	0.52%	0.00%
Pork lard	1.94%	5.05%	0.64%	0.00%	0.00%
Chicken fat	0.96%	1.87%	0.13%	0.00%	0.00%
Palm oil	0.00%	0.00%	1.25%	9.27%	4.10%
Sunflower oil	0.00%	0.00%	0.00%	0.00%	0.00%
Castor oil	0.00%	0.00%	0.00%	0.00%	0.00%
Fodder radish oil	0.00%	0.00%	0.00%	0.00%	0.00%
<i>Jatropha curcas</i> oil	0.00%	0.00%	0.00%	0.00%	0.00%
Corn oil	0.00%	0.00%	0.4%	0.00%	0.00%
Canola oil	0.00%	0.18%	0.00%	0.00%	0.00%

Source: ANP (January, 2018)

Table 1 shows the percentage of raw materials used in biodiesel production in 2018, in Brazil. The southeast region uses the highest percentage of waste cooking oil (9.16%) compared to south, center-west, northeast and north regions.

The most common method to synthesize biodiesel is transesterification of vegetable oil or animal fats, with a short-chain alcohol (Buyukkaya, 2010), as shown in Figure 3. Conventionally, this renewable fuel is produced using a homogeneous strong basic catalyst. Sodium or potassium hydroxides, carbonates or alkoxides are the most commonly used in the industry, since they present high performance under milder conditions and because of their low cost (Pereira et al., 2014). However, the use of homogeneous catalysts for the process has some drawbacks: it requires the use of refined feedstock, since the presence of free fatty acids and water adversely causes saponification reaction during transesterification of triglycerides (Song et al., 2016), the energy costs are high, the recovery of glycerol is difficult and the catalyst must be removed from the product, among other problems (Silva et al., 2007).

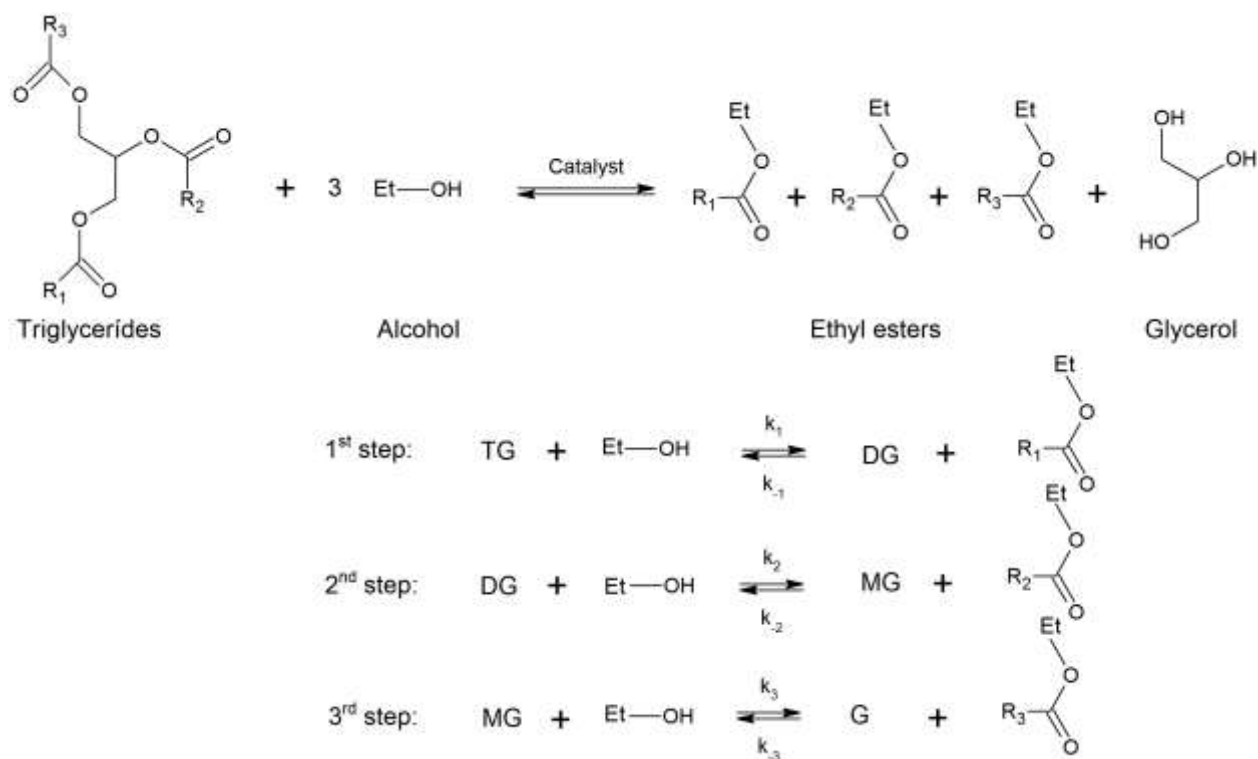


Figure 3- Global transesterification reaction, where  $R_1$ ,  $R_2$ ,  $R_3$  are long chain alkyl groups (Richard et al., 2013)

Considering that the refined feedstock represents up to 75% of the overall biodiesel production cost (Atabani et al., 2012), the importance of esterification reaction studies is growing. This reaction uses free fatty acids (FFA), present in second-generation feedstock, as an alternative feedstock for biodiesel production and generates water as byproduct (Figure 4).

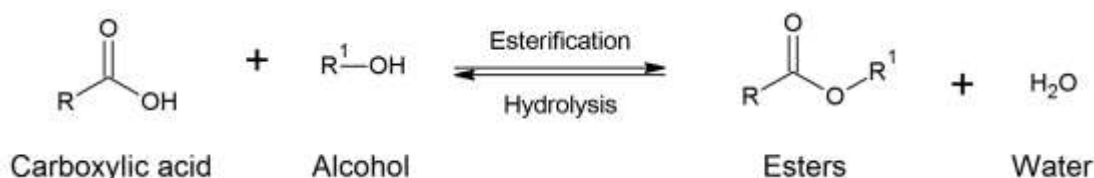


Figure 4- Esterification reaction (Pereira et al., 2014)

In addition to the use of any source of FFA, hydrolysis of oils and fats can be used as a pretreatment to improve the FFA concentration and producing a more complete conversion in this feedstock (Aranda et al., 2009). This process is known as hydroesterification. Firstly, the vegetable oil is hydrolyzed to free fatty acids (FFAs) and glycerol. The FFAs produced are separated and esterified using a short-chain alcohol, generating biodiesel and water (Cavalcanti-Oliveira et al., 2011). Although both steps can be catalyzed by acid materials (Aranda et al., 2009), all the studies reported about the hydroesterification process applied enzymes to catalyze the hydrolysis step. However, it is known that enzymes are very expensive and may turn the process not feasible. For esterification reaction, sulfuric acid is the most commonly catalyst used. However, this catalyst presents some disadvantages, such as generation of wastes that impact both the cost and environmental production of biodiesel (Hernández-Montelongo et al., 2017), reactor corrosion and salts formation due to neutralization of the mineral acid (Pereira et al., 2014). The use of heterogeneous catalysts can be an alternative to overcome these problems and has other advantages, such as easier catalyst separation and product purification, which allows obtaining a high purity glycerol and avoiding the alkaline catalyst neutralization. Moreover, the catalyst can be easily reused and there is no need to replace the consumed catalyst in a short time. All these advantages make the operation of the reactor in continuous mode easier and may increase the profitability of the process (Aranda et al., 2009).

According to studies about biodiesel production, there are some features that a catalyst must possess to achieve good catalytic performance such as: i) high porosity, ii) high concentration of strong acid sites and iii) little or no sensitivity to water. The acid solid catalysts commonly used in the esterification reaction (ion-exchange organic resins, zeolites, silica-supported heteropolyacids and  $\text{ZrO}_2$ ) have some limitations, such as low thermal stability, mass transfer resistance or loss of acidic active sites in the presence of a polar medium (Bassan et al., 2013). Niobia based materials have a great potential as catalysts in the production of biodiesel. In some cases, these catalysts showed better catalytic performances than some zeolites in the esterification of free fatty acids (Aranda et al., 2009).

Niobium is a shiny and silvery metal, with a typical metallic bcc structure. It has an atomic number of 41 and an atomic mass of 92.9064. Niobium belongs to group VA, but is very similar to its predecessors in group IVA (Nowak and Ziolk, 1999). When pure, niobium is comparatively soft and ductile, but impurities make it harder. It reacts with most nonmetals at high temperatures and is resistant to most aggressive compounds and, thus, to corrosion (Nowak and Ziolk, 1999). Niobium materials have been shown very promising in heterogeneous catalysis as catalyst components or when they are added in small amounts to catalysts (Nowak and Ziolk, 1999). These materials exhibit special properties not shown by the compounds of neighboring elements in the periodic table. Some of them such as stability and strong metal support interaction (SMSI) are very important for a good quality catalyst (Ziolk, 2003). In addition to this features, niobium-containing catalysts also have strong acid properties that are preserved in polar liquids (Carniti et al., 2006). The vast majority of acid solids used as catalysts cannot maintain the desirable activity and stability without deactivation of the acid sites in water or very highly protic medium. In this context, the development of insoluble water-tolerant solid acids, as niobic acid and niobium phosphate, are expected to give great benefits in industrial applications (Carniti et al., 2006).

There are many studies reported in the literature on the production of biodiesel using niobium catalysts, however, the majority of them are works whose reactions were carried out in batch reactors.

Aranda et al. (2009) studied the influence of the molar alcohol: fatty acid ratio, the presence of water, temperature and catalyst concentration on the yield of the esterification of palm fatty acids using heterogeneous acid catalysts in a batch reactor. The authors tested several catalysts: poly naphthalene sulfonic acid (PSA), niobium oxide ( $\text{Nb}_2\text{O}_5$ ) and four types of zeolites: Hbeta

(H $\beta$ ), HMordenite (HMOR), HZSM-5 and HY (CBV-760). Niobium oxide was used in three different granulometries: powder (2.94  $10^{-3}$  mm), small pellet (1 x 0.8 mm) and large pellet (5 x 4 mm). The results showed that the zeolites had a higher surface area compared to the other catalysts, especially HY (CBV760). Among all the catalysts, PSA and niobium oxide presented the best catalytic performance, even though they had smaller surface areas than the zeolites, due to their high acidity and because the zeolites presented problems of internal diffusion and inhibition by the presence of water. Niobium oxide in smaller pellets showed better results compared to powder and larger pellets. Finally, calcined niobium oxides showed better yields in the reaction, showing that calcination is an important step for the activation of the catalytic acid sites, since it eliminates excess of water and other molecules adsorbed on the surface of the niobium compound.

Bassan et al. (2013) evaluated the performance of two niobium-based catalysts: niobic acid and niobium phosphate in the esterification reaction of fatty acids (lauric, oleic and stearic) with different alcohols (methanol, ethanol and 1-butanol), in a batch reactor. The catalysts were characterized by N<sub>2</sub> adsorption, XRD, FTIR and pyridine adsorption techniques. In X-ray diffraction, no peak for the niobium acid and niobium phosphate samples were observed when they are calcined at 300 °C, indicating that these materials are amorphous at this temperature. In addition, the results showed that both catalysts have reasonable values of specific area: 152 and 165 m<sup>2</sup>/g for niobic acid and niobium phosphate, respectively. The acidity of Bronsted and Lewis was evaluated by the adsorption-desorption of pyridine and the results showed that niobic acid has lower concentration acidic sites than niobium phosphate. The quantification of acidic sites showed that niobium phosphate has a higher concentration of Bronsted acid sites (BAS) than of Lewis acid sites (LAS). Comparing the catalytic activities of both catalysts, it was observed that niobic acid presented a conversion of 41% in the esterification reaction of lauric acid with butanol. Niobium phosphate presented the best result, with conversion of 81%. According to the authors, the superior catalytic activity of niobium phosphate can be related to the higher number of sites on the surface, maintaining the acidic characteristics, even in the presence of polar or protic solvents. The presence of the POH group in the structure provides a larger Bronsted acidity than in the niobic acid. Niobic acid has only NbOH sites, which are weaker Bronsted acids than the POH groups. The authors investigated the reuse of niobium phosphate after regeneration. The results showed that the catalyst could be reused up to three times without significant loss of activity.



Mohammed and co-workers (2016) studied the biodiesel synthesis through esterification of hydrolysate (FFA) produced by enzymatic hydrolysis reaction of *Jatropha curcas* oil. The free fatty acids obtained were esterified with methanol, using niobic acid as catalyst in a batch reactor. The catalyst was calcined at 150 °C for 4 hours. The effect of temperature (45 to 65 °C), catalyst loading (1 to 5 wt.%), methanol:oil molar ratio (3:1 to 7:1), reaction time (3 to 7 h) and agitation rate (10 to 500 rpm) were evaluated. Results showed that the highest biodiesel yield and FFA conversion were 96% and 100%, respectively, at the following conditions: 5:1 methanol:FFA molar ratio, agitation of 400 rpm, catalyst loading of 4 wt.%, temperature of 60 °C and reaction time of 6 h. Thus, the results revealed that powdered niobic acid is a viable catalyst in esterification of hydrolysate FFA for biodiesel synthesis.

Based on what was presented and accounting for the fact that there are much less studies in the literature devoted to biodiesel production using a continuous reactor and niobia based catalysts, the objective of this PhD project were: i) to investigate the catalytic activity of niobia based catalysts calcined at different temperatures in the continuous esterification reaction of oleic acid by ethanol. For this purpose, niobic acid and niobium phosphate were calcined from 300 to 600 °C. W/F tests were carried out, to avoid mass transfer problems and, then, the catalytic activities of all the samples were evaluated. For the samples which presented the highest catalytic activities, the experimental conditions of temperature, amount of catalyst and ethanol:oleic acid molar ratio were optimized by using design of experiments (DOE) and canonical analysis; ii) to simulate a plant for production of biodiesel through hydroesterification process, using UniSim software and perform a preliminary economic analysis of this process. In this simulation, conversions data obtained in laboratory for hydrolysis and esterification reactions were used as input data of the simulated reactors.

Chapter 2 presents the relevant results from this research obtained for niobic acid, which were published in the journal Renewable Energy. Chapter 3 presents the manuscript containing the results obtained for niobium phosphate, which was also submitted in journal Renewable Energy. Chapter 4 presents the manuscript containing the results obtained for the simulation step and economic analysis. Finally, Chapter 5 presents the conclusions and perspectives of this Doctorate research.

## REFERENCES

Anuário Estatístico Brasileiro do Petróleo, Gás Natural e Biocombustíveis. Accessed at <http://www.anp.gov.br/wwwanp/publicacoes/anuario-estatistico/3819-anuario-estatistico-2017>, on 8<sup>th</sup>, August, 2017.

Aranda, D. A. G., Gonçalves, J. A., Peres, J. S., Ramos, A. L. D., Melo Junior, C. A. R., Antunes, O. A. C., Furtado, N. C., Tafté, C. A. **The use of acids, niobium oxide, and zeolite catalysts for esterification reactions**, *Journal of Physical Organic Chemistry*. 22 (2009) 709. <https://doi.org/10.1002/poc.1520>

Atabani, A. E., Silitonga, A. S., Badruddin, I. A., Mahlia, T. M. I., Masjuki, H. H., Mekhilef, S. **A comprehensive review on biodiesel as an alternative energy resource and its characteristics**, *Renewable and Sustainable Energy Reviews*. 16 (2012) 2070– 2093. <https://doi.org/10.1016/j.rser.2012.01.003>

Agência Nacional do Petróleo, Gás Natural e Biocombustíveis (ANP). Accessed at <http://www.anp.gov.br/wwwanp/producao-de-biocombustiveis/biodiesel/informacoes-de-mercado> on 8<sup>th</sup> March, 2018.

Bassan, I. A. L., Nascimento, D. R., San Gil, R. A. S., Silva, M. I. P., Moreira, C. R., Gonzales, W. A., Faro Jr, A. C., Onfroy, T., Lather, E. R. **Esterification of fatty acids with alcohols over niobium phosphate**, *Fuel Processing Technology*. v. 106 (2013) p. 19–624. <https://doi.org/10.1016/j.fuproc.2012.09.054>

Boletim dos Biocombustíveis, Ministério de Minas e Energia Secretaria de Petróleo, Gás Natural e Biocombustíveis, Departamento de Biocombustíveis. 107 (2017) Jan/Feb.

Buyukkaya, E. **Effects of biodiesel on a DI diesel engine performance, emission and combustion characteristics**, *Fuel*. 89 (2010) 3099–3105. <https://doi.org/10.1016/j.fuel.2010.05.034>

Carniti, P., Gervasini, A., Biella, S., Auroux, A. **Niobic acid and niobium phosphate as highly acidic viable catalysts in aqueous medium: fructose dehydration reaction**, *Catal. Today*. 118 (2006) 373–378. <https://doi.org/10.1016/j.cattod.2006.07.024>

Cavalcanti-Oliveira, E. D. A., Silva, P. R. D., Ramos, A. P., Aranda, D. A. G., Freire, D. M. G. **Study of soybean oil hydrolysis catalyzed by *Thermomyces lanuginosus* lipase and its application to biodiesel production via hydroesterification**, *Enzyme Research*. v 2011 (2011). <http://dx.doi.org/10.4061/2011/618692>

De França, C. G. B. **O setor de biodiesel no Brasil: uma análise do período de 2010 a 2014**. Monograph presented to the Agribusiness Management course, Faculty of Agronomy and Veterinary Medicine, University of Brasília (UnB) (2014).

Guarieiro, L. L., Vasconcellos, P. C., Solci, M. C. **Poluentes atmosféricos provenientes da queima de combustíveis fósseis e biocombustíveis: uma breve revisão**. *Revista Virtual de Química*, 3(5) (2011) 434-445. <https://doi.org/10.5935/1984-6835.20110047>

Hernández-Montelongo, R., García-Sandoval, J. P., Gonzáles-Álvarez, A., Dochain, D., Aguilar-Garnica, E. **Biodiesel production in a continuous packed bed reactor with recycle: A modeling approach for an esterification system**, *Renewable Energy*. Accepted Manuscript (2017). <https://doi.org/10.1016/j.renene.2017.09.030>

Lotero, E., Liu, Y., Lopez, D. E., Suwannakarn, K., Bruce, D. A. and Goodwin Jr, J. G. **Synthesis of Biodiesel via Acid Catalysis**, *Ind. Eng. Chem. Res.* 44 (2005) 5353-5363. <https://doi.org/10.1021/ie049157g>

Mohammed, N. I., Kabbashi, N. A., Alam, M. Z., Mirghani, M. E. S. **Esterification of Jatropha curcas hydrolysate using powdered niobic acid catalyst**, *Journal of the Taiwan Institute of Chemical Engineers*. 63 (2016) 243-249. <https://doi.org/10.1016/j.jtice.2016.03.007>

Nowak, I., Ziolk, M. **Niobium compounds: preparation, characterization, and application in heterogeneous catalysis**, *Chemical Reviews*. 99(12) (1999) 3603-3624. <https://doi.org/10.1021/cr9800208>

Pereira, C. O., Portilho, M. F., Henriques, C. A., Zotin, F. M. **SnSO<sub>4</sub> as catalyst for simultaneous transesterification and esterification of acid soybean oil**, *Journal of the Brazilian Chemical Society*. 25(12) (2014) 2409-2416. <http://dx.doi.org/10.5935/0103-5053.20140267>

Silva, C., Weschenfelder, T. A., Rovani, S., Corazza, F. C., Corazza, M. L., Dariva, C., Oliveira, J. V. **Continuous Production of Fatty Acid Ethyl Esters from Soybean Oil in Compressed Ethanol**, *Industrial & Engineering Chemistry Research*. 46(16) (2007) 5304. <https://doi.org/10.1021/ie070310r>

Song, C., Liu, Q., Ji, N., Deng, S., Zhao, J., Li, S., Kitamura, Y. **Evaluation of hydrolysis–esterification biodiesel production from wet microalgae**, *Bioresource Technology*. 214 (2016) 747-754. <https://doi.org/10.1016/j.biortech.2016.05.024>

Ziolk, M. **Niobium-containing catalysts—the state of the art**, *Catalysis Today*. 78 (1-4) (2003) 47-64. [https://doi.org/10.1016/S0920-5861\(02\)00340-1](https://doi.org/10.1016/S0920-5861(02)00340-1)

---

## 2. MANUSCRIPT PUBLISHED IN RENEWABLE ENERGY

---

### Optimization of continuous esterification of oleic acid with ethanol over niobic acid

Letícia L. Rade<sup>a</sup>, Caroline O. T. Lemos<sup>a</sup>, Marcos Antônio S. Barrozo<sup>a</sup>, Rogério M. Ribas<sup>b</sup>, Robson S. Monteiro<sup>b,c</sup>, Carla E. Hori<sup>a,\*</sup>

<sup>a</sup>Universidade Federal de Uberlândia, Faculdade de Engenharia Química, 38408-144, Uberlândia, Brazil

<sup>b</sup>Companhia Brasileira de Metalurgia e Mineração - CBMM, 38183-903, Araxá, Brazil

<sup>c</sup>Catalysis Consultoria Ltda, 22793-081, Rio de Janeiro, Brazil

[\\*cehori@ufu.br](mailto:cehori@ufu.br)

**Version of record on ScienceDirect <https://doi.org/10.1016/j.renene.2017.08.035>**

**ABSTRACT:** The aim of this work was to evaluate the continuous production of biodiesel through the esterification reaction between oleic acid and ethanol using niobic acid as a solid acid catalyst. In this study, different calcination temperatures of niobic acid were tested. W/F tests were carried out, to avoid mass transfer problems and, then, the catalytic activities of all the samples were evaluated. Results showed that niobic acid calcined at 350°C presented the highest catalytic activity. The experimental conditions of temperature, amount of catalyst and ethanol:oleic acid molar ratio were optimized by using design of experiments (DOE) and canonical analysis. All three single parameters were significant on the yield of esters. The esterification reaction of oleic acid led to yields of esters up to 70% and conversion up to 90%, at 249 °C, ethanol:oleic acid molar ratio of 10.83:1 and 0.7 g of niobic acid.

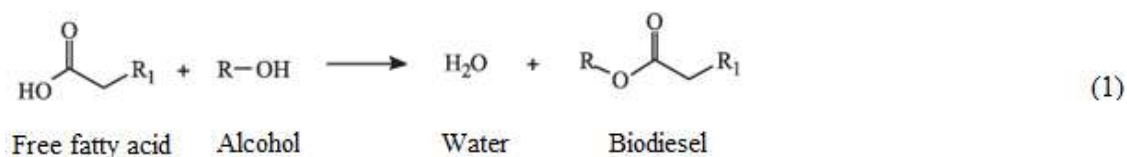
**KEYWORDS:** continuous esterification, oleic acid, niobium, niobic acid, design of experiments, canonical analysis.

\* Reproduction copyright clearance can be seen on Appendix I.

## 1. INTRODUCTION

Most of the energy currently consumed in the world in the transportation sector comes from fossil fuel sources. However, due to environmental concerns, restrictions on the fuel combustion emissions are imposed through legislation in most developed countries [1]. Furthermore, the demand for energy is increasing continuously. In this context, the development of alternative energy sources has been stimulated [1]. Biodiesel is a promising alternative to petroleum-based fuels because it is produced from renewable sources [2, 3], is biodegradable and nontoxic and emits less polluting gases during combustion [1]. Biodiesel can be produced by transesterification of triglycerides or esterification of free fatty acids (FFA) using short chain alcohols. Conventionally, it is synthesized by transesterification. However, the importance of esterification reaction studies is growing, once this reaction uses feedstocks that present high percentage of FFA, which could make the conventional transesterification unfeasible [4]. According to Nandiwale and Bokade [5], the esterification of long chain carboxylic acids such as oleic acid can represent well the biodiesel production process, because this compound is present in most of oil crops (*Jatropha curcas*, soybean, sunflower, rapeseed, palm).

Esterification is the process of forming esters from carboxylic acids and alcohol. In the esterification reaction, in the presence of an acid catalyst and heat, the hydroxyl (-OH) from the carboxylic acid is removed and, after that, the hydrogen from the alcohol is removed. The hydroxyl and the hydrogen combine to form water as byproduct of the reaction and ester as a main product (biodiesel). The esterification reaction between free fatty acid and alcohol is shown in Equation 1:



Among the esterifying agent options, methanol is the most used because it presents lower cost and is widely available. However, this alcohol is toxic and it is obtained from petroleum, which makes the final biodiesel product not a truly renewable energy source. On the other hand, ethanol is less toxic for humans, renewable, derived from agricultural products and produced in large scale in Brazil.

Conventionally, mineral liquid acids (sulfuric acid, hydrochloric acid) and organic acids like p-toluenesulfonic are used to catalyze esterification reactions [1, 6]. These homogeneous catalysts are very effective. However, they can lead to serious contamination problems, since they are toxic, corrosive and form by-products, which are difficult to separate from the reaction medium. Besides that, homogeneous catalysts cannot be reused and generate high amounts of waste and effluents [3]. All these problems can result in higher production costs [1]. The use of heterogeneous catalysts shows easier catalyst separation, product purification, high activity and stability [5]. In addition, these catalysts can be reused, decreasing production costs.

Amberlyst 15 [7], zeolites [8] and  $\text{ZrO}_2$  [9] are the most used solid acid catalysts for esterification of oleic acid with some promising results. However, niobia based materials, such as niobic acid and niobium phosphate, may present great potential as catalysts in the production of biodiesel [6], for many reasons: the acidity is maintained in aqueous reactions, they present large surface area and regular porosity. In some cases, these catalysts showed better catalytic performances than some zeolites [10]. However, the reports on the use of niobium compounds for esterification reaction are still scant.

The vast majority of the esterification studies use batch type reactors. One problem of using batch reactors is that the water is not removed from the reaction medium. The presence of water promotes a loss of active acid sites of the catalysts and shifts the reaction equilibrium to the reagents side. Moreover, in batch reactors, the energy costs are high and the catalysts must be separated from the product. On the other hand, continuous reactors present many advantages such as smaller reactors, better productivity, no separation and recycle of catalysts, among others.

Response surface methodology (RSM) is an efficient statistical technique used for modeling experimental data and evaluation of the influence of parameters on the response process [5]. This methodology allows obtaining much information by performing a small number of experiments and permits the evaluation not just of the single experimental parameters but also of their interactions [5]. Design of experiments coupled with response surface method gives more information than unplanned approaches, reduces waste of materials and time and leads to better knowledge of the process studied [2].

Accounting for the fact that there are not many studies in the literature devoted to esterification reaction using continuous reactor and niobium catalysts, the objective of this work is to investigate the continuous production of biodiesel from oleic acid and ethanol and niobic acid

as a heterogeneous catalyst. The catalytic activity of a series of samples was evaluated and after selecting the best catalyst, the experimental conditions were optimized using design of experiments (DOE). The parameters investigated were: temperature (from 220-290 °C), mass of catalyst (from 0 to 0.8 g) and ethanol:oleic acid molar ratio (from 2:1 to 14:1). The effect of each parameter and their interactions on the yield of esters were studied using a central composite design (CCD) coupled with response surface method (RSM), developed by Statistica software and optimized by canonical analysis technique.

## **2. MATERIAL AND METHODS**

### **2.1. Materials and reagents**

The substrates used in the esterification reactions were oleic acid (Synth) and ethanol (Synth 99.5%). N-heptane (Química Moderna, 99.9%) was used as a solvent for the gas chromatography analysis. The catalysts were prepared by heating  $\text{Nb}_2\text{O}_5 \cdot n\text{H}_2\text{O}$  (HY-340, supplied by Companhia Brasileira de Metalurgia e Mineração - CBMM) at different calcination temperatures, in air (20 mL/min) for 2 hours. The calcination temperatures varied from 300 to 600 °C.

### **2.2. Catalysts characterization**

BET surface areas were determined from nitrogen adsorption measurements at 77 K on a Quantachrome Nova-1200 apparatus. Adsorption isotherms were used to determine the specific area of the catalysts. The specific pore volume and pore dimension were obtained by the desorption isotherm. In all samples, the validity of the BET method was based on the value of the constant C associated to the adsorbate/adsorbent interaction in which  $C > 0$  was the adjustment region of the isotherms. Pore sizes were calculated from BJH distribution method.

The combined thermogravimetric (TGA) and differential scanning calorimetric (DSC) analyses were performed using Q600 SDT differential analyzer (TA instruments) coupled to a thermo-balance. For the analyses, the niobic acid sample (12 mg) was heated from 25 °C to 800 °C at a rate of 20 °C/min and air flow rate of 100 mL/min.

The ex-situ X-ray powder diffraction (XRD) patterns were obtained on a Rigaku diffractometer, using Cu K $\alpha$  radiation ( $\lambda = 1.540 \text{ \AA}$ ) over a  $2\theta$  range of  $20^\circ$  to  $70^\circ$ , at a scan rate of  $0.05^\circ/\text{step}$  and scan time of  $2 \text{ s/step}$ .

X-ray diffraction in-situ was carried out at the XPD-D10B beamline, at Brazilian Synchrotron Light Laboratory (LNLS). For the analysis, samples were sieved (20 mesh), heated at a rate of  $10^\circ\text{C}/\text{min}$  and, then, maintained at the desired temperature of calcination for 2 hours, with a synthetic air flow rate of  $20 \text{ mL}/\text{min}$ . Scans were obtained from  $20^\circ$  to  $40^\circ$ , with a step size of 0.003 and a counting time of 1 s, using a wavelength of  $1.54056 \text{ \AA}$  and a resolution of 8 keV.

Temperature-programmed desorption of ammonia ( $\text{NH}_3$ -TPD) was performed using a ChemBET-3000 equipment. The samples (0.18g) were treated under nitrogen flow rate of  $20 \text{ mL}/\text{min}$  at  $300^\circ\text{C}$  for 1 hour, followed by adsorption of ammonia at  $100^\circ\text{C}$  for 30 minutes. After that, the removal of physically adsorbed ammonia was carried under nitrogen flow rate of  $20 \text{ mL}/\text{min}$ , at  $100^\circ\text{C}$  for 2 hours. Finally, the  $\text{NH}_3$ -TPD was performed between 100 and  $700^\circ\text{C}$  with a heating rate of  $10^\circ\text{C}/\text{min}$  under nitrogen flow.

### **2.3. Esterification reaction**

Reactions were carried out in a fixed bed stainless steel tubular reactor (o.d.,  $3/8 \text{ in}$ ; i.d.  $12.5 \text{ mm}$ ; length,  $29.5 \text{ cm}$ ). The substrate (oleic acid and ethanol) was continuously fed into the system using a high-pressure liquid pump (LabAlliance, Series III), at a volumetric flow rate of  $0.30 \text{ mL}/\text{min}$ . After filling the system with substrate, the reactor was heated by two electric furnaces (heating power of  $2000 \text{ W}$ ) connected to temperature controllers (Novus N1100), with a heating rate of  $10^\circ\text{C}/\text{min}$  and precision of  $\pm 2^\circ\text{C}$ . Samples were collected after waiting at least two residence times at the desired condition. A schematic diagram of the experimental apparatus used for the synthesis of esters is illustrated in Figure 1.



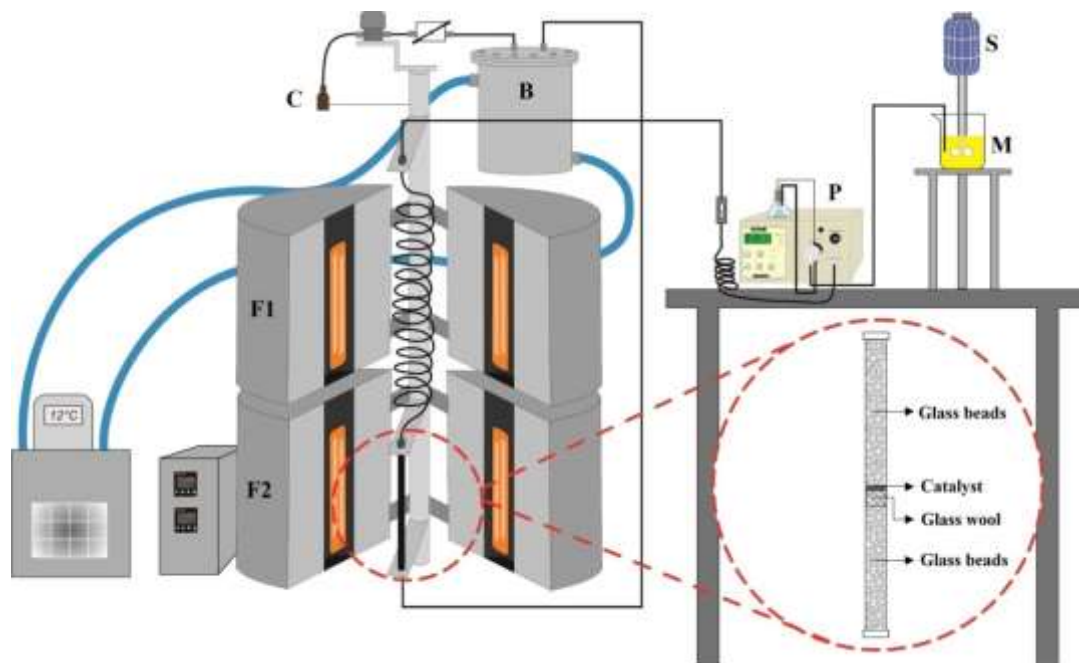


Figure 1- Schematic diagram of the experimental apparatus. S- stirrer, M- substrate mixture, P- high-pressure liquid pump, F1- pre-heating zone furnace, F2- furnace of the fixed bed reactor, B- water bath, C- product collector.

## 2.4. Sample analysis

The samples obtained were dried in incubator at 80°C to constant weight, to ensure the total evaporation of the ethanol.

The oleic acid conversion was calculated as shown in Equation 2:

$$\text{Oleic acid conversion (\%)} = \frac{FFA_i - FFA_f}{FFA_i} \quad (2)$$

Where  $FFA_i$  and  $FFA_f$  are free fatty acid content at the initial substrate and at the samples collected, respectively (mg of FFA/100 mg of sample).

The percentage of free fatty acid of the samples was determined according to method Ca 5a-40, as presented by Abdala et al. [4]. This method is based on acid-base titration using as titrant

methanol solution of potassium hydroxide (KOH) previously standardized. The free fatty acid content was defined as Equation 3:

$$FFA\ content\left(\frac{mg}{100mg}\right)=\frac{282.MC.V}{10\ w}\quad (3)$$

Where  $MC$  is the molar concentration of KOH,  $V$  is the volume of KOH used in the titration and  $w$  is the sample weight.

The esters content of the samples were analyzed by gas chromatography (GC). The analytical method was the same used by Rade et al. [11].

## 2.5. Design of experiments

The design of experiments (DOE) was used to optimize the operational conditions for the yield of esters in the esterification reaction using niobic acid as a solid acid catalyst. The experiments were carried out according to a central composite design with four center points, resulting in 18 experiments, using alpha for orthogonality ( $\alpha$ ) of 1.414. The process parameters were defined as reaction temperature (220-290 °C), mass of catalysts (0-0.8 g) and ethanol-to-oleic acid molar ratio (2:1–14:1). The selection of the levels was defined according to results obtained in preliminary tests. The effect of each parameter and their interactions on the yield of esters were studied using a central composite design (CCD) coupled with response surface method (RSM), developed by Statistica software. The actual and coded values of the variables are given in Table 1. Yields of esters obtained were fitted in a quadratic model using regression analysis and p-value less than 0.05 were considered statistically significant. The coded variables were defined as follow:

$$X_T = \frac{T(^{\circ}C)-255}{25}\quad (4)$$

$$X_{MC} = \frac{AC(g)-0.4}{0.3}\quad (5)$$

$$X_{MR} = \frac{MR-8}{4}\quad (6)$$

Where  $X_T$ ,  $X_{MC}$ ,  $X_{MR}$  are coded variables of temperature, mass of catalyst and ethanol-to-oleic acid molar ratio, respectively.

Table 1- Coded and uncoded levels of variables used for central composite design

Parameters	Symbol	Coded levels				
		-1.414	-1	0	+1	+1.414
Temperature (°C)	$X_T$	220	230	255	280	290
Mass of catalyst (g)	$X_{MC}$	0	0.1	0.4	0.7	0.8
Ethanol:oleic acid molar ratio	$X_{MR}$	2:1	4:1	8:1	12:1	14:1

## 2.6. Optimization

Canonical analysis technique was employed to determine the optimal conditions of temperature ( $X_T$ ), mass of catalyst ( $X_{MC}$ ) and ethanol-to-oleic acid molar ratio ( $X_{MR}$ ) for the continuous esterification reaction. According to Box and Tiao [12], the response function can be expressed in terms of new variables  $w_1, w_2, \dots, w_K$ , whose axes correspond to the principal axes of the contour system. Thus, the canonical form consists in the function in terms of these new variables and is given according to Equation 7:

$$\hat{y} = \hat{y}_0 + \lambda_1 w_1^2 + \lambda_2 w_2^2 + \dots + \lambda_K w_K^2 \quad (7)$$

The nature of the fitted surface stationary point ( $x_0$ ) can be determined by the sign and magnitude of the characteristic roots ( $\lambda_i$ ). If  $\lambda_i < 0$ , a move in any direction from the stationary results in a decrease in  $\hat{y}$ , which means that the stationary point is a point of maximum. In contrast, if  $\lambda_i > 0$ , the stationary point is a point of minimum. If  $\lambda$ 's differ in sign, the stationary point represents a saddle point [12]. In this work, the canonical analysis was implemented using the software *Maple 17*.

### 3. RESULTS AND DISCUSSION

#### 3.1. Characterization

##### 3.1.1. Nitrogen adsorption

Table 2 shows the BET surface area, pore volume and the average pore size for niobic acid calcined from 300 °C to 600 °C. According to the results, it is possible to observe that increasing calcination temperature causes a decrease in the surface area, from 111 to 15 m<sup>2</sup>/g. The same effect was observed for pore volume of the samples (from 0.114 to 0.015 cm<sup>3</sup>/g). However, the average pore sizes did not varied significantly with the increase of calcination temperature. These results were consistent with data reported by Florentino et al. [13].

Table 2- Textural properties of niobic acid calcined between 300 and 600 °C

Calcination temperature (°C)	Surface area (m <sup>2</sup> /g)	Total pore volume (cm <sup>3</sup> /g)	Pore size (Å)
300	111	0.114	20.5
350	95	0.097	20.3
400	86	0.083	19.3
450	66	0.060	18.0
500	34	0.034	20.2
600	15	0.015	20.3

##### 3.1.2. Thermogravimetric analysis

The results of TGA and DSC analysis for fresh niobic acid are presented in Figure 2. According to the TGA, niobic acid presents a weight loss of 11% between 40 and 350 °C. This weight loss is an endothermic process, which can be attributed to the elimination of adsorbed and structural water [14]. For temperatures higher than 350 °C, no significantly weight loss was observed. These results are in good agreement with the ones obtained by Iizuka et al. [15] and Lebarbier et al. [14].

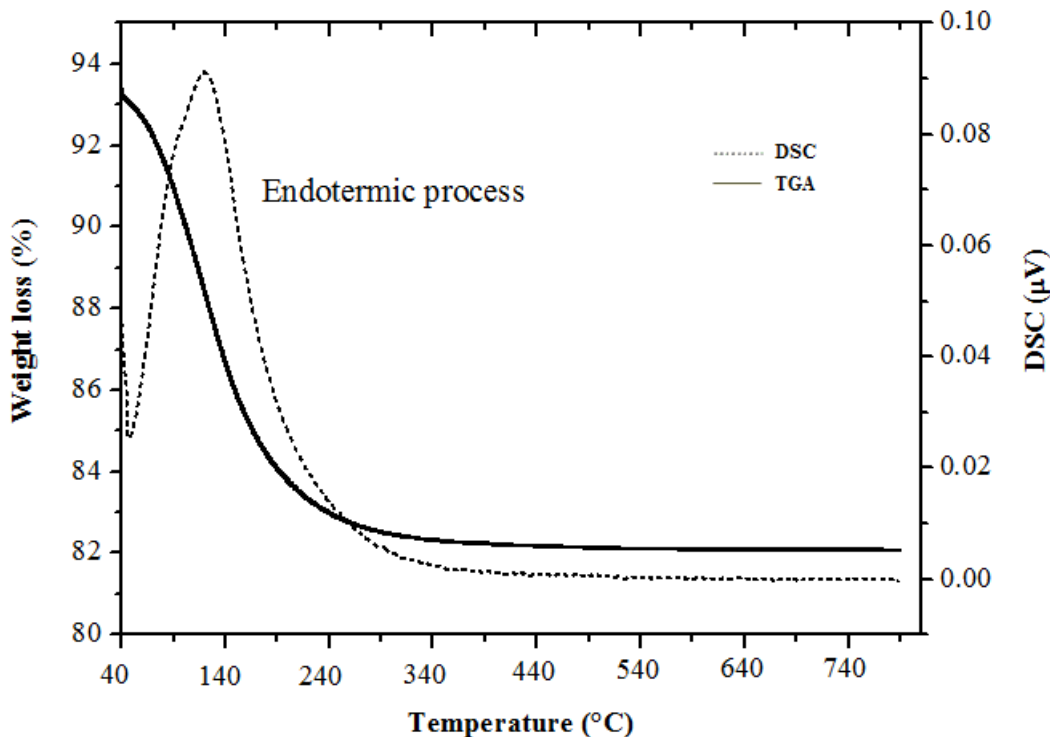


Figure 2- TGA and DSC analysis of fresh niobic acid

### 3.1.3. Ex-situ X-ray diffraction (ex-situ XRD)

Figure 3 shows the XRD pattern of niobic acid calcined at 300, 400, 500 and 600 °C. Samples calcined at 300 and 400 °C showed an amorphous structure. However, when the calcination temperatures were 500 or 600 °C, the samples changed their structure from amorphous to crystalline. The analysis of the XRD pattern of the niobic acid calcined at 500 °C indicates the presence of  $\text{Nb}_2\text{O}_5$  with hexagonal structure, whereas analysis of samples calcined at 600 °C indicates the presence of essentially orthorhombic  $\text{Nb}_2\text{O}_5$ . These results are coherent with the ones reported by Paulis et al. [16] for niobic acid samples calcined at 400, 500, 700 and 900 °C. In their work, the behavior of phase changes of this material while studying the aldol condensation of acetone was investigated. The surface area of niobium oxide decreases from 144 to 4  $\text{m}^2/\text{g}$  with the increase of calcination temperature from 400 to 900 °C, while the structure of  $\text{Nb}_2\text{O}_5$  also changes from amorphous to crystalline in different phases.

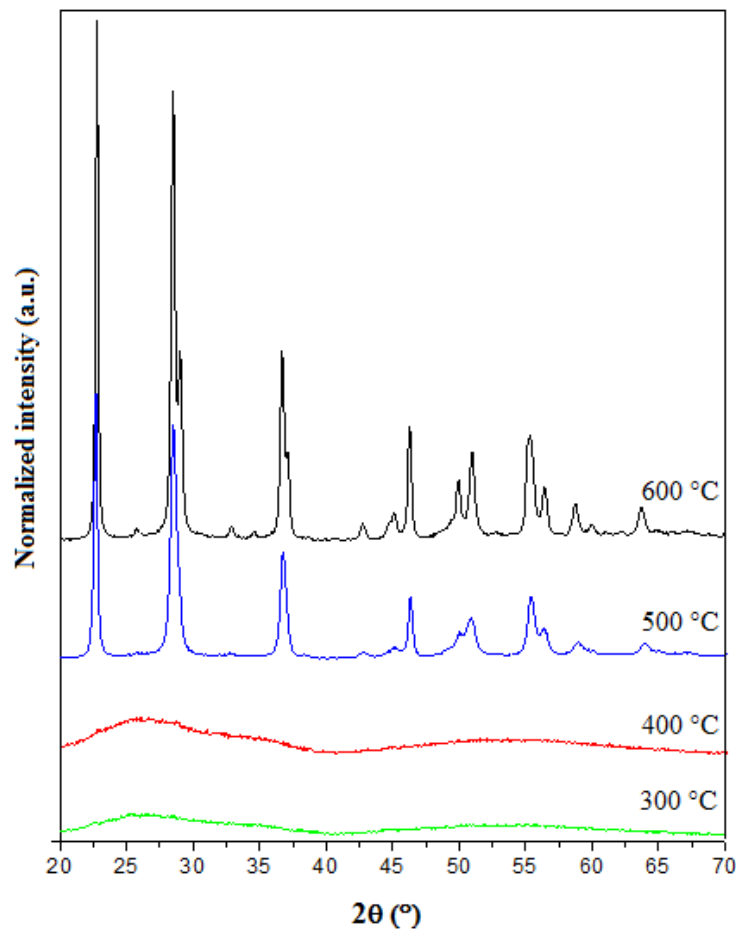


Figure 3- XRD pattern of niobic acid calcined between 300 and 600 °C

#### 3.1.4. In-situ X-ray diffraction (in-situ XRD)

Figure 4 presents the results obtained for the in-situ X-ray diffraction technique for niobic acid calcined from room temperature to 500 °C. As it was observed in ex-situ XRD analyses, samples calcined at temperatures higher than 500 °C changed their structure from amorphous to crystalline. As indicated by Figure 4, the sample changed its structure with a calcination time of only five minutes at 500 °C. This result proves that a calcination time of 2 hours is more than enough to fully change the structure from amorphous to crystalline for calcination temperatures equal or above 500 °C. For lower temperatures, this calcination time is also adequate to ensure an amorphous structure.

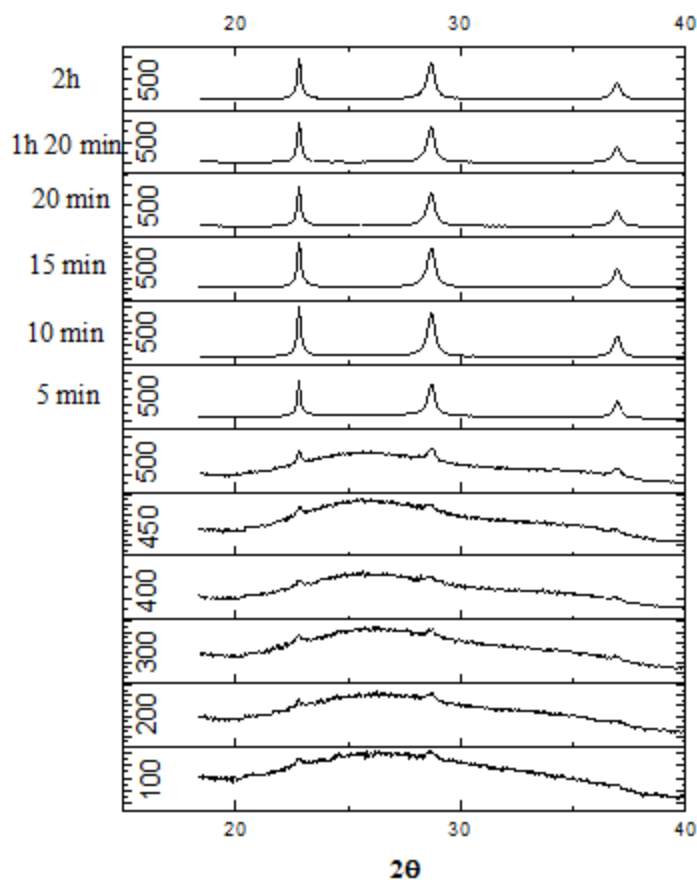


Figure 4- In-situ XRD pattern of niobic acid calcined from room temperature to 500 °C

### 3.1.5. Temperature-programmed desorption of ammonia (NH<sub>3</sub>-TPD)

The total acidity of the niobic acid calcined at different temperatures was evaluated by NH<sub>3</sub>-TPD and the results are shown in Table 3. The concentration of the acid sites decreases from 0.10 to 0.03 mmol NH<sub>3</sub>/g with the increase of calcination temperature, showing that the acid properties are affected by the thermal treatment. According to Iizuka et al. [15], niobic acid has acidic OH groups, which are Bronsted acid sites, even after heat treatment at 100 °C. After a pretreatment at 300 °C, the water present at the surface of the catalyst is almost removed and the Lewis sites increase with the decrease of Bronsted sites. However, according to their results, after a heat treatment at 500 °C, niobic acid starts to show weak acidic properties and becomes inactive due to the phase transformation of amorphous Nb<sub>2</sub>O<sub>5</sub>.nH<sub>2</sub>O to crystalline, that happens around 500-600 °C.

Table 3- Total acidity of niobic acid calcined at different temperatures

Calcination Temperature (°C)	Total acidity (mmol NH <sub>3</sub> /g)
300 °C	0.10129
350 °C	0.08207
400 °C	0.07426
450 °C	0.06053
500 °C	0.03471
600 °C	—*

\* Total acidity present in the sample was at the noise level

### 3.2. W/F tests and catalytic activity in the esterification reaction

Initially, tests with niobic acid calcined at 300 °C were performed, in order to define the conditions of kinetic regime, without external diffusion limitations [17]. For these tests, experiments were carried out using a fixed feed flow rate and varying the catalyst mass, evaluating the conversion of the reaction. W/F value was defined as the ratio of catalyst mass (g) to organic feed flow rate (mol/min). For this purpose, reactions were performed at 250 °C, ethanol:oleic acid molar ratio of 6:1 and flow rate of 0.3 mL/min. The mass of catalysts varied from 0 to 0.8 g. The results obtained are presented in Figure 5 and Table 4.

It can be observed that when an amount of niobic acid up to 0.4 g (W/F of 888 g.min/mol of oleic acid) is used, there are no mass transfer limitations. After this point, the conversion is not proportional to the amount of catalyst, which is an indication of mass transfer limitations. Moreover, this means that the evaluation of the catalytic activity of niobic acid calcined at different temperatures can be performed with 0.3 g of catalyst. Therefore, the catalytic activity of niobic acid calcined at 300, 350, 400, 450, 500 and 600 °C were tested at 250 °C, ethanol:oleic acid molar ratio of 6:1, flow rate of 0.3 mL/min and 0.3 g of catalyst.



Table 4- Data of W/F tests performed at 250 °C, ethanol:oleic acid molar ratio of 6:1, flow rate of 0.3 mL/min (0.00045 mol OA/min) and mass of catalyst from 0 to 0.8 g

Mass of niobic acid (g)	W/F (g min/mol AO)	Conversion (%)
0	0	8.8
0.1	222	20.7
0.3	666	47.1
0.4	888	73.6
0.6	1332	81.5
0.8	1776	84.8

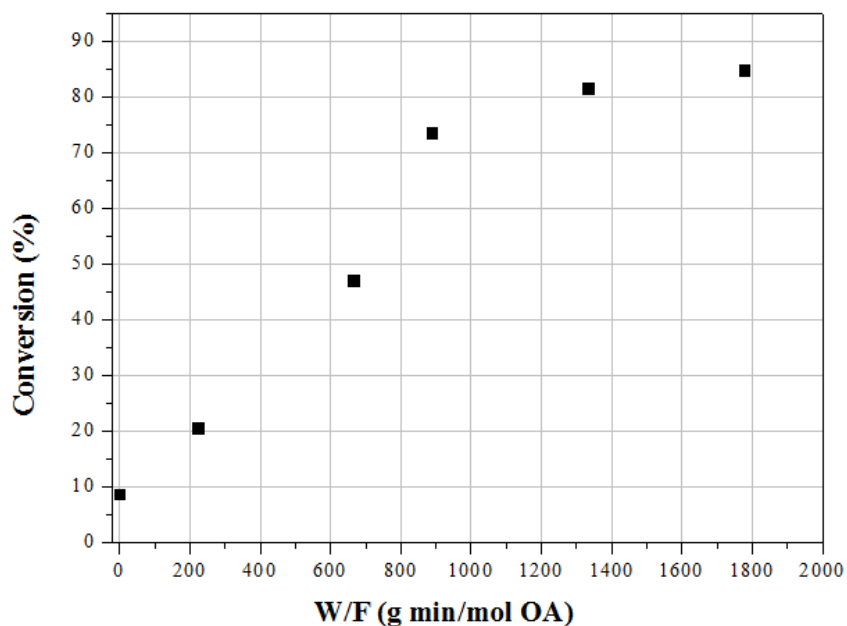


Figure 5- Conversion versus W/F, for esterification reaction of oleic acid and ethanol, at 250 °C, ethanol:oleic acid molar ratio of 6:1 and flow rate of 0.3 mL/min. Mass of niobic acid varied from 0 to 0.8 g.

Figure 6 shows the catalytic tests performed with niobic acid calcined at different temperatures. There is a progressive decrease of the catalytic activity with increasing calcination temperature. The conversions obtained using niobic acid calcined at 300, 350 and 400°C were 44%, 50% and 48%, respectively. These results were analyzed using analysis of variance

(ANOVA). The analysis showed that there is no significant difference between the conversions obtained for these three temperatures. However, lower conversions were obtained for samples calcined at 450, 500 and 600°C (24%, 16% and 7%, respectively).

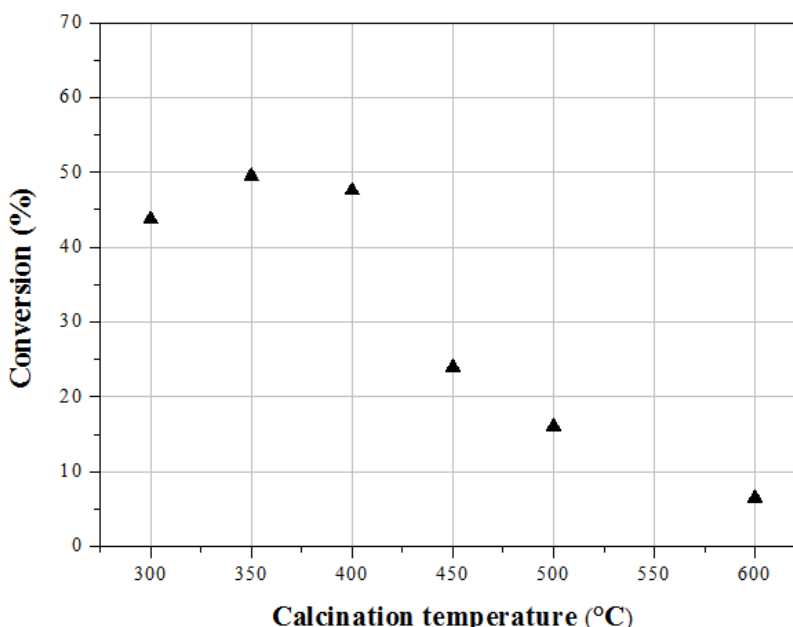


Figure 6- Conversion of the continuous esterification reaction versus niobic acid calcination temperature. Reaction conditions: 250 °C, ethanol:oleic acid molar ratio of 6:1, flow rate of 0.3 mL/min and 0.3 g of catalyst.

The results of the catalytic activity can be correlated with the characterization of niobic acid. According to the characterizations performed with samples calcined at different temperatures, it was possible to conclude that the textural and acid properties were affected by the thermal treatment. BET area, pore volume and acidity of niobic acid decreased with increasing the calcination temperature from 111 to 15 m<sup>2</sup>/g, 0.11 to 0.02 cm<sup>3</sup>/g and 0.10 to 0.03 mmol NH<sub>3</sub>/g, respectively. Consequently, the conversion of esterification reaction also decreased with the increase of calcination temperatures from 300 to 600 °C. According to X-ray diffraction data (Fig. 4), with the increase of calcination temperatures, niobic acid starts to change the structure from amorphous (non-crystalline) to crystalline and these changes on the structure make Nb<sub>2</sub>O<sub>5</sub>.nH<sub>2</sub>O inactive with very weak acidity [15]. Lebarbier et al. [14] obtained similar results. In their work, they tested samples of niobium oxide calcined at different temperatures (from 150 to 550 °C) and

investigated the relationship between the structure obtained, acidity and the catalytic performance for the propan-2-ol dehydration. Results showed that the catalytic activity of niobium oxide samples decreases with increasing calcination temperatures. The authors suggest that the decrease in the catalytic activity is result of a decrease in the surface area and in the abundance of the Brønsted acid sites, which were monitored by lutidine adsorption followed by desorption at 250 °C.

Summarizing, these results show that the conversion of esterification reaction decreases with increasing the calcination temperature. Knowing that surface area and total acidity of niobic acid decrease with increasing calcination temperatures, it is possible to say that there is a direct relationship between the amount of acid sites, the surface area and the esterification activity.

### **3.3. Effects of process parameters for central composite design**

Based on the fact that niobic acid calcined at 300, 350 and 400 °C showed similar conversions on the esterification reaction (with no significant difference), the sample calcined at 350 °C, which presented the highest value of conversion (50%), was selected to the next step of this work. In this step, the experimental conditions of temperature, mass of catalyst and ethanol-to-oleic acid molar ratio were evaluated using design of experiments (DOE). As already mentioned, the experiments were carried out according to a central composite design (CCD) in the following ranges: temperature from 220 to 290 °C, mass of catalysts from 0 to 0.8 g and ethanol-to-oleic acid molar ratio from 2:1 to 14:1.

The results obtained for the experiments based on the CCD matrix using niobic acid calcined at 350 °C are presented in Table 5. The yield of esters obtained varied from 6 to 62%, depending on the experimental conditions. On the other hand, the yield of esters of center points (runs 15, 16, 17 and 18) range from 38 % to 42% with an average of 41%. Therefore, the experimental error obtained was smaller than 2%.

Table 5- Experimental conditions studied in CCD matrix, with uncoded values of parameters and results obtained

Run number	Temperature (°C)	Mass of catalyst (g)	Ethanol:oleic acid molar ratio	Yield of esters (%)
1	230	0.1	4:1	8
2	280	0.1	4:1	19
3	230	0.7	4:1	33
4	280	0.7	4:1	51
5	230	0.1	12:1	17
6	280	0.1	12:1	29
7	230	0.7	12:1	55
8	280	0.7	12:1	60
9	220	0.4	8:1	27
10	290	0.4	8:1	51
11	255	0	8:1	6
12	255	0.8	8:1	62
13	255	0.4	2:1	29
14	255	0.4	14:1	59
15	255	0.4	8:1	40
16	255	0.4	8:1	42
17	255	0.4	8:1	38
18	255	0.4	8:1	42

Table 6- Analysis of variance (ANOVA) for response surface quadratic model for the yield of ester

	Sum of squares	DF	Mean square	F value	Prob> F	Significance (at 95% confidence interval)
Model	5088.90	9	565.43	28.25	0.00	Significant
$X_T$	551.37	1	551.37	23.73	0.01238	Significant
$X_T^2$	32.94	1	32.94	1.42	0.267934	Not Significant
$X_{MC}$	3591.63	1	3591.63	154.56	0.000002	Significant
$X_{MC}^2$	167.57	1	167.57	7.21	0.027695	Significant
$X_{MR}$	711.58	1	711.58	30.62	0.000551	Significant
$X_{MR}^2$	1.18	1	1.18	0.05	0.827677	Not Significant
$X_T.X_{MC}$	0.004	1	0.004	0.0002	0.989790	Not Significant
$X_T.X_{MR}$	14.15	1	14.15	0.61	0.457635	Not Significant
$X_{MC}.X_{MR}$	18.48	1	18.48	0.80	0.398499	Not Significant

$X_T$ : variable for temperature,  $X_{MC}$ : variable for mass of catalyst and  $X_{MR}$ : variable for ethanol:oleic acid molar ratio.

The esters content (y) was defined as the response of the process. These values were used to develop a quadratic polynomial equation that correlates the yield of esters as a function of the independent parameters and their interactions. The multiple regression was carried out, using Statistica software, by eliminating the insignificant parameters, which presented p-values were higher than 0.05 (Table 6). The equation obtained, expressed in coded factors, is given by Equation 8.

$$y (\%) = 40.14 + 6.78X_T + 17.30X_{MC} + 7.70X_{MR} - 4.58X_{MC}^2 \quad (8)$$

Where  $X_T$ : coded variable for temperature,  $X_{MC}$ : coded variable for mass of catalyst and  $X_{MR}$ : coded variable for ethanol:oleic acid molar ratio.

The quality of developed model was determined by the value of correlation ( $R^2$ ). Equation 8 had a correlation coefficient ( $R^2$ ) of 0.95, indicating a good agreement between predicted and experimental yields of biodiesel in this regression model [18]. As shown in Figure 7, there are no tendencies in the regression fit and the points are close to the regression line. Therefore, it is possible to affirm that Equation 8 is statistically consistent and describes very accurately the experimental data.

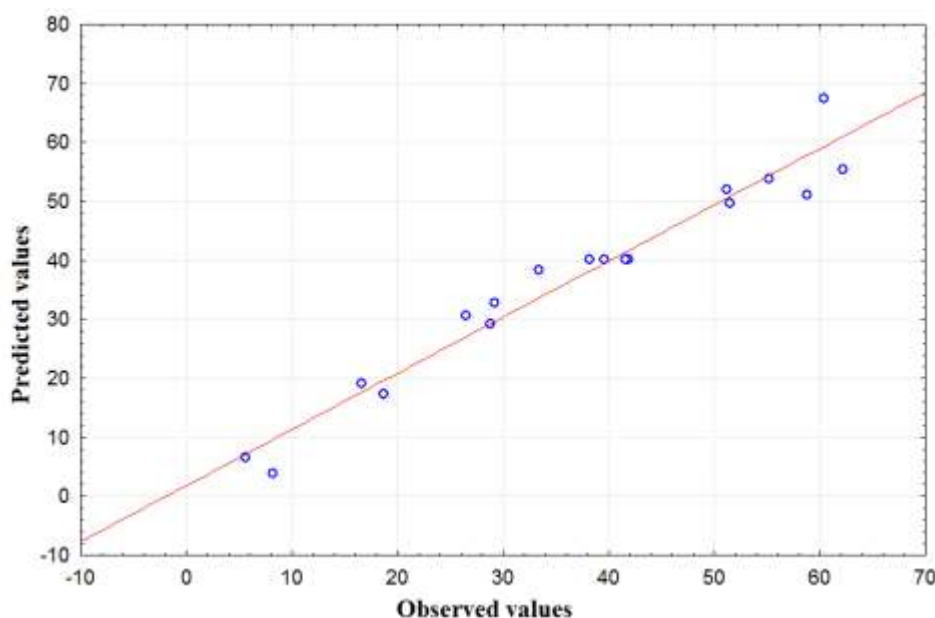


Figure 7- Predicted values versus observed values obtained in the CCD experiments

According to the regression coefficients obtained in Eq. 8 and the ANOVA (Table 6), the three single parameters temperature ( $X_T$ ), mass of catalyst ( $X_{MC}$ ) and ethanol:oleic acid molar ratio ( $X_{MR}$ ) are significant and affect the yield of esters, as well as the quadratic term of the mass of catalyst ( $X_{MC}.X_{MC}$ ). No interaction between variables was significant. Analyzing the regression coefficient obtained, it can be noticed that all three parameters showed a positive effect. The mass of catalysts is the most significant variable, with a coefficient value of 17.30, followed by ethanol:oleic acid molar ratio (7.70) and temperature (6.78). The quadratic term obtained for the mass of catalysts ( $X_{MC}.X_{MC}$ ) indicates a non-linear behavior of the system. This means that at

higher amounts of catalyst, this parameter will not increase the yield of esters anymore, probably due to mass transfer limitations.

The positive effects of the parameters can also be observed in the Table 5. Comparing runs 1 and 5, one can notice that the temperature and mass of catalysts are the same (230°C and 0.1 g, respectively), but the ethanol:oleic acid molar ratio is increased from 4:1 to 12:1. This increase of the ethanol:oleic acid molar ratio causes an increase in the yields of esters from 8 to 17%. The same behavior can be observed comparing runs 2 and 6 (from 19 to 29%), 3 and 7 (from 33 to 55%), 4 and 8 (from 51 to 60%) and 13, center points and 14 (29, 41 and 59%, respectively). Therefore, consistently with the literature, these results show that an increase in the ethanol:oleic acid molar ratio positively affects the response of the process. According to Alinezi et al. [19], the stoichiometric ratio for the esterification reaction requires an ethanol:oleic acid molar ratio equals to 1. Thus, higher molar ratios result in greater production of esters, because the excess of alcohol provides a better contact between the reactants and causes the equilibrium to shift the reaction to esters formation.

The effect of mass of catalyst on the yield of esters, keeping temperature and ethanol:oleic acid molar ratio constants, can be observed by comparing runs 1 and 3 (from 8 to 33%), 2 and 4 (from 19 to 51%), 5 and 7 (from 17 to 55%), 6 and 8 (from 29 to 60%) and 11, point centers and 12 (6, 41 and 62%, respectively). As expected, an increase in the mass of niobic acid promotes an increase on the number of acid sites and, consequently, favors the formation of esters.

Maintaining the mass of catalyst and ethanol:oleic acid molar ratio constant and raising the temperature of the process, promotes an increase in the esters content. This can be observed comparing runs 1 and 2 (from 8 to 19%), 3 and 4 (from 33 to 51%), 5 and 6 (from 17 to 29%), 7 and 8 (from 55% to 60%) and 9, point centers and 10 (27, 41 and 51%, respectively). This result is consistent with others reported in literature [6, 19, 20, 21]. At higher temperatures, the solubility of fatty acid in alcohol increases, benefiting the conversion of the reaction.

Response surfaces were constructed using the multiple regression of CCD. The response surface plot of yield of esters against coded ethanol:oleic acid molar ratio and coded mass of catalysts is shown in Figure 8. The response surface plot of yield of esters against coded mass of catalysts and coded temperature is shown in Figure 9. Analyzing Fig. 8 and 9, it is possible to observe a convex behavior, caused by the quadratic term of the mass of catalysts. As already

mentioned, the yield of esters will start to stabilize even with higher amount of catalyst, probably due to the mass transfer limitations.

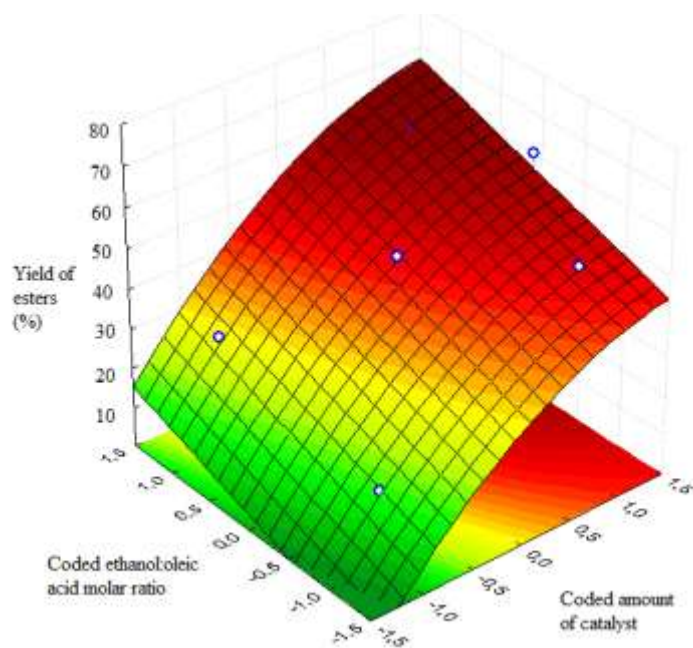


Figure 8- CCD Response surface plot of FAEE yield versus coded ethanol:oleic acid molar ratio and coded amount of catalyst (temperature at level zero)

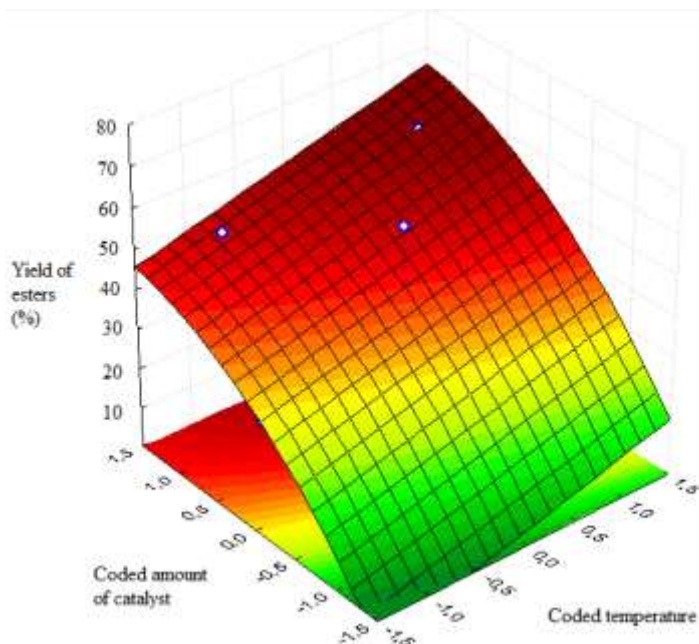


Figure 9- CCD response surface plot of FAEE yield versus coded amount of catalyst and coded temperature (ethanol:oleic acid molar ratio at level zero)



### 3.4. Optimization

The highest yield of esters obtained in the central composite design (CCD) was 62%. The optimization using canonical analysis was used to determine the maximum yield of esters that could be obtained in this reaction system. The empirical model was expressed in the canonical form and the model obtained was:

$$y = 28.76 - 4.58w_1^2 - 2.23w_2^2 + 0.20w_3^2 \quad (9)$$

Equation 9 shows two characteristic roots ( $\lambda_1$  and  $\lambda_2$ ) with a negative sign (-4.58 and -2.23, respectively) and that the last one ( $\lambda_3$ ) with a positive sign (+0.20). This fact means that the stationary point is a saddle point. Thus, to maximize Equation 9,  $w_1$  and  $w_2$  shall be zero, for different values of  $w_3$ .

Testing different values of  $w_3$ , the optimum conditions of temperature, mass of catalyst and ethanol:oleic acid molar ratio optimized were defined. These conditions are presented in Table 7.

Table 7- Temperature, ethanol:oleic acid molar ratio and mass of catalyst optimized using canonical analysis and predicted yield of esters for each test

Run	Temperature (°C)	Mass of catalysts (g)	Ethanol:oleic acid molar ratio	Predicted yield of esters (%)	Yield of esters obtained (%)
19	292	0.960	15:1	73	67
20	285	0.965	18.9:1	79	69
21	278	0.965	22.8:1	86	68
22	271	0.966	26.6:1	93	69

With the experimental results presented in Table 7, it is possible to conclude that yield of esters higher than 62% can be obtained. However, the values of predicted yield of esters and the experimental yield of esters were not the same. This fact means that Eq. 9 did not represent with accurate the extrapolated ranges of the parameters. The reactions presented in Table 7 were

coupled at the CCD matrix and the optimization was carried out again, also using the canonical analysis technique. The new model obtained was:

$$y = 72.04 - 14.45w_1^2 - 12.17w_2^2 - 2.26w_3^2 \quad (10)$$

Equation 10 shows that all three characteristic roots ( $\lambda_1$ ,  $\lambda_2$  and  $\lambda_3$ ) presented negative signs (-14.45, -12.17 and -2.26, respectively). This means that any displacement from the stationary point causes a decrease of the response and that the stationary point is a maximum point. Then, the optimal conditions were defined at: 249 °C, ethanol:oleic acid molar ratio of 10.83:1 and 0.7 g of niobic acid. Under these operational conditions, the canonical model predicts a yield of esters of 72%. Experimentally, this reaction got a yield of esters of 71%, confirming the result predicted by the canonical analysis.

#### 4. CONCLUSIONS

In this work, niobic acid was calcined at temperatures between 300 and 600 °C. As the calcination temperatures of niobic acid were increased, there was a decrease on the surface area, total acidity and activity for esterification reaction. In the catalytic tests performed at 250 °C, ethanol:oleic acid molar ratio of 6:1, flow rate of 0.3 mL/min, the samples calcined at 300, 350 and 400 °C presented higher catalytic activity on the esterification reaction, with no significant difference at the conversions obtained. For niobic acid calcined at 350 °C, which presented higher catalytic activity, all three parameters: temperature, mass of catalyst and ethanol:oleic acid molar ratio significantly affected the yield of esters, in the experimental ranges studied. The highest yield of ester obtained in the central composite design (CCD) was 62%, at 255 °C, 0.8 g of niobic acid and 8:1 ethanol:oleic acid molar ratio. With the optimization, a yield of esters of 71% was obtained, at 249 °C, 0.7 g of niobic acid and ethanol:oleic acid molar ratio of 10.83:1. Finally, niobic acid calcined at 350 °C was an effective catalyst for the continuous esterification with ethanol and oleic acid.

## ACKNOWLEDGEMENTS

The authors are grateful to CBMM for the financial support and for providing the niobic acid (HY-340) used in this work, to CNPq, FAPEMIG, CAPES and Vale S.A. for the financial support and to LNLS (Laboratório Nacional de Luz Síncrotron – Campinas – Brazil) for the use of the XPD beamline.

## REFERENCES

- [1] M.E. Borges, L. Díaz. **Recent developments on heterogeneous catalysts for biodiesel production by oil esterification and transesterification reactions: A review**, *Renew. and Sust. Energ. Rev.* 16 (2012) 2839– 2849. <https://doi.org/10.1016/j.rser.2012.01.071>
- [2] A. Bouaid, M. Martinez, J. Aracil. **A comparative study of the production of ethyl esters from vegetable oil as a biodiesel fuel optimization by factorial design**, *Chem. Eng. J.* 134 (2007) 93-99. <https://doi.org/10.1016/j.cej.2007.03.077>
- [3] Navjot Kaur, Amjad Ali. **Preparation and application of Ce/ZrO<sub>2</sub>-TiO<sub>2</sub>/SO<sup>-2</sup><sub>4</sub> as solid catalyst for the esterification of fatty acids**, *Renew. Energ.* 81 (2015) 421-431. <https://doi.org/10.1016/j.renene.2015.03.051>
- [4] A.C.A. Abdala, V.A.S. Garcia, C.P. Trentini, L. Cardozo Filho, E.A. da Silva, C. Silva. **Continuous catalyst-free esterification of oleic acid in compressed ethanol**, *Int. J. of Che. Eng.* (2014) Article ID 803783, 1-5. <http://dx.doi.org/10.1155/2014/803783>
- [5] K.Y. Nandiwale, V.V. Bokade. **Process Optimization by Response Surface Methodology and Kinetic Modeling for Synthesis of Methyl Oleate Biodiesel over H<sub>3</sub>PW<sub>12</sub>O<sub>40</sub> Anchored Montmorillonite K10**, *Ind. Eng. Chem. Res.* 53 (2014) 18690–18698. <https://doi.org/10.1021/ie500672v>
- [6] I.A.L. Bassan, D.R. Nascimento, R.A.S. San Gil, M.I.P. da Silva, C.R. Moreira, W.A. Gonzalez, A.C. Faro Jr., T. Onfroy, E.R. Lachter. **Esterification of fatty acids with alcohols over niobium phosphate**, *Fuel Process. Technol.* 106 (2013) 619–624. <https://doi.org/10.1016/j.fuproc.2012.09.054>

- [7] J. Park, D. Kim, J. Lee. **Esterification of free fatty acids using water-tolerable Amberlyst as a heterogeneous catalyst**, *Bio. Technol.* 101 (2010) 62-65. <https://doi.org/10.1016/j.biortech.2009.03.035>
- [8] A. M. Doyle, T. M. Albayati, A. S. Abbas, Z. T. Alismaeel. **Biodiesel production by esterification of oleic acid over zeolite Y prepared from kaolin**, *Renew. Energ.* 97 (2016) 19-23. <https://doi.org/10.1016/j.renene.2016.05.067>
- [9] D. E. López, J. G. Goodwin Jr., D. A. Bruce, S. Furuta. **Esterification and transesterification using modified-zirconia catalysts**, *Appl. Catal. A.* 339 (2008) 76-83. <https://doi.org/10.1016/j.apcata.2008.01.009>
- [10] D.A.G. Aranda, J.A. Gonçalves, J.S. Peres, A.L.D. Ramos, C. A.R. de Melo Jr, O.A.C. Antunes, N.C. Furtado, C.A. Taft. **The use of acids, niobium oxide, and zeolite catalysts for esterification reactions**, *J. Phys. Org. Chem.* 22 (2009) 709–716. <https://doi.org/10.1002/poc.1520>
- [11] L.L. Rade, S. Arvelos, M.A.S. Barrozo, L.L. Romanielo, E.O. Watanabe, C.E. Hori. **Evaluation of the use of degummed soybean oil and supercritical ethanol for non-catalytic biodiesel production**, *J. Supercrit. Fluids.* 105 (2015) 21-28. <https://doi.org/10.1016/j.supflu.2015.05.017>
- [12] G.E. Box, G.C. Tiao. **A canonical analysis of multiple time series**, *Biometrika.* 64(2) (1977) 355-365. <https://doi.org/10.1093/biomet/64.2.355>
- [13] A. Florentino, P. Cartraud, P. Magnoux, M. Guisnet. **Textural, acidic and catalytic properties of niobium phosphate and of niobium oxide**, *Appl. Catal., A*, 89 (1992) 143-153. [https://doi.org/10.1016/0926-860X\(92\)80229-6](https://doi.org/10.1016/0926-860X(92)80229-6)
- [14] V. Lebarbier, M. Houalla, T. Onfroy. **New insights into the development of Bronsted acidity of niobic acid**, *Catal. Today.* 192 (2012), 123-129. <https://doi.org/10.1016/j.cattod.2012.02.061>
- [15] T. Iizuka, K. Ogasawara, K. Tanabe. **Acidic and catalytic properties of niobium pentoxide**, *Bull. Soc. Jpn.* 56 (1983) 2927-2931. <https://doi.org/10.1246/bcsj.56.2927>
- [16] M. Paulis, M. Martín, D.B. Soria, A. Díaz, J.A. Odriozola, M. Montes. **Preparation and characterization of niobium oxide for the catalytic aldol condensation of acetone**, *Appl. Catal. A.* 180 (1999) 411-420. [https://doi.org/10.1016/S0926-860X\(98\)00379-2](https://doi.org/10.1016/S0926-860X(98)00379-2)

- [17] H.S. Fogler. **Elements of Chemical Reaction Engineering**, Prentice Hall International Series, 3<sup>rd</sup>ed., Upper Saddle River, New Jersey, USA, 1999.
- [18] K.T. Tan, M.M. Gui, K.T. Lee, A.R. Mohamed. **An optimized study of methanol and ethanol in supercritical alcohol technology for biodiesel production**, *J. Supercrit. Fluids*. 53 (2010) 82–87. <https://doi.org/10.1016/j.supflu.2009.12.017>
- [19] R. Alenezi, G.A. Leeke, J.M. Winterbottom, R.C.D. Santos, A.R. Khan. **Esterification kinetics of free fatty acids with supercritical methanol for biodiesel production**, *Energy Conversion and Manage.* 51 (2010) 1055–1059. <https://doi.org/10.1016/j.enconman.2009.12.009>
- [20] A.S. Ramadhas, S. Jayaraj, C. Muraleedharan. **Biodiesel production from high FFA rubber seed oil**, *Fuel*. 84 (2005) 335–340. <https://doi.org/10.1016/j.fuel.2004.09.016>
- [21] J.A. Gonçalves, A.L.D. Ramos, L.L.L. Rocha, A.K. Domingos, R.S. Monteiro, J.S. Peres, N.C. Furtado, C.A. Taft, D.A.G. Aranda. **Niobium oxide solid catalyst: esterification of fatty acids and modeling for biodiesel production**, *J. Phys. Org. Chem.* 24 (2011) 54–64. <https://doi.org/10.1002/poc.1701>

Optimization of esterification reaction over niobium phosphate in a packed bed  
tubular reactor

L. L. Rade<sup>a</sup>, C. O. T. Lemos<sup>a</sup>, M. A. S. Barrozo<sup>a</sup>, R. M. Ribas<sup>b</sup>, R. S. Monteiro<sup>b,c</sup>, C. E. Hori<sup>a,\*</sup>

<sup>a</sup>Universidade Federal de Uberlândia, Faculdade de Engenharia Química, 38408-144,  
Uberlândia, MG, Brazil

<sup>b</sup>Companhia Brasileira de Metalurgia e Mineração - CBMM, 38183-903, Araxá, MG, Brazil

<sup>c</sup>Catalysis Consultoria Ltda, 22793-081, Rio de Janeiro, RJ, Brazil

\* cehori@ufu.br

**ABSTRACT:** The aim of this work was to investigate the effect of the calcination temperature on the textural properties, structure and acidity of niobium phosphate and the relationship between those properties and the catalytic activity for the continuous esterification reaction using oleic acid and ethanol. For this purpose, samples of niobium phosphate were prepared by calcination at 300, 350, 400, 450 500 and 600 °C. Despite the good thermal stability presented by niobium phosphate, best results were achieved for samples pretreated at 300 °C, which presented higher acidity, surface area and catalytic activity. For this sample, the experimental conditions of temperature (from 220 to 290 °C), amount of catalyst (from 0 to 0.8 g) and ethanol:oleic acid molar ratio (from 2:1 to 14:1) were studied using design of experiments (DOE) and optimized with canonical analysis. The esterification reaction of oleic acid led to yields of esters up to 70% and conversion up to 90% at optimized conditions.

**KEYWORDS:** biodiesel, continuous esterification, niobium, niobium phosphate, design of experiments.

## 1. INTRODUCTION

Niobium materials have been shown very promising in heterogeneous catalysis as catalyst components or when they are added in small amounts to catalysts [1]. These materials exhibit special properties that are very important for a good quality catalyst such as stability and strong metal support interaction [2]. In addition to this features, niobium-containing catalysts also have strong acid properties that are preserved in polar liquids [3]. The vast majority of acid solids used as catalysts cannot maintain the desirable activity and stability without deactivation of the acid sites in water or very highly protic medium. In this context, the development of insoluble water-tolerant solid acids, as niobium phosphate, are expected to give great benefits in industrial applications [3].

Niobium phosphate ( $\text{NbOPO}_4 \cdot n\text{H}_2\text{O}$ ) is an amorphous solid acid catalyst ( $H_0 \leq -8.2$ ) with a high ratio of Lewis/Brønsted acidity. This compound shows a very high activity in acid-catalyzed reactions in which water molecules participate or are liberated [3]. Niobium phosphate shows textural, acidic, and catalytic properties similar to niobic acid and conserves these properties at higher pretreatment temperatures [1]. According to Florentino et al. [4], the BET area of niobic acid becomes practically zero after a pretreatment at 500 °C. However, for niobium phosphate, the BET area remains very high at this temperature, with a surface area of approximately 140 m<sup>2</sup>/g. Besides that, niobium phosphate maintains higher amount of strong acid sites with increasing pretreatment temperatures than niobium oxide.

Considering the urgency to develop alternatives to petroleum-based fuels, esterification reaction is a very promising route to synthesize biodiesel. Esterification consists in an acid-catalyzed reaction, which produces long-alkyl chain fatty acid alkyl esters that can be used as biofuel [5]. In this reaction, the alcohol in contact with the free fatty acid generates esters as a main product (biodiesel) and water as a byproduct. The advantage presented by esterification reaction is that this route accepts low quality feedstock with high concentration of free fatty acids (FFA) and no formation of glycerin. The vast majority of low cost feedstocks available for biodiesel production present a very high percentage of FFA, making the conventional alkali-catalyzed transesterification impracticable [6]. Because of that, a previous free fatty acids esterification reaction is an alternative process to transesterification reaction when low-quality oils and fats are used as feedstock [7].

Considering that esterification reaction involves water as product, niobium-containing materials can be a good option as catalysts for this process. Bassan et al. [5] evaluated two niobium based catalysts (niobic acid, niobium phosphate) in the esterification reaction of fatty acids (C12–C18) with different alcohols (methanol, ethanol, butanol). The results showed that niobium phosphate was the most active in esterification of lauric acid with butanol, at a temperature of 120 °C, molar ratio butanol:acid of 10:1, and reaction time of 4 hours. In those conditions, niobium phosphate presented a conversion of 81%, while niobic acid presented a conversion of 41%. According to the characterizations carried out for both catalysts, niobium phosphate showed a surface area and pore volume higher than niobic acid. Besides that, the acid sites quantification indicated that niobium phosphate presented higher concentration of Brønsted acid sites (BAS) than the other catalyst.

Based on the advantages showed for the use of niobium phosphate in the esterification reaction and accounting for the fact that there are much less studies in the literature devoted to biodiesel production using this catalyst, especially in continuous reactor, the objective of this work was to investigate the use of niobium phosphate as a solid acid catalysts in the continuous esterification of oleic acid and ethanol. Our group has already researched this reaction using niobic acid as solid catalyst [8]. Aiming at comparing the materials, we applied the same methodology used in the previous work. Thus, different temperatures of calcination were evaluated. After selecting the best calcination temperature, design of experiments (DOE) approach was applied, aiming to evaluate the effect of some parameters on the biodiesel production. The parameters were defined as: temperature (from 220 to 290 °C), amount of catalyst (from 0 to 0.8 g) and ethanol:oleic acid molar ratio (from 2:1 to 14:1). It is known that when many parameters affect the biodiesel production, the application of a statistical experimental design is recommended, as this type of approach allows analyzing the influence of the process variables on the response with a smaller number of experiments, which reduces reagent consumption and laboratory work [9]. The effect of each parameter as well as of their interactions on the yield of esters was studied using a central composite design (CCD) coupled with response surface method (RSM) and optimized by canonical analysis technique.



## 2. EXPERIMENTAL SECTION

### 2.1. Materials

Oleic acid (Synth) and ethanol (Synth 99.5%) were used as substrates in the esterification reactions. Solvent n-heptane (Química Moderna, 99.9%) was used for the gas chromatography analysis. For the titration of samples, ethanol (Synth 99.5%), ethyl ether (Dinâmica 98%), sodium hydroxide (Impex 99%), and phenolphthalein reagent (Dinâmica) were used.

The niobia based catalyst used in this work was niobium phosphate,  $\text{NbOPO}_4 \cdot n\text{H}_2\text{O}$  (AD-5970), supplied by Companhia Brasileira de Metalurgia e Mineração (CBMM). The catalyst was prepared by heating  $\text{NbOPO}_4 \cdot n\text{H}_2\text{O}$  at different calcination temperatures, under air flow of 20 mL/min for 2 hours. The calcination temperatures tested were 300, 350, 400, 450, 500 and 600 °C.

### 2.2. Catalyst Characterization

The catalysts were analyzed by nitrogen adsorption, thermogravimetric analysis (TGA-DSC), X-ray diffraction in-situ (XRD) and temperature-programmed desorption of ammonia (TPD of ammonia).

BET surface areas were determined on a Quantachrome Nova-1200 apparatus, from nitrogen adsorption measurements at 77 K. The pore volume was estimated using BJH method.

The combined thermogravimetric (TGA) and differential scanning calorimetric (DSC) analysis were carried out using Q600 SDT differential analyzer (TA instruments) coupled to a thermo-balance. Niobium phosphate (weight of 12 mg) was placed inside an alumina vessel and heated from 25 °C to 800 °C at a temperature rate of 20 °C/min and air flow rate of 100 mL/min.

X-ray diffraction in-situ was obtained at the XPD-10B beamline, at Brazilian Synchrotron Light Laboratory (LNLS). Samples were sieved (20 mesh) and heated to the desired temperature of calcination, at a rate of 10 °C/min and synthetic air flow rate of 20 mL/min. Then, they were maintained at this temperature for 2 hours. Scans were obtained from 20° to 47°, with a step size of 0.003 and a counting time of 1 s, using a wavelength of 1.54056 Å and a resolution of 8 keV.

Temperature-programmed desorption of ammonia ( $\text{NH}_3$ -TPD) was carried out to evaluate the total acidity of the catalysts. The analyses were obtained using a ChemBET-3000 equipment. Samples (weight  $\pm 0.18$  g) were treated at 300 °C for 1 hour, under nitrogen flow rate of 20 mL/min. Then, the adsorption of ammonia was performed at 100 °C for 30 minutes. After that, the removal of physically adsorbed ammonia was purged for 2 hours at 100 °C, under nitrogen flow rate of 20 mL/min. Finally, desorption of chemisorbed ammonia was performed by heating the samples from 100 to 700 °C under nitrogen flow and temperature rate of 10 °C /min.

### 2.3. Experimental Procedure

The continuous esterification reactions were performed using an experimental apparatus, which is composed of: i) a mechanical stirring (Ika, RW 20), ii) a high pressure liquid pump (LabAlliance, Series III), iii) pre-heating zone (made of stainless steel tubing, 218 cm, 1/16 in OD inner diameter 0.79 mm) and fixed bed reactor (made of stainless steel tubing, 29.5 cm, 3/8 in OD inner diameter 6.8 mm) placed in furnaces (heating power of 2000 W) connected to temperature controllers (Novus N1100) and iv) a cooling system. The experimental apparatus is illustrated in Figure 1.

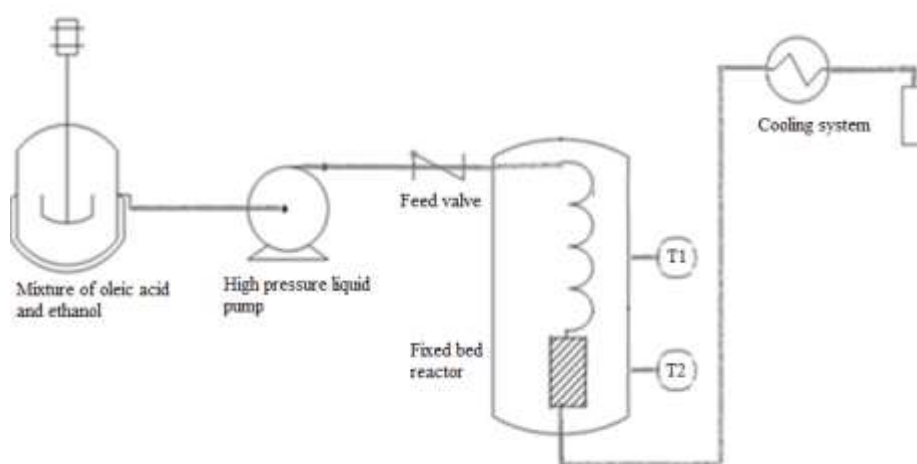


Figure 1- Schematic diagram of the experimental apparatus for esterification reaction of ethanol and oleic acid. ( $T_1$ ) temperature indicator at the pre-heating zone; ( $T_2$ ) temperature indicator at the fixed bed reactor

Experiments were carried out as follows: the substrate composed by ethanol and oleic acid in predetermined proportions, was mixed by the mechanical stirring device. The substrate was charged into the reaction system by a high-pressure liquid pump adjusted to a flow rate of 0.30 mL/min. After filling the system with the reactants, the process of heating the furnaces started, with a heating rate of 10 °C/min and precision of  $\pm 2$  °C. Finally, when the temperatures were stabilized at the desired conditions and after waiting at least two residence times with the temperature stabilized, samples were collected. To ensure total evaporation of ethanol, samples were dried using an incubator at 80 °C. The residence time was calculated as the time that the substrate remains in contact with the catalyst, which ranged from 12 to 106 seconds for 0.10 and 0.80 g of catalyst respectively.

#### 2.4. Sample analysis

The free fatty acid (FFA) content of the sample was determined based on the acid-base titration using as titrant ethanol solution of sodium hydroxide (NaOH) previously standardized (method Ca 5a-40) [6]. FFA content was calculated according to Equation 1:

$$FFA\ content\left(\frac{mg}{100mg}\right)=\frac{282.M.V}{10\ w}\quad (1)$$

Where  $M$  is the molar concentration of NaOH,  $V$  is the volume of NaOH used in the titration process and  $w$  is the sample weight.

The total conversion of the reaction was calculated using Equation 2:

$$Oleic\ acid\ conversion(\%)=\frac{FFA_i-FFA_f}{FFA_i}\quad (2)$$

Where  $FFA_i$  correspond to free fatty acid content at the initial substrate and  $FFA_f$  at the samples collected (mg of FFA/100 mg of sample).

The yield of ester was calculated by gas chromatography (GC), according to Rade et al. [10].

## 2.5. Statistical analysis using design of experiments

In order to study the influence of the operational conditions in the yield of esters, the esterification reactions were performed according to a central composite design (CCD) coupled with response surface method (RSM). Three independent variables were defined: reaction temperature, varying from 220 to 290 °C; amount of catalyst, varying from 0 to 0.8 g and ethanol:oleic acid molar ratio, varying from 2:1 to 14:1. Five levels were used to code these variables:  $-\alpha$ , -1, 0, +1 and  $+\alpha$  (Table 1), where  $\alpha$  is the axial point of 1.414 (alpha for orthogonality).

A quadratic model using regression analysis was fitted for the values of yields of esters obtained, in which p-value less than 0.05 were considered statistically significant.

Table 1- Parameters of central composite design, with coded and uncoded levels

Parameters	Coded levels				
	-1.414	-1	0	+1	+1.414
Temperature (°C)	220	230	255	280	290
Amount of catalyst (g)	0	0.1	0.4	0.7	0.8
Ethanol:oleic acid molar ratio	2:1	4:1	8:1	12:1	14:1

## 2.6. Optimization by canonical analysis

Canonical analysis technique was used to optimize the operational conditions for the yield of esters. Considering the response function can be expressed in terms of the parameters, according to Equation 3:

$$\hat{y} = b_0 + \underline{x}' \underline{b} + \underline{x}' B \underline{x} \quad (3)$$

Where

$$\underline{x} = \begin{bmatrix} x_1 \\ x_2 \\ \vdots \\ x_k \end{bmatrix}, \underline{b} = \begin{bmatrix} b_1 \\ b_2 \\ \vdots \\ b_k \end{bmatrix}, B = \begin{bmatrix} b_{11} & b_{12}/2 & \dots & b_{1k}/2 \\ b_{11}/2 & & & b_{2k}/2 \\ \dots & & \dots & \dots \\ & & & b_{k-1,k}/2 \\ & & & & b_{kk} \end{bmatrix}$$

The point of the maximum response is defined in a set of conditions  $(x_1, x_2, \dots, x_k)$  which turn the partial derivatives  $\frac{\partial \hat{y}}{\partial x_1}, \frac{\partial \hat{y}}{\partial x_2}, \dots, \frac{\partial \hat{y}}{\partial x_k}$  equal to zero. Deriving Equation 3 and equaling to zero, the stationary point is obtained (Eq. 4):

$$\underline{x}^0 = -\frac{1}{2}B^{-1}\underline{b} \quad (4)$$

To define the nature of the stationary point the adjusted surface has to be translated from the origin  $(x_1, x_2, \dots, x_k)$  to the stationary point  $\underline{x}^0$ . Thus, the response surface is expressed in new variables  $(w_1, w_2, \dots, w_k)$ , whose axes correspond to the principal axes of the contour system. The form of the function in terms of these variables is called the canonical form and is given according to Equation 5:

$$\hat{y} = \hat{y}_0 + \lambda_1 w_1^2 + \lambda_2 w_2^2 + \dots + \lambda_K w_K^2 \quad (5)$$

Where  $\hat{y}_0$  is the estimated response in the stationary point and  $\lambda_i$  are the characteristic roots of matrix B.

The sign and magnitude of the characteristic roots  $\lambda_i$  can determine the nature of the stationary point of the fitted surface  $(x_0)$ . If  $\lambda_i < 0$ , a move in any direction from the stationary brings a decrease in  $\hat{y}$ . This means that the stationary point is a point of maximum response for the

fitted surface. On the other hand,  $\lambda_i > 0$ ,  $x_0$  will be a minimum for the fitted surface. Finally, in the case where the  $\lambda$ 's differ in sign, the stationary point is a saddle point.

### 3. RESULTS AND DISCUSSION

#### 3.1. Characterization of catalysts

##### 3.1.1. Nitrogen adsorption

Figure 2 shows the evolution of the BET surface area of niobium phosphate as a function of calcination temperature. It is possible to observe that increasing calcination temperature brings a decrease in the surface area, from 165 to 113 m<sup>2</sup>/g. However, the decrease only starts to be pronounced at a calcination temperature of 600 °C.

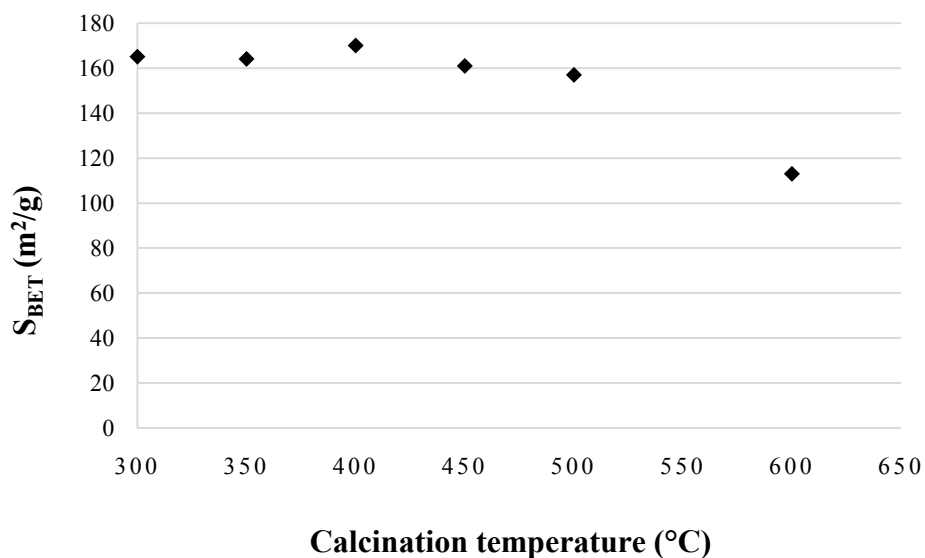


Figure 2- Evolution of the BET surface area of niobium phosphate with increasing the calcination temperatures

### 3.1.2. In-situ X-ray diffraction (in-situ XRD)

Figure 3 shows the result obtained for the in-situ X-ray diffraction technique for niobium phosphate calcined from room temperature to 700 °C. Niobium phosphate calcined at temperatures up to 700°C presents an amorphous structure. However, above this temperature, the structure changes from amorphous to crystalline. The analysis of the XRD pattern of the solid calcined at 700 °C indicates the presence of tetragonal niobium oxide phosphate [11], with  $2\theta = 25.8, 27.9, 29.4, 38.4, 39.9, 44.8^\circ$ . The result also shows that even maintained at 700 °C for 2 hours, the sample does not suffers modification, proving that a calcination time of 2 hours is enough to guarantee a stable structure.

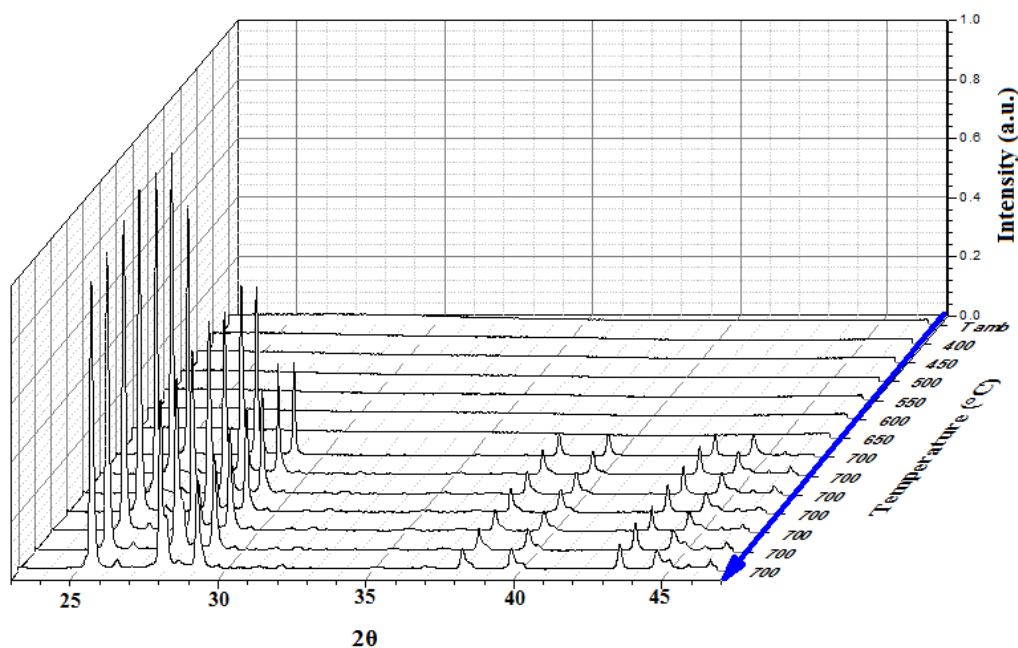


Figure 3- In-situ XRD pattern of niobium phosphate calcined from room temperature to 700 °C

### 3.1.3. Thermogravimetric analysis

Figure 4 shows the results of TGA and DSC analysis for fresh sample niobium phosphate. Niobium phosphate presented a weight loss of 11.3% between room temperature and 350 °C. This

weight loss corresponds to the elimination of the water, which is in agreement with literature data [12]. For temperatures higher than 350 °C, no significantly weight loss was observed.

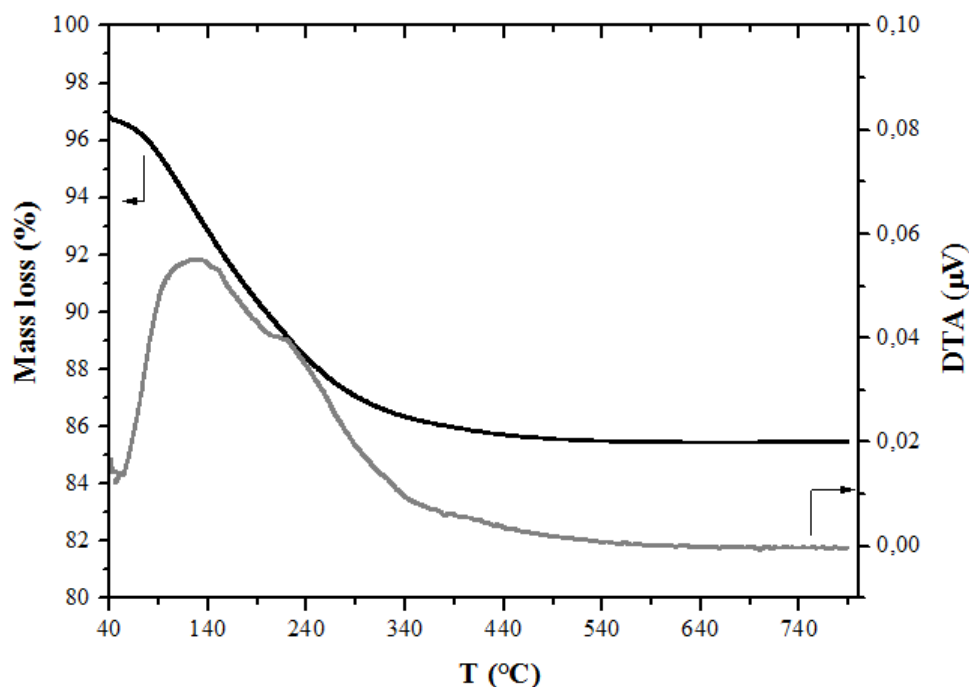


Figure 4- TGA and DTA analysis of fresh niobium phosphate

#### 3.1.4. Temperature-programmed desorption of ammonia (NH<sub>3</sub>-TPD)

Table 2 shows the ammonia TPD results obtained for niobium phosphate samples calcined at 300, 350, 400, 450, 500 and 600 °C. This analysis was performed to measure the total acidity of the samples, once that the yield of esters in the esterification reaction depends on the quantity and strength of acid sites of the solid catalyst.

One may observe that an increase in calcination temperature of the samples reduces the amount of desorbed ammonia/mass of niobium phosphate. However, as it can be seen in Table 2, the decrease is not very pronounced until 500 °C. Thus, it is possible to affirm that this material presents a good thermal stability, starting to suffer the effects of calcination temperatures only at temperatures above 600 °C.



Table 2- Total acidity of niobium phosphate calcined from 300 to 600 °C

Calcination Temperature (°C)	Total acidity (mmol NH <sub>3</sub> /g)
300 °C	0.25256
350 °C	0.27518
400 °C	0.22212
450 °C	0.21388
500 °C	0.22803
600 °C	0.12897

### 3.2. Catalytic activity in the esterification reaction

Aiming at investigating the relationship between the effect of calcination temperatures and the catalytic activity for the continuous esterification reaction using oleic acid and ethanol, samples of niobium phosphate calcined from 300 to 600 °C were subjected to catalytic tests. W/F tests had to be carried out before the catalytic tests, to verify the amount of catalysts that can be used without external diffusive problems. Performing these tests, a graph of conversion versus W/F is obtained and, with this graph, it is possible to verify the region where the conversion is not proportional to the amount of catalyst, which is an indicative of mass transfer limitations. Thus, for those tests, experiments were conducted by varying the catalyst mass with a fixed flow rate, evaluating the conversion of the reaction. W/F value was defined as the ratio of catalyst mass (g) to substrate flow rate (mol/min). The follow conditions were used: 250 °C, 6:1 ethanol:oleic acid molar ratio and flow rate of 0.3 mL/min. The mass of niobium phosphate varied from 0 to 0.8 g. Figure 5 shows the results obtained.

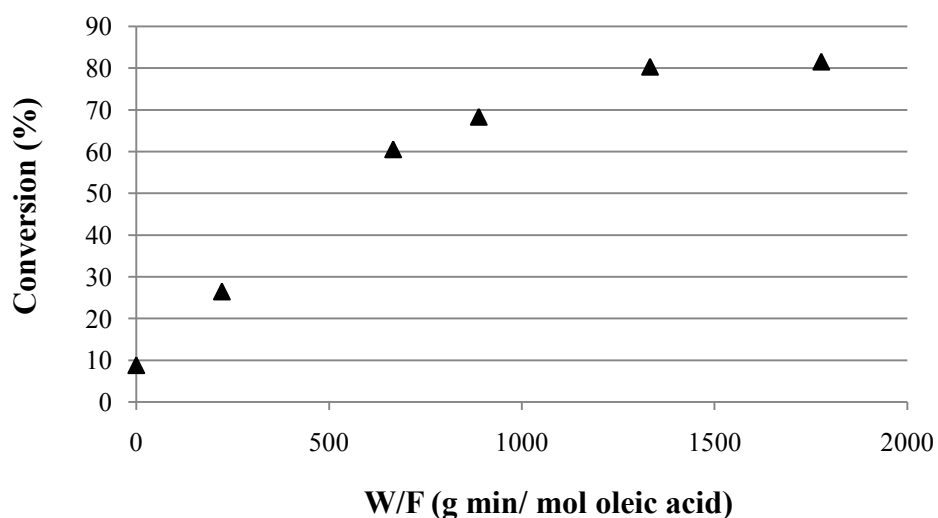


Figure 5- Conversion versus W/F at 250 °C, ethanol:oleic acid molar ratio of 6:1 and flow rate of 0.3 mL/min. Mass of niobium phosphate varied from 0 to 0.8 g.

It can be observed that at W/F up to 888 g.min/mol of oleic acid, corresponding to an amount of niobium phosphate of 0.4 g, there are no mass transfer limitations. However, after this point, the conversion starts to be not proportional to the mass of catalyst, indicating a mass transfer limitation. Thus, the catalytic tests of niobium phosphate calcined from 300 to 600 °C were tested at the same operational conditions of the W/F tests and 0.3 g of catalyst. Figure 6 shows the results obtained.

The conversions obtained using niobium phosphate calcined at 300, 350, 400, 450, 500 and 600 °C were 61%, 55%, 54%, 53%, 53% and 50%, respectively. Although all conversions were similar, it is possible to affirm that there was a declining trend, with a conversion difference of 11% for calcination temperature varying from 300 to 600 °C. The results of the catalytic activity can be correlated with the previous characterization, which showed that the thermal treatment affected the textural and acid properties of the material. BET area and total acidity of niobium phosphate decreased with increasing the calcination temperature from 165 to 113 m<sup>2</sup>/g, and from 0.25 to 0.13 mmol NH<sub>3</sub>/g, respectively. Therefore, the conversion of esterification reaction also decreased with increasing the calcination temperature.

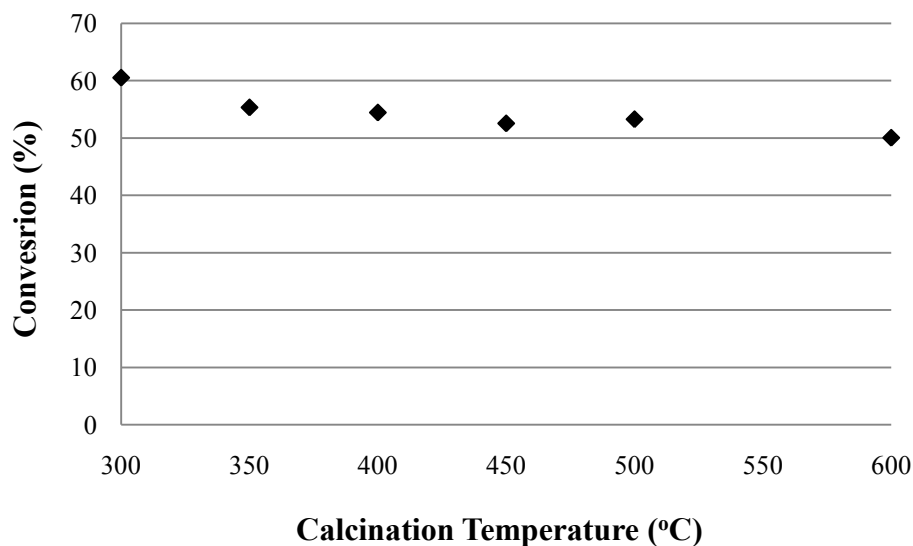


Figure 6- Conversion of the continuous esterification reaction versus calcination temperature. Reaction conditions: 250 °C, ethanol:oleic acid molar ratio of 6:1, flow rate of 0.3 mL/min and 0.3 g of niobium phosphate

According to X-ray diffraction data (Figure 3), with the increase of calcination temperature, niobium phosphate starts to change its structure from non-crystalline (amorphous) to crystalline. These structure changes also happen with niobic acid ( $\text{Nb}_2\text{O}_5 \cdot n\text{H}_2\text{O}$ ). According to Rade et al. [8] and Lebarbier et al. [13], niobic acid changes from amorphous to crystalline in different phases, when calcined at temperatures higher than 500 °C. The authors suggest that increasing the calcination temperature of amorphous niobic acid leads to the formation of crystalline niobium oxide and a progressive decrease in the BET surface area and a in the abundance of Brønsted acid sites. The same behavior is observed with niobium phosphate, although it presents higher thermal stability than niobic acid. Because of that, the catalytic activity of niobium phosphate did not suffer a very significant decline, as it happen with niobic acid.

Despite the good thermal stability of niobium phosphate, results showed that the conversion of esterification reaction decreases with increasing the calcination temperature. Knowing that surface area and total acidity decrease with increasing calcination temperature, is it possible to say that there is a direct relationship between amount of acid sites, surface area and esterification activity.

### 3.3. Experimental design

Niobium phosphate calcined at 300 °C presented the highest catalytic activity (conversion of 61%). Thereby, the sample calcined at this temperature was chosen to be used in the next steps of the study. In this step, a set of experiments was carried out to determine the influence of three parameters and their interactions (temperature  $X_T$ ; amount of catalyst  $X_{AC}$  and ethanol:oleic acid molar ratio  $X_{MR}$ ) on the process response, which was defined as yield of esters ( $y$ ). The yield corresponds to the conversion of free fatty acid (FFA) into ethyl esters. The experiments were performed according to a central composite design (CCD), with four repetition at the central point (coded at zero), resulting in 18 experiments. The selection of the levels was carried according to preliminary tests, considering the experimental limits. Table 3 shows the CCD matrix and the results obtained, using niobium phosphate calcined at 300 °C.

As can be seen, the yield of esters showed a large sensitivity to the parameters tested, varying from 6 to 60%. Besides that, the arithmetical average of the center points (runs 15, 16, 17 and 18) was 52.5%, with an experimental error smaller than 2%.

The values of yield of esters ( $y$ ) were applied to multiple regression analysis by eliminating the parameters which presented p-values higher than 0.05. Thus, Equation 6 gives the yield model, expressed in coded factors:

$$y = 51.73 + 5.17X_T + 15.83X_{AC} + 7.33X_{MR} - 9.37X_{AC}^2 - 4.92X_{MR}^2 \quad (6)$$

Where  $X_T$ : coded temperature,  $X_{AC}$ : coded amount of catalyst and  $X_{MR}$ : coded ethanol:oleic acid molar ratio.

Equation 6 had a correlation coefficient ( $R^2$ ) of 0.96. This means that 96% of the experimental response variability can be explained by Equation 6. Based on the value of  $R^2$  and analyzing the graph of predicted values versus observed values obtained for the model equation (Figure 7), which does not present tendencies and where experimental points are very close to the regression line; it is possible to conclude that Equation 6 is statistically consistent and describes very accurately the experimental data.

Table 3- Experimental conditions studied in CCD matrix, with uncoded parameters and results obtained

Run	Temperature (°C)	Amount of catalyst (g)	Ethanol:oleic acid molar ratio	Yield of esters (%)
1	230	0.1	4:1	11
2	280	0.1	4:1	28
3	230	0.7	4:1	44
4	280	0.7	4:1	46
5	230	0.1	12:1	20
6	280	0.1	12:1	35
7	230	0.7	12:1	56
8	280	0.7	12:1	59
9	220	0.4	8:1	41
10	290	0.4	8:1	57
11	255	0	8:1	6
12	255	0.8	8:1	60
13	255	0.4	2:1	25
14	255	0.4	14:1	58
15	255	0.4	8:1	51
16	255	0.4	8:1	52
17	255	0.4	8:1	53
18	255	0.4	8:1	56

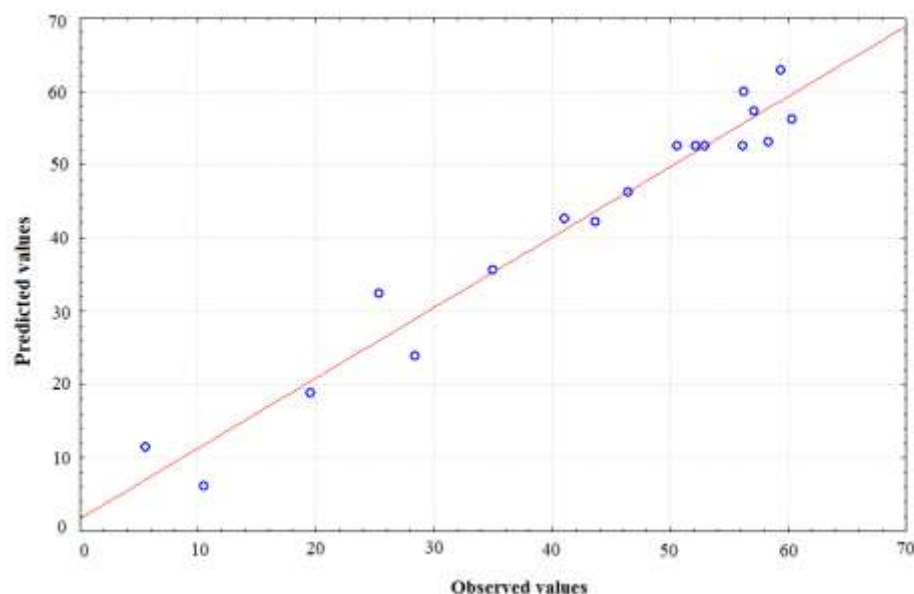


Figure 7- Predicted values of yield of esters versus observed values obtained in the CCD experiments

Analyzing the regression coefficients obtained for each term in Equation 6, it is possible to evaluate if the parameters positive or negatively affect the yield of esters. The highest coefficient obtained were +15.83 for the amount of catalyst ( $X_{AC}$ ). This means that this variable is the most significant on the response of the process. Besides that, the positive sign in front of the term indicates a synergistic effect. This positive effect can also be observed in Table 3. Comparing runs: 1 and 3; 2 and 4; 5 and 7; 6 and 8; 11, point centers and 12 is it possible to observe that the amount of niobium phosphate was increased, maintaining temperature and ethanol:oleic acid constant. In all cases, as expected, an increase in the amount of catalysts promoted an increase in the yield of esters. With a higher mass of catalysts, the number of acid sites, which catalyze the reaction, also increased, favoring the formation of esters [14].

The second most significant parameter on the yield of esters was ethanol:oleic acid molar ratio ( $X_{MR}$ ), which presented a regression coefficient of +7.33. This variable also showed a positive effect. Comparing runs: 1 and 5; 2 and 6; 3 and 7; 4 and 8; 13, center points and 14 in Table 3, it can be seen that the increase in the ethanol:oleic acid molar ratio caused an increase in the yields of esters in all cases. Therefore, consistently with the literature ref, these results show that an

increase in the ethanol:oleic acid molar ratio positively affects the response of the process, once that the excess of alcohol provides a better contact between the reactants and causes the equilibrium to shift the reaction to esters formation [15].

The last linear term significant on the response process was temperature ( $X_T$ ), with a coefficient of +5.17. Maintaining the mass of catalyst and ethanol:oleic acid molar ratio constant and varying the temperature of the process, an increase on the esters content occurs with an increase at the reaction temperature. This can be observed comparing runs 1 and 2; 3 and 4; 5 and 6; 7 and 8; and 9, point centers and 10. At higher temperatures, the solubility of fatty acid in alcohol increases, benefiting the conversion of the reaction [14, 15, 16, 17].

Finally, the quadratic terms of amount of catalyst and ethanol:oleic acid molar ratio ( $X_{AC}X_{AC}$  and  $X_{MR}X_{MR}$ , respectively) were also significant on the response of the process and were responsible of a non-linear behavior of the system. These terms mean that at higher amounts of catalyst and ethanol:oleic acid molar ratios, they will not increase the yield of esters anymore, due to mass transfer limitations and the highest dilution of the oleic acid in the reaction medium, which may slow down the reaction and decrease the yield of esters. No interaction between variables was significant.

Figures 8 and 9 show the response surfaces for the yield of esters predicted by the multiple regression (Eq. 6). Analyzing the response surfaces it is possible to observe the positive effect of all three parameters already discussed and the convex behavior, due to quadratic terms of amount of catalyst and ethanol:oleic acid molar ratio.

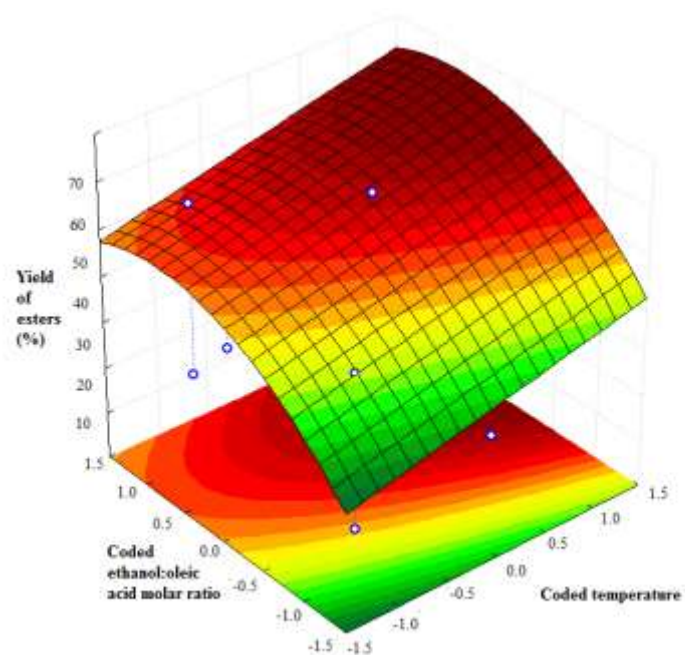


Figure 8- Response surface of yield of esters versus coded ethanol:oleic acid molar ratio and coded temperature, with amount of catalyst fixed at 1.414.

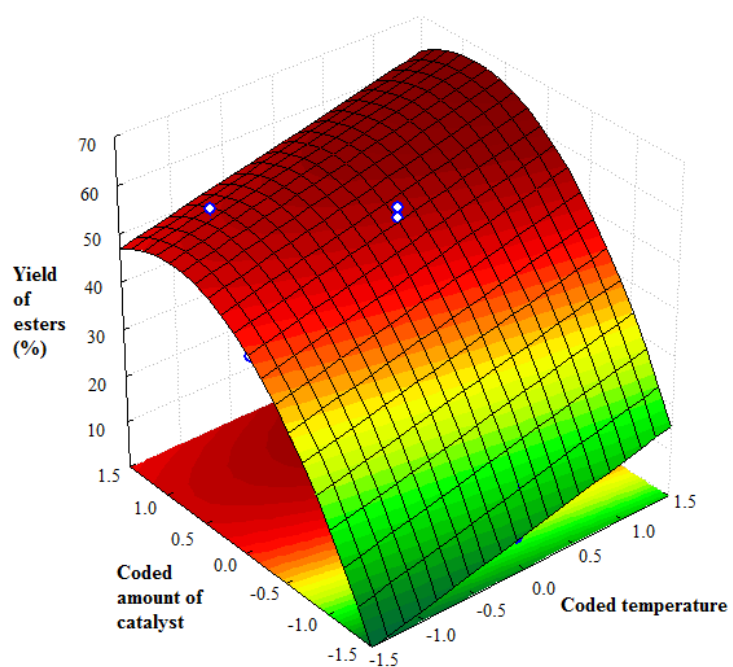


Figure 9- Response surface of yield of esters versus coded amount of catalyst and coded temperature, with ethanol:oleic acid molar ratio fixed at 1.414



### 3.4. Optimization

In order to generate optimal conditions and obtain yields of esters higher than 60%, the canonical analysis was applied. For this, the empirical model was expressed in the canonical form and given by Equation 7:

$$y = -9.79 w_1^2 - 4.87 w_2^2 - 0.93 w_3^2 + 63.73 \quad (7)$$

As already mentioned, the sign and magnitude of the characteristic roots  $\lambda_i$  can determine the nature of the stationary point of the fitted surface. According to Equation 7, all three characteristic roots ( $\lambda_1$ ,  $\lambda_2$  and  $\lambda_3$ ) showed negative sign (-9.79, -4.87 and -0.93, respectively), which means that the stationary point is a maximum point.

The canonical analysis defined the following optimal conditions: 279 °C, ethanol:oleic acid molar ratio of 11:1 and 0.62 g of niobium phosphate. Under these operational conditions, the maximum yield of esters predicted was 71%. The experimental value obtained was 69%, confirming the result predicted by the canonical analysis.

## 4. CONCLUSIONS

Samples of niobium phosphate were calcined at different temperatures: 300, 350, 400, 450, 500 and 600 °C and were tested for the continuous esterification reaction of oleic acid. Results showed that increasing the calcination temperature promoted a decrease on the BET surface area, total acidity and, consequently, on the catalytic performance of the samples for the esterification reaction. However, compared to niobic acid, niobium phosphate showed higher thermal stability, avoiding a more significant decline in the conversion. Niobium phosphate calcined at 300 °C, which presented the highest catalytic activity (61% at 250 °C, ethanol:oleic acid molar ratio of 6:1, 0.3 g of catalyst and flow rate of 0.3 mL/min), was submitted to a design of experiments, to evaluate the effect of three parameters on the yield of esters: temperature, mass of catalyst and ethanol-to-oleic acid molar ratio. All the parameters significantly affected the response of the process. The highest yield of ester obtained in the central composite design (CCD) was 60%. With

the optimization, a yield of esters of 69% could be obtained, at 279 °C, 0.62 g of catalyst and ethanol:oleic acid molar ratio of 11:1. The results proved that niobium phosphate is an effective catalyst for the continuous esterification with ethanol and oleic acid when it is calcined at 300 °C, since it presents high BET surface area, high total acidity and good thermal stability.

## ACKNOWLEDGMENT

The authors are grateful to CBMM for the financial support and for providing the niobium phosphate used in this work, to CNPq, FAPEMIG, CAPES and Vale S.A. for the financial support and to LNLS (Laboratório Nacional de Luz Síncrotron – Campinas – BRAZIL) for the use of the XPD beamline.

## REFERENCES

- [1] I. Nowak, M. Ziolek. **Niobium compounds: preparation, characterization, and application in heterogeneous catalysis**, *Chem. Rev.* 99 (1999) 3603-3624. <https://doi.org/10.1021/cr9800208>
- [2] M. Ziolek. **Niobium-containing catalysts- the state of the art**, *Catal. Today.* 78 (2003) 47–64. [https://doi.org/10.1016/S0920-5861\(02\)00340-1](https://doi.org/10.1016/S0920-5861(02)00340-1)
- [3] P. Carniti, A. Gervasini, S. Biella, A. Auroux. **Niobic acid and niobium phosphate as highly acidic viable catalysts in aqueous medium: fructose dehydration reaction**, *Catal. Today.* 118 (2006) 373–378. <https://doi.org/10.1016/j.cattod.2006.07.024>
- [4] A. Florentino, P. Cartraud, P. Magnoux, M. Guisnet. **Textural, acidic and catalytic properties of niobium phosphate and of niobium oxide**, *Appl. Catal. A.* 89 (1992) 143-153. [https://doi.org/10.1016/0926-860X\(92\)80229-6](https://doi.org/10.1016/0926-860X(92)80229-6)
- [5] I.A.L. Bassan, D.R. Nascimento, R.A.S. San Gil, M.I.P. da Silva, C.R. Moreira, W.A. Gonzalez, A.C. Faro Jr., T. Onfroy, E.R. Lachter, **Esterification of fatty acids with alcohols over niobium phosphate**. *Fuel Process. Technol.* 106 (2013) 619–624. <https://doi.org/10.1016/j.fuproc.2012.09.054>
- [6] A.C.A. Abdala, V.A.S. Garcia, C.P. Trentini, L. Cardozo Filho, E.A. da Silva, C. Silva. **Continuous catalyst-free esterification of oleic acid in compressed ethanol**, *Int. J. of Che. Eng.* Article ID 803783, (2014) 1-5. <http://dx.doi.org/10.1155/2014/803783>

- [7] M.E. Borges, L. Díaz. **Recent developments on heterogeneous catalysts for biodiesel production by oil esterification and transesterification reactions: A review**, *Renew. and Sust. Energ. Rev.* 16 (2012) 2839–2849. <https://doi.org/10.1016/j.rser.2012.01.071>
- [8] L.L. Rade, C.O.T. Lemos, M.A.S. Barrozo, R.M. Ribas, R.S. Monteiro, C.E. Hori. **Optimization of continuous esterification of oleic acid with ethanol over niobic acid**, *Renew. Energ.* 115 (2018) 208-216. <https://doi.org/10.1016/j.renene.2017.08.035>
- [9] M.R. Miladinović, O.S. Stamenković, P.T. Banković, A.D. Milutinović-Nikolić, D.M. Jovanović, V.B. Veljković. **Modeling and optimization of sunflower oil methanolysis over quicklime bits in a packed bed tubular reactor using the response surface methodology**, *Energy Convers. Manage.* 130 (2016) 25-33. <https://doi.org/10.1016/j.enconman.2016.10.020>
- [10] L.L. Rade, S. Arvelos, M.A.S. Barrozo, L.L. Romanielo, E.O. Watanabe, C.E. Hori. **Evaluation of the use of degummed soybean oil and supercritical ethanol for non-catalytic biodiesel production**, *J. Supercrit. Fluids.* 105 (2015) 21-28. <https://doi.org/10.1016/j.supflu.2015.05.017>
- [11] J.M. Longo & P. Kierkegaard. **The crystal structure of NbOPO<sub>4</sub>**, *Acta Chemica Scandinavica*. 2001 (1996) 72-78.
- [12] M. H. C de la Cruz., J. F. C da Silva, E. R. Lachter. **Catalytic activity of niobium phosphate in the Friedel–Crafts reaction of anisole with alcohols**, *Catal. Today.* 118 (2006) 379–384. <https://doi.org/10.1016/j.cattod.2006.07.058>
- [13] V. Lebarbier, M. Houalla, T. Onfroy. **New insights into the development of Bronsted acidity of niobic acid**, *Catal. Today*, 192 (2012) 123-129. <https://doi.org/10.1016/j.cattod.2012.02.061>
- [14] A. Hykkerud, J. M. Marchetti. **Esterification of oleic acid with ethanol in the presence of Amberlyst 15**, *Biomass Bioenerg.* 95 (2016) 340-343. <https://doi.org/10.1016/j.biombioe.2016.07.002>
- [15] R. Alenezi, G.A. Leeke, J.M. Winterbottom, R.C.D. Santos, A.R. Khan. **Esterification kinetics of free fatty acids with supercritical methanol for biodiesel production**, *Energy Conversion and Manage.* 51 (2010) 1055–1059. <https://doi.org/10.1016/j.enconman.2009.12.009>
- [16] A.S. Ramadhas, S. Jayaraj, C. Muraleedharan. **Biodiesel production from high FFA rubber seed oil**, *Fuel.* 84 (2005) 335–340. <https://doi.org/10.1016/j.fuel.2004.09.016>

[17] J.A. Gonçalves, A.L.D. Ramos, L.L.L. Rocha, A.K. Domingos, R.S. Monteiro, J.S. Peres, N.C. Furtado, C.A. Taft, D.A.G. Aranda. **Niobium oxide solid catalyst: esterification of fatty acids and modeling for biodiesel production**, *J. Phys. Org. Chem.* 24 (2011) 54–64.  
<https://doi.org/10.1002/poc.1701>

---

#### 4. MANUSCRIPT THAT WILL BE SUBMITTED IN BIORESOURCE TECHNOLOGY

---

Process synthesis and economic assessment of biodiesel production by  
hydroesterification of waste cooking oil using heterogeneous catalyst

L. L. Rade<sup>a</sup>, R. S. Monteiro<sup>b,c</sup>, R. M. Ribas<sup>b</sup>, S. M. S. Neiro<sup>a</sup>, C. E. Hori<sup>a,\*</sup>

<sup>a</sup>Universidade Federal de Uberlândia, Faculdade de Engenharia Química, 38408-144,  
Uberlândia, MG, Brazil

<sup>b</sup>Companhia Brasileira de Metalurgia e Mineração - CBMM, 38183-903, Araxá, MG, Brazil

<sup>c</sup>Catalysis Consultoria Ltda, 22793-081, Rio de Janeiro, RJ, Brazil

\*cehori@ufu.br

**ABSTRACT:** Biodiesel production by continuous hydroesterification using acid solid catalysts on a commercial scale was synthesized and simulated in UniSim Design. Operational conditions and equipment designs for the process were obtained. An economic analysis was carried out to evaluate the feasibility of the process. Total capital investment and total manufacturing cost were calculated and the cash flow diagram of the process was generated. The results showed that the continuous hydroesterification acid-catalyzed using waste cooking oil as the raw material was technically feasible and capable of producing biodiesel with high purity (97%). However, the process presented limitations in the economic aspect. The cost of the utilities employed in the process was, in general, the factor that most affected the economic viability, especially the utilities used in the reboilers of the distillation towers.

**KEYWORDS:** biodiesel, hydroesterification, heterogeneous catalyst, process synthesis, economic analysis.

## 1. INTRODUCTION AND BACKGROUND

The development and use of alternatives to petroleum-based fuels is a way to meet the growing energy demand in the world. One such fuel that exhibits great potential is biofuel, in special, biodiesel (Demirbas, 2007). Biodiesel is produced from renewable sources, such as vegetable oils and animal fats, is biodegradable, nontoxic (West et al., 2008) and emits less polluting gases during the combustion process. This biofuel has physical properties similar to petroleum diesel and it can be used individually or mixed with diesel in diesel engines (Kapilakarm and Peugtong, 2007).

Conventionally, biodiesel is produced by transesterification of triglycerides with short chain alcohols catalyzed by basic homogeneous catalysts. Despite the advantages such as low cost and mild reaction conditions, the alkali-catalyzed transesterification shows some limitations (Aranda et al., 2007a). This process is very sensitive to water and free fatty acids contents in the feedstock used and, because of that, vegetable oils and alcohol must be anhydrous (Silva et al., 2007). Furthermore, the recovery of glycerol is difficult, the catalyst must be removed from the product and the energy costs are high, among other problems. Depending on the operational conditions and the water and free fatty acid contents, the saponification reaction can be promoted and the soap produced decreases the biodiesel selectivity, hinders the separation of the esters and glycerol and favors the emulsion formation during the washing step (Aranda et al., 2009a).

Hydroesterification was recently established as a way to overcome those problems related to the conventional biodiesel production methods using second-generation feedstock, such as animal fats, non-edible oils and waste cooking oils (Pourzolfaghar et al., 2016). This process consists of a two-stage process, as presented in Figure 1. First, the vegetable oil is hydrolyzed to free fatty acids (FFAs) and glycerol. Then, the FFAs produced in the first step are separated and esterified using a short-chain alcohol, generating biodiesel and water (Cavalcanti-Oliveira et al., 2011). Both steps can be catalyzed by acid materials (Aranda et al., 2009a) and become more attractive when coupled to the use of heterogeneous catalysts, which can be reused and minimize waste generation. Besides that, this process allows the use of low quality raw materials, with any acidity and any water content, obtains a more pure glycerin as sub product (Aranda et al., 2009b) and shows an easier product purification (Nandiwale and Bokade, 2014).

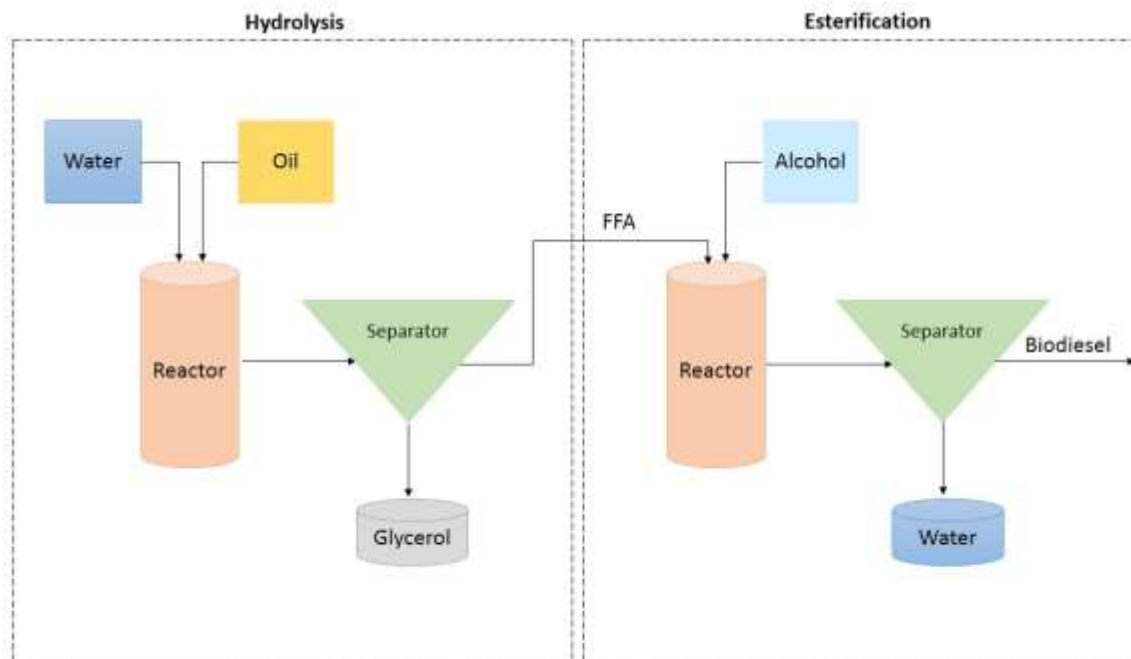


Figure 1- Schematic diagram of the hydroesterification process (Adapted from Pourzolfaghar et al., 2016)

The high cost of biodiesel production is considered the biggest obstacle to its large-scale commercialization (Canakci and Van Gerpen, 2001; Zhang et al., 2003a), one of the main focus of biodiesel research nowadays is to explore ways to reduce the process cost (Zhang et al., 2003a; West et al., 2008). The refined feedstock represents up to 75% of the overall biodiesel production cost (Atabani et al., 2012). Thus, the use of waste cooking oil as raw material is very attractive, since it is estimated to be about half the price of refined oil (Zhang et al., 2003a).

All the studies reported about the hydroesterification process, using waste cooking oil or any other raw material, applied enzymes to catalyze the hydrolysis step, which are very expensive and may turn the process not feasible. There are few studies available in the literature that use an acid solid catalyst for both steps of the hydroesterification route. Reyes et al. (2012) studied the hydroesterification process for the production of biodiesel from *Monoraphidium contortum* (MORF-1) microalgae biomass, using niobium oxide powder as solid catalyst for esterification reaction. However, for the hydrolysis step, no catalyst was used. The reactions were carried out in batch reactor. The authors obtained a product with an ester content of 94.27%. Thus, the hydroesterification process revealed a very promising alternative to the transesterification process

as it allows the use of feedstocks with any free fatty acid and water contents and may be performed with acid catalyst, which favors high conversions in a small reaction time.

Song et al. (2016) performed a techno-economic evaluation of hydrolysis–esterification biodiesel production process and compared this route with the conventional biodiesel production process. The authors evaluated the energy and material balance by Aspen Plus. Results showed that the high energy required for the conventional route (5.42 MJ/L biodiesel) is mainly contributed to the drying and transesterification stages (2.36 and 1.89 MJ/L biodiesel, respectively). However, the hydroesterification process can reduce this energy consumption to 1.81 MJ/L biodiesel (33.39% of conventional process).

The vast majority of biodiesel studies investigate the processes in a laboratory/bench-scale. This way, steps as product separation and purification are not evaluated (Zhang et al., 2003a). Evaluating the technological and economic feasibility of a biodiesel plant involves all operating units, not only one reactor. Therefore, there is a need to design a complete continuous process and assess its performance from the viewpoint of an entire plant (Zhang et al., 2003a). It is important to emphasize that, for hydroesterification process, in particular, information on process simulation and design are not available.

In this context, the objectives of this work were to develop a simulation of acid catalyzed hydroesterification to produce biodiesel from waste cooking oil using UniSim Design and to perform an economic analysis of the process. Conversions obtained in laboratory were used as input data of the simulated reactors. Both reactions were catalyzed by niobic acid (CBMM's HY- 340) using a continuous reactor.

## **2. PROCESS SIMULATION**

UniSim Design (Honeywell) was used as the basic platform for the synthesis of the complete process. Initially, chemical components were selected to integrate the base case out of the simulator data base, thermodynamic models were selected for describing each of the chemical and physical operations and systems in the model. Then, the reactions were configured and grouped in different reaction sets, as shown in Figure 2. It was not observed any side reaction at the experimental conditions used in the simulation. The waste cooking oil was represented by triolein. Thus, ethyl oleate was taken as the resulting biodiesel product.



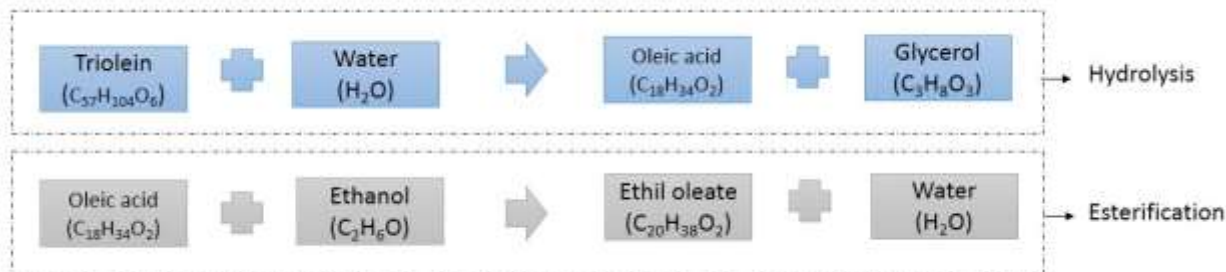


Figure 2- Two reactions used in the simulation of the hydroesterification process

Information for the components ethanol, glycerol and water was available at UniSim library. The components that were not available in the library were defined as hypothetical components using the ‘‘Hypo Manager’’ tool. These components were: triolein ( $C_{57}O_{104}O_6$ ), oleic acid ( $C_{18}H_{34}O_2$ ) and ethyl oleate ( $C_{20}H_{38}O_2$ ). Aiming to create the hypothetical components, some specification were required as input. Table 1 shows the properties that were used for this purpose. All other physical properties were estimated using UNIFAC by providing a molecular structure.

Table 1- Input properties of oleic acid, triolein and ethyl oleate

Component	Tc [°C]	Pc [kPa]	$\omega$	Boiling point [°C]	Density [kg/m <sup>3</sup> ]	Molecular weight
Oleic acid <sup>1</sup>	522.1	1220	1.214	358.9	893.4	282.5
Triolein <sup>2</sup>	704.8	730	1.594	416.2	900.0	885.4
Ethyl oleate <sup>2</sup>	523.1	1050	1.3282	217.0	870.0	310.5

Sales-Cruz et al. (2010)<sup>1</sup>, Arvelos et al. (2014)<sup>2</sup>

The non-random two liquid (NRTL) thermodynamic/activity model was selected for the description of the liquid phase (Zhang et al., 2003a), due to the presence of polar compounds such as ethanol and glycerol in the process, whereas Soave-Redlich-Kwong (SRK) was chosen to describe the vapor phase for all systems in the simulation, including supporting utilities.

The plant capacity was specified to take in a feedstock flowrate of 925 kg/h vegetable oil and 1111 kg/h of water. The main operations included reactors, pumps, heat exchangers, distillation columns and process vessels, which are the typical operations used in biodiesel processes (Zhang et al., 2003a; West et al., 2008; Karmee et al., 2015). The reactors were modeled

as conversion reactors and were assumed to operate continuously (Zhang et al., 2003a; West et al., 2008). As already mentioned, conversions obtained in laboratory were used as input data for the simulated reactors. A conversion of 92% was obtained for continuous esterification using niobic acid as solid acid catalyst, at the optimal conditions (1 atm, 250 °C and 11:1 ethanol:oleic acid molar ratio, substrate flow rate of 0.3 ml/min) (Rade et al., 2018). The continuous hydrolysis using niobic acid as solid acid catalyst was also investigated and a conversion of 86% was obtained (1 atm pressure, 400 °C and 52:1 water:waste cooking oil, substrate flow rate of 0.2 ml/min). The European standard (EN 14214:2008) for purity of biodiesel product (i.e., 96.5 wt.%) was applied to the process in the present study. For the current analysis, pressure drops on heat exchangers, furnaces, process vessels and reactors were all considered to be negligible (Zhang et al., 2003).

Distillation columns were used to recover the excess ethanol, triolein and in the purification of oleic acid and biodiesel produced. The columns sizing were performed by using a shortcut model based on Fenske (for the minimum stages number), Underwood (for the minimum reflux rate) and Gilliland (for the real stages number) and using information such as desired separation between the key components and the real reflux ratio. Triolein, ethanol and oleic acid were recycled in the process. Two and three-phase vessels were also used to separate components.

### **3. PROCESS SYNTHESIS**

The continuous hydroesterification process was synthesized as depicted in Figure 3. In the first reactor, the waste cooking oil was hydrolyzed to free fatty acids (FFAs) and glycerol, using niobic acid as catalyst. Then, the products were sent for downstream purification, which consisted of the following steps: i) glycerol separation using a three-phase separator by gravity and ii) remained triolein recovery and oleic acid separation by distillation. The FFAs produced and separated in the first step of the process were esterified in the second reactor, also using niobic acid as catalyst. The reaction synthesized biodiesel (FAEE) and water as products. The products of the second reactor were purified using the following steps: i) ethanol recovery by distillation, ii) separation of biodiesel and remained oleic acid using two-phase separator, iii) separation of biodiesel from the other components by distillation. The biodiesel was obtained in two liquid phases due to the presence of water. Thus, the product was submitted to two two-phase separators.

The hydroesterification process obtained a biodiesel with a purity of 97%. The process stream summary is presented in Table 2.

### **3.1. Hydrolysis reaction**

The continuous hydrolysis was performed at 400 °C, 52:1 water:oil molar ratio, 100 kPa and 1 g of niobic acid. Water (at 1111 kg/h), triolein (925 kg/h) and recycled triolein (127 kg/h) were mixed and heated in exchangers E-101 and E-102 to 400 °C, before entering into the hydrolysis reactor R-101. In R-101, 86% of the waste cooking oil was assumed to be converted to FFA, producing glycerol as by-product. The products (stream 104) were cooled to 130 °C and introduced to a three-phase vessel V-101. The glycerol remained in the bottom stream (90 kg/h), which contained 87% glycerol, 9% water, 3% triolein and 1% oleic acid. The residual gas, containing 98% of water and 2% of triolein, was separated in the top of the vessel. Stream 106 (1001.5 kg/h), containing 86% oleic acid, 13% triolein and 1% glycerol were pumped by pump P-101 into the column distillation T-201.

### **3.2. Triolein recovery**

In T-201, 17 theoretical stages and a reflux ratio of 3 were used to obtain a good separation between oleic acid, remained triolein and other components. Recycled triolein was a pure triolein distillate, containing 99% of total stream and was recycled to reactor R-101. Pure oleic acid (99%), also separated in T-201, was mixed with fresh ethanol and recycled ethanol. The mixture (stream 201) was heated to 250 °C and, then, charged into esterification reactor R-201.

### **3.3. Esterification reaction**

The continuous esterification was performed at 250 °C, 11:1 ethanol:oleic acid molar ratio, 100 kPa and 0.7 g of niobic acid, at reactor R-201. In R-201, 92% of the oleic acid was assumed to be converted to ethyl esters, producing water as a by-product. The products (stream 203) were cooled in exchanger E-201 to 78 °C and pumped by pump P-102 to ethanol distillation T-301.

### **3.4. Ethanol recovery**

At column distillation T-301, the ethanol was separated from the other components and recycled (containing 72% of ethanol, 23% ethyl oleate and 6% water). 15 theoretical stages and a reflux ratio of 4 were used. The biodiesel produced remained in the bottom stream 301, which contained 84% ethyl oleate, 7% ethanol, 5% oleic acid and 4% water. This stream was sent to process vessels and columns distillation aiming to obtain a final biodiesel product that meets European standard specifications (greater than 96.5% pure).

### **3.5. FAEE purification**

Aiming to purify biodiesel produced, stream 301 was heated in exchanger E-301 to 250 °C and sent to a two-phase vessel (V-301). Using this vessel, the remained oleic acid could be separated in the bottom stream (stream 304) and recycled to reactor R-201. The stream at the top of the vessel was cooled in exchanger E-302 to 127 °C and sent to a column distillation (T-401), which separated the FAEE produced. The biodiesel was obtained in the bottom stream (stream 401) that contained 96% ethyl oleate, 2% water, 1% oleic acid and 1% glycerol. However, it was obtained in two liquid phases and, because of that, stream 401 had to be sent to two other vessels (V-401 and V-402). The water content could be separated by using these two vessels and the product was then purified. Thus, the final product (FAEE) was produced at the rate of 769 kg/h and FAEE purity of 97%.

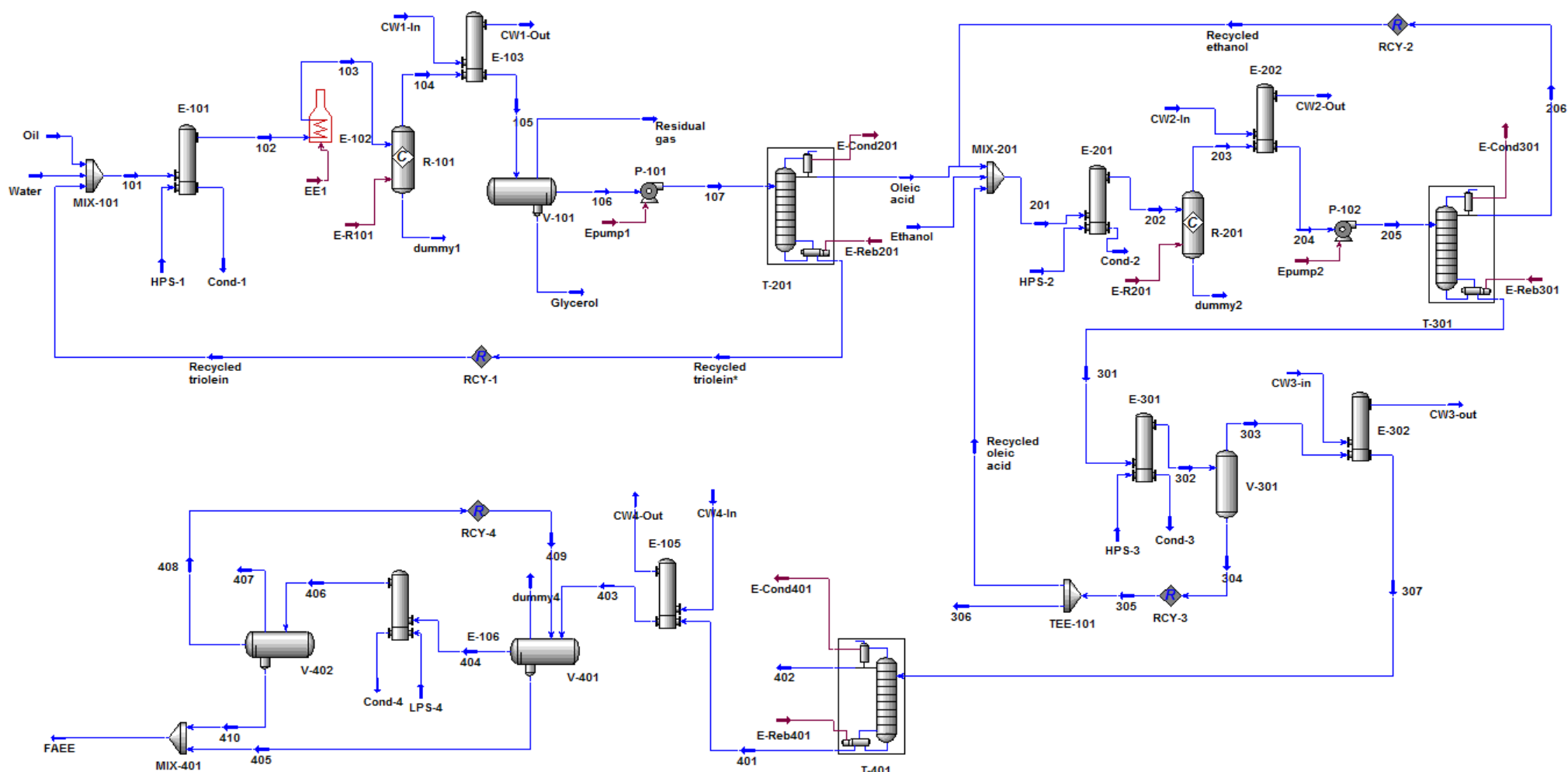


Figure 3- Heterogeneous acid-catalyzed hydroesterification process flow sheet to produce biodiesel from waste oils.

Table 2- Feed and product stream information for the hydroesterification process

Stream name	Oil	Water	101	104	106	Residual gas	Glycerol	Recycled triolein	Ethanol	Oleic acid	201	203	Recycled ethanol
Temperature (°C)	25.0	25.0	46.9	400.0	130.0	130.0	130.0	489.0	25.0	155.2	79.2	250.0	124.7
Pressure (kPa)	100.0	100.0	100.0	100.0	100.0	100.0	100.0	200.0	100.0	200.0	100.0	100.0	500.0
Molar flow (kgmol/h)	1.04	61.67	62.86	62.86	3.45	58.12	1.29	0.15	5.12	3.31	51.04	51.04	41.48
Mass flow (kg/h)	925.00	1111.00	2162.70	2162.70	1001.54	1071.35	89.81	126.70	236.00	874.80	3577.15	3577.15	2130.69
Component mass fraction													
Water	0.000	1.000	0.514	0.488	0.003	0.976	0.087	0.000	0.000	0.003	0.035	0.050	0.057
Oleic acid	0.000	0.000	0.000	0.400	0.862	0.001	0.010	0.007	0.000	0.986	0.259	0.021	0.000
Glycerol	0.000	0.000	0.000	0.043	0.009	0.006	0.870	0.000	1.000	0.011	0.003	0.003	0.000
Ethanol	0.000	0.000	0.000	0.000	0.000	0.000	0.000	0.000	0.000	0.000	0.493	0.454	0.717
Ethyl oleate	0.000	0.000	0.000	0.000	0.000	0.000	0.000	0.000	0.000	0.000	0.210	0.472	0.226
Triolein	1.000	0.000	0.486	0.068	0.126	0.017	0.032	0.993	0.000	0.000	0.000	0.000	0.000
Stream name	301	303	304	306	Recycled oleic acid	401	402	404	405	407	408	410	FAEE
Temperature (°C)	133.5	250.0	250.0	250.0	250.0	102.5	78.8	87.0	87.0	112.0	112.0	112.0	87.5
Pressure (kPa)	500.0	500.0	500.0	500.0	500.0	100	100.0	100.0	100.0	100.0	100.0	100.0	100.0
Molar flow (kgmol/h)	9.56	8.41	1.15	0.02	1.12	3.81	4.60	1.93	2.68	0.95	0.81	0.17	2.85
Mass flow (kg/h)	1447.49	1103.96	343.53	6.85	335.66	859.22	244.74	340.09	759.22	90.32	239.69	10.07	769.29
Component mass fraction													
Water	0.040	0.052	0.000	0.000	0.000	0.021	0.158	0.043	0.006	0.003	0.003	0.139	0.008
Oleic acid	0.051	0.007	0.193	0.193	0.193	0.009	0.000	0.010	0.010	0.014	0.014	0.000	0.010
Glycerol	0.007	0.008	0.001	0.001	0.001	0.011	0.000	0.026	0.001	0.001	0.001	0.860	0.012
Ethanol	0.068	0.088	0.002	0.002	0.002	0.000	0.396	0.000	0.000	0.000	0.000	0.000	0.000
Ethyl oleate	0.835	0.845	0.803	0.803	0.803	0.958	0.446	0.920	0.983	0.982	0.982	0.001	0.970
Triolein	0.000	0.000	0.000	0.000	0.000	0.000	0.000	0.000	0.000	0.000	0.000	0.000	0.000

#### 4. ECONOMIC ASSESSMENT

Whereas the hydroesterification process proposed in this work could produce biodiesel with 97% of purity, techniques of economic analysis were used to assess the profitability of this process. The evaluation of fixed capital investment and the economic calculations were performed using CAPCOST program (CAPCOST\_2008.xls) from Turton et al. (2003). The program requires, as input data, information about the equipment (capacity, operating pressure and materials of construction). Using the current value of The Chemical Engineering Plant Cost Index (CEPCI) the cost data could be adjusted for inflation. Other data necessary to determine material and energy costs were obtained from the flowsheets. Table 3 gives the capacity of the equipment simulated in the hydroesterification process. These values were defined by the simulator. The material of construction of all equipment was carbon steel.

Table 3- Equipment sizes for various process units in all processes

Equipment	Description	Dimension
Reactors	Hydrolysis reactor (R-101)	5 m <sup>3</sup>
	Esterification reactor (R-201)	5 m <sup>3</sup>
Towers	T-201	10.5 m x 1.2 m
	T-301	9.5 m x 1.2 m
	T-401	7 m x 1.2 m
Vessels	V-101	3.2 m x 0.91 m
	V-301	2.5 m x 0.46 m
	V-401	1.23 m x 0.41 m
	V-402	2.1 m x 0.61 m

Dimension of towers and vessels are given as height x diameter (m)

##### 4.1. Basis of calculation

The economic assessment performed is classified as a “study estimate” with estimates accurate in the range of +40% to –25% (Turton et al., 2003). The CEPCI used was 541.7 (value for 2016). The time for the plant construction was defined in two years, with a plant life of ten

years after start-up. 10% of annual interest rate and a taxation rate of 42% were applied (Turton et al., 2003). Operating hours were set at 8322 h/year (Turton et al., 2003). The cost of the land was \$1250000 (Turton et al., 2003). The pump and furnace efficiencies were assumed 70% and 90%, respectively (Turton et al., 2003). Low and high-pressure steam were used as heating media and water was the cooling medium.

The process was evaluated based on fixed capital investment and cost of manufacturing. The capital cost for a chemical plant takes into consideration many other costs than the purchased cost of the equipment (Turton et al., 2003). It consists of three parts: total bare module capital cost (sum of direct and indirect costs), contingencies and fees, and costs of auxiliary facilities (Turton et al., 2003).

The costs associated with the day-to-day operation of a chemical plant consist of the cost of manufacturing. It includes raw material prices, operating labor, utilities, maintenance and repairs, operating supplies, laboratory charges, expenses for patents and royalties, research and development, administrative costs, local taxes and insurance, among others. The cost of manufacturing can be determined when the following costs are known: fixed capital investment, cost of operating labor, cost of utilities (such as fuel gas, electric power, steam, cooling water, among others) and cost of raw materials (Turton et al., 2003).

In the present study, the prices of the raw materials and product were researched in different sources (Neste, accessed in 2018; Zhang et al., 2003; Trading Economics, accessed in 2018 and Turton et al., 2003) and their flow rate was obtained from the UniSim simulation. The utilities costs were obtained from Turton et al. (2003). Table 4 gives the specifications of utilities and costs (US\$) adopted in the economic assessment.



Table 4- Basic conditions for the economic assessment

Item	Description	Price
<b>Chemicals</b>		
Biodiesel <sup>a</sup>		920 \$/ton
Waste cooking oil <sup>b</sup>		200 \$/ton
Ethanol <sup>c</sup>		430 \$/ton
Glycerol <sup>b</sup>		750 \$/ton
<b>Utilities</b>		
Cooling water <sup>d</sup>	(30 °C to 45°C)	0.354 \$/GJ
Low-pressure steam <sup>d</sup>	(5 barg, 160 °C)	13.28 \$/GJ
High-pressure steam <sup>d</sup>	(41 barg, 254 °C)	17.7 \$/GJ
Electricity <sup>d</sup>	(110-440 V)	16.8 \$/GJ
Fuel oil (no. 2) <sup>d</sup>		14.2 \$/GJ

<sup>a</sup>Neste, <sup>b</sup>Zhang et al., 2003, <sup>c</sup>Trading Economics, <sup>d</sup>Turton et al., 2003

## 4.2. Fixed capital investment

For the fixed capital cost calculation, the bare module cost ( $C_{BM}$ ) of each equipment were evaluated. The bare module cost of an equipment is the sum of direct and indirect costs (direct: purchased cost, materials required for installation and labor to install. Indirect: freight, insurance, taxes, construction overhead and engineering expenses) (Turton et al., 2003). The  $C_{BM}$  of each equipment were calculated using the CAPCOST program, according to Equations (1)-(3).

$$C_{BM} = C_P^0 F_{BM} \quad (1)$$

$$F_{BM} = B_1 + B_2 F_M F_P \quad (2)$$

$$\log_{10} C_P^0 = K_1 + K_2 \log_{10}(A) + [K_3 \log_{10}(A)]^2 \quad (3)$$

where  $F_{BM}$  is the bare module cost factor,  $C_P^0$  is the purchased cost of the equipment.  $B_1$  and  $B_2$  are constants specific to equipment type and  $F_M$  and  $F_P$  are the material and pressure factors,

respectively.  $K_i$  is a constant specific to the unit type and  $A$  is the capacity of the unit (Turton et al., 2003).

The equipment costs, fixed capital costs and total capital investments of the process, obtained using CAPCOST program (Turton et al., 2003), are presented in Table 5.

The total bare module cost of the hydroesterification plant proposed in this study was \$2.52 million. As shown in Table 5, the cost of the heat exchangers contributed with a significant part of the capital cost. The costs associated with these equipment units amounted to 73.8% of the total bare module. Thus, other separation methods must be evaluated, in order to minimize these costs.

Table 5- Equipment costs and fixed capital costs and fixed capital

Type	Description	Purchased Cost	Bare Module Cost	Total Module Cost	Grass Roots Cost
<b>Reactors</b>	Hydrolysis	\$9810	\$39200	\$46300	\$51200
	Esterification	\$9810	\$39200	\$46300	\$51200
<b>Towers</b>	T-201	\$41600	\$100000	\$118000	\$165000
	T-301	\$37600	\$117000	\$138000	\$181000
	T-401	\$27500	\$78800	\$93000	\$127000
<b>Fired Heater</b>	E-102	\$54100	\$117000	\$138000	\$197000
<b>Others</b>	Separators	\$20900	\$63200	\$74600	\$103800
	Heat exchangers	\$563900	\$1863000	\$2195000	\$3125000
	Pumps	\$26800	\$106600	\$125600	\$170000
<b>Total</b>		\$792020	\$2524000	\$2970000	\$4170000
Fixed Capital Investment (FCI)			\$4170000		
Working Capital (WC)			\$670000		

#### 4.3. Total manufacturing cost

Results for the total manufacturing cost of the process are shown in Table 6. The results showed that the direct manufacturing costs (raw materials, operating labor and utilities)

represented 70% of the total manufacturing. The raw materials and utilities comprised 33.3% and 34.6% of the total manufacturing, respectively. Only the pumps used the electricity required in the process. The electricity annual costs for these equipment was \$545, which has an order of magnitude much lower than the other values presented in Table 6. Considering just utilities, it is also possible to observe that the hydroesterification process applied an amount of low-pressure steam higher than the amount of high-pressure steam. Furthermore, the reboilers and condensers of the distillation columns used 51.6% of the total annual utility. As was mentioned, separation methods also must be evaluated and optimized, in order to minimize the operational costs.

Table 6- Total annual manufacturing cost obtained for the hydroesterification process

<b>Raw material</b>	\$2.39
Waste cooking oil	\$1.54
Ethanol	\$0.85
<b>Operating labor</b>	\$0.16
<b>Utilities</b>	\$2.48
Low-Pressure steam	\$1.26
High-Pressure steam	\$1.07
Electricity	\$0.00
Cooling water	\$0.05
<b>Total manufacturing cost</b>	\$7.17
Revenue from sales	\$6.27

Costs reported as \$ millions

Figure 4 presents the Cash Flow Diagram generated for the hydroesterification process, considering a Modified Accelerated Cost Recovery System depreciation (MACRS) of five years. Is it possible to observe that the process is not economically reasonable with a biodiesel cost of \$0.92/kg, even though is technologically feasible. The economic viability of the process highly depend on the biodiesel cost. With a biodiesel cost of \$1.30/kg, the process proposed starts to be feasible, with a discounted payback period of 4.9 years (after starting the operation), as shown in Figure 5.

Zhang et al. (2003b) also evaluated the economic feasibilities of four continuous processes to produce biodiesel (from virgin vegetable oil or waste cooking oil, by using alkali- and acid-catalysts). Despite the fact that it was possible to compare the processes proposed, all the processes showed a negative after-tax rate of return. The authors affirmed that the analysis showed a preliminary nature, with uncertain absolute values. They suggested that suitable government subsidies might be required to produce positive rates of return.

West et al. (2008) also evaluated the economic profitability of four processes to produce biodiesel. Two processes using traditional homogeneous alkali and acid catalysts, a process with heterogeneous acid catalyst and a supercritical method. The results showed that three of the processes presented negative after-tax rate of return. Just heterogeneous acid catalyst process had a positive after tax rate-of-return, with the lowest total capital investment and manufacturing costs. The viable process configuration employed a heterogeneous acid-catalyst (tin(II) oxide), in a multiphase reactor fed, for the transesterification of waste vegetable oil with methanol. The reaction conditions were: 60 °C, 101.3 kPa, residence time of 3 hours and alcohol:oil molar ratio of 4.5:1. Thus, the one-step reaction using mild conditions (so much lower than the conditions used in the present work) and the relatively small sizes of equipment used contributed to the lowest total capital investment and the highest rate-of-return obtained for this process.

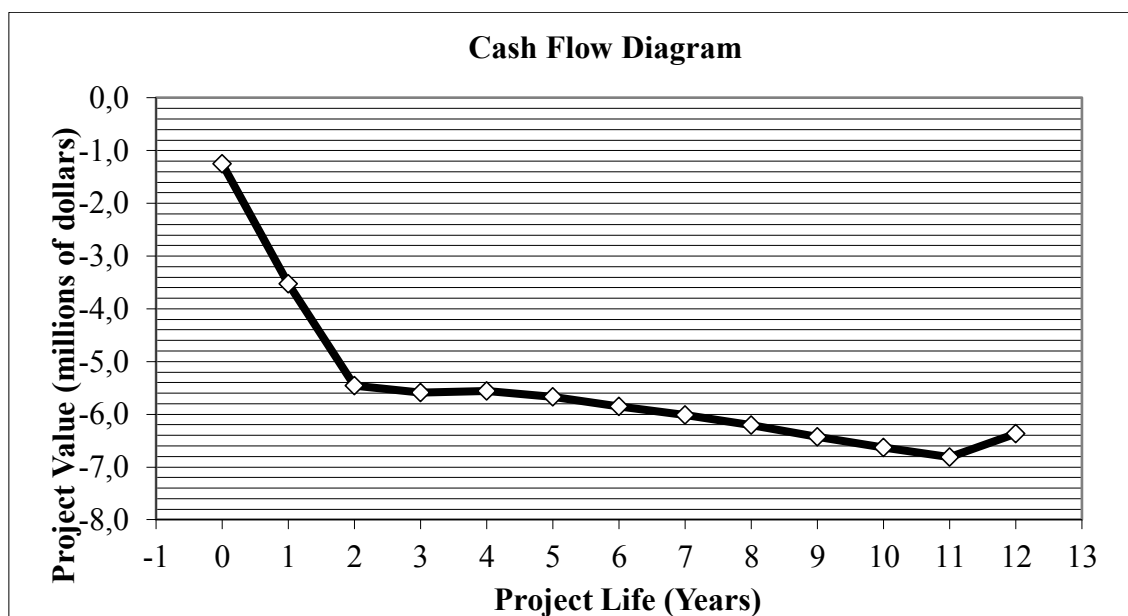


Figure 4- Cash flow diagram obtained for the hydroesterification process, for biodiesel cost of \$0.92/kg

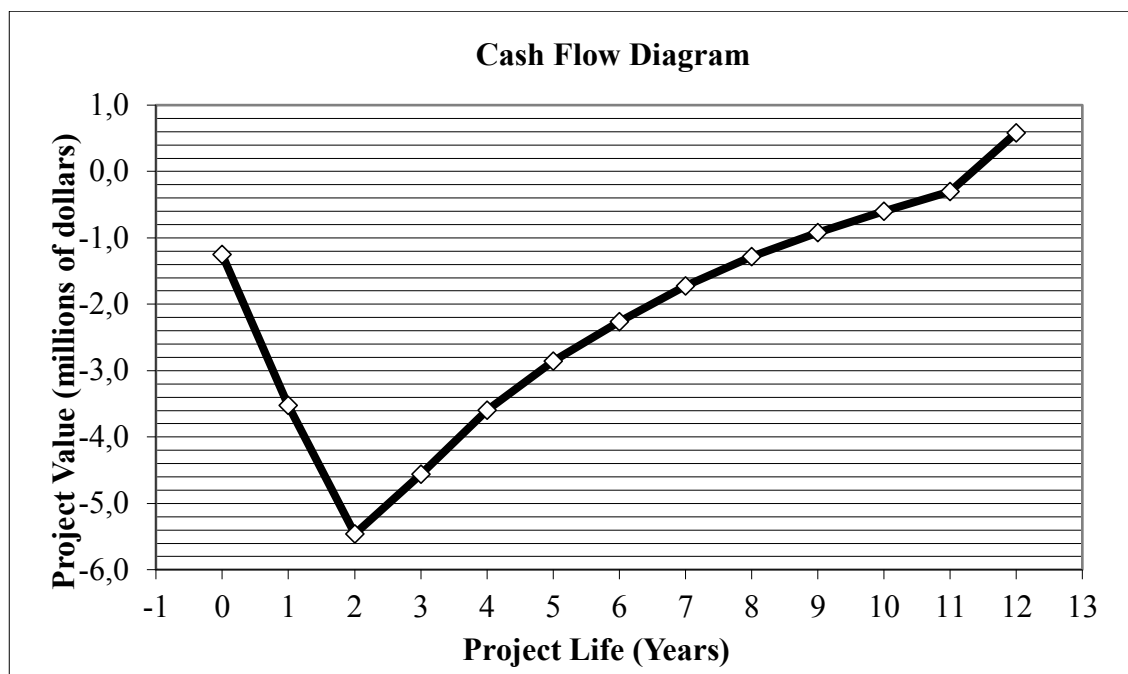


Figure 5- Cash flow diagram obtained for the hydroesterification process, for biodiesel cost of \$1.3/kg

A Monte-Carlo simulation using CAPCOST was applied in order to quantify the risks by investigating the following variables: fixed capital investment, price of product, working capital, income tax rate, interest rate and raw material price. According to Turton et al. (2003), this method is the concept of assigning probability distributions to parameters, repeatedly choosing variables from these distributions, and using these values to calculate a function dependent on the variables. The resulting distribution of calculated values of the dependent function is the result of the Monte-Carlo simulation. Therefore, by specifying the ranges over which these terms are likely to vary, a Monte-Carlo analysis can be achieved and the cumulative distribution of net present values of a project can be obtained. Table 7 presents the variation of each parameters, which were considered in the Monte-Carlo simulation. Figure 6 presents the net present value data obtained for the hydroesterification process.

Table 7- Probable variation of parameters over plant life

	Lower Limit	Upper Limit	Base Value
Fixed capital investment	-20	30	\$4170000
Price of Product	-20	50	\$6274401
Working Capital	-50	10	\$671000
Income Tax Rate	-20	20	42%
Interest Rate	-10	20	10%
Raw Material Price	-10	15	\$2384087

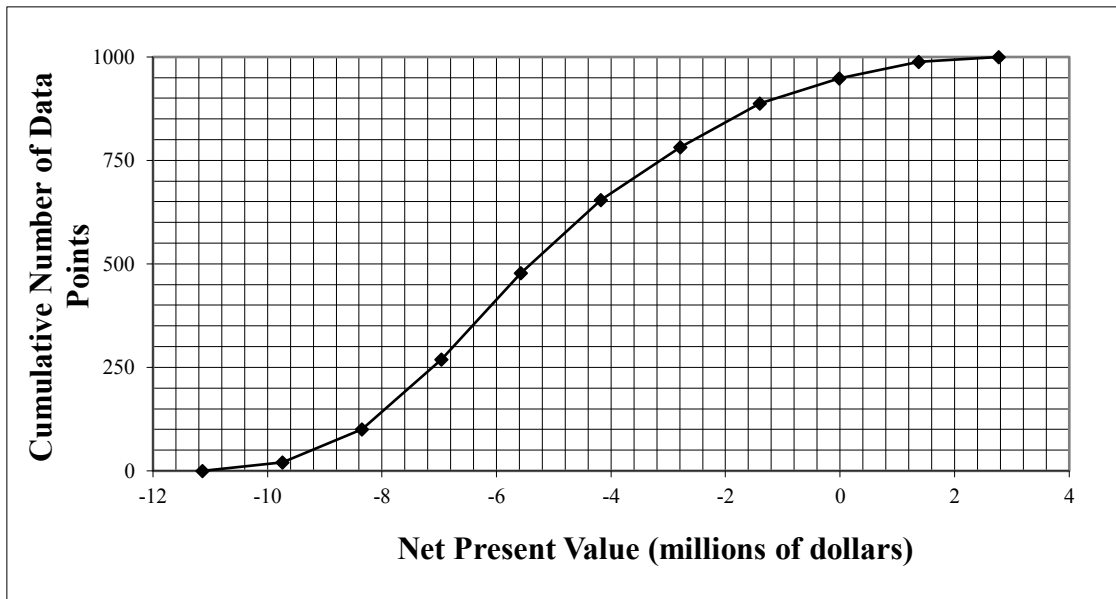


Figure 6- Net present value data obtained for the hydroesterification process

According to Figure 6, by varying some parameters, almost all scenarios led to a negative net present value (NPV). The net present value varied from -11.1 to 2.8 in the parameters ranges tested. Therefore, the probability that this process becomes viable is very low, since that only 5% of the scenarios tested in the Monte Carlo simulation (50 of 1000) resulted in positive NPV. Thus, we can conclude that this process presents high risks and is not feasible within the range of parameters studied.

## 5. CONCLUSIONS

The hydroesterification process proposed in this work proved feasible from the technical assessment, producing biodiesel in a flowrate of 770 kg/h (6736 ton/year) with high purity (97%). Besides that, it presents environmental benefits as it uses waste cooking oil as raw material, which is an inexpensive feedstock, and produces glycerol with high purity. However, this process showed limitations in the economic analysis. Even reducing the raw material cost by using waste cooking oil and using the glycerin credit, a factor that affected the economic viability of the process were the utilities, especially the utilities used in distillation towers. The distillation columns uses a very high amount of energy, which increased the annual utility cost of the process. Thus, it is necessary to evaluate alternatives to decrease the high temperatures used in the reactors and optimize the separation steps of the process.

## ACKNOWLEDGEMENT

The authors are grateful to CBMM for the financial support and for providing the niobic acid (HY-340) used in this work.

## REFERENCES

- Aranda, D. A. G., Gonçalves, J. D. A., Peres, J. S., Ramos, a. L. D., de Melo, C. A. R., Antunes, O. A. C., Furtado, N. C., Taft, C. A. **The use of acids, niobium oxide, and zeolite catalysts for esterification reactions.** *J. Phys. Org. Chem.*, v. 22 (2009a) p. 709–716. <https://doi.org/10.1002/poc.1520>
- Aranda, D. A., da Silva, C. C. C. M., Detoni, C. **Current processes in Brazilian biodiesel production.** *International Review of Chemical Engineering*, 1(6) (2009b) 603-608.
- Atabani, A. E., Silitonga, A. S., Badruddin, I. A., Mahlia, T. M. I., Masjuki, H. H., Mekhilef, S. **A comprehensive review on biodiesel as an alternative energy resource and its characteristics.** *Renewable and Sustainable Energy Reviews*, 16 (2012) 2070– 2093. <https://doi.org/10.1016/j.rser.2012.01.003>

Arvelos, S., Rade, L. L., Watanabe, E. O., Hori, C. E., Romanielo, L. L. **Evaluation of different contribution methods over the performance of Peng–Robinson and CPA equation of state in the correlation of VLE of triglycerides, fatty esters and glycerol + CO<sub>2</sub> and alcohol.** *Fluid Phase Equilibria*, 362 (2014) 136-146. <https://doi.org/10.1016/j.fluid.2013.09.040>

Canakci, M., Van Gerpen, J. **Biodiesel production from oils and fats with high free fatty acids.** *Transactions of the ASAE*, 44 (2001) 1429–1436. <https://doi.org/10.13031/2013.7010>

Cavalcanti-Oliveira, E. D. A., Silva, P. R. D., Ramos, A. P., Aranda, D. A. G., Freire, D. M. G. **Study of soybean oil hydrolysis catalyzed by *Thermomyces lanuginosus* lipase and its application to biodiesel production via hydroesterification.** *Enzyme Research*, (2011) v 2011. <http://dx.doi.org/10.4061/2011/618692>

Demirbas, A. **Importance of biodiesel as transportation fuel.** *Energy policy*, 35(9) (2007) 4661-4670. <https://doi.org/10.1016/j.enpol.2007.04.003>

Nandiwale, K.Y., Bokade, V.V. **Process Optimization by Response Surface Methodology and Kinetic Modeling for Synthesis of Methyl Oleate Biodiesel over H<sub>3</sub>PW<sub>12</sub>O<sub>40</sub> Anchored Montmorillonite K10.** *Ind. Eng. Chem. Res.* 53 (2014) 18690–18698. <https://doi.org/10.1021/ie500672v>

Kapilakarn, K., Peugtong, A. **A comparison of costs of biodiesel production from transesterification.** *International Energy Journal*, (2007) 8(1).

Karmee, S. K., Patria, R. D., Lin, C. S. K. **Techno-economic evaluation of biodiesel production from waste cooking oil—a case study of Hong Kong.** *International journal of molecular sciences*, 16(3) (2015) 4362-4371. <https://doi.org/10.3390/ijms16034362>

Neste, accessed at <https://www.neste.com/en/corporate-info/investors/market-data/biodiesel-prices-sme-fame>, on 24<sup>th</sup>, January, 2018.

Rade, L. L., Lemos, C. O., Barrozo, M. A. S., Ribas, R. M., Monteiro, R. S., Hori, C. E. **Optimization of continuous esterification of oleic acid with ethanol over niobic acid.** *Renewable Energy*, 115 (2018) 208-216. <https://doi.org/10.1016/j.renene.2017.08.035>

Reyes, Y., Chenard, G., Aranda, D., Mesquita, C., Fortes, M., João, R., Bacellar, L. **Biodiesel production by hydroesterification of microalgal biomass using heterogeneous catalyst.** *Natural Science*, 4(10) (2012) 778. <http://dx.doi.org/10.4236/ns.2012.410102>



Sales-Cruz, M., Aca-Aca, G., Sánchez-Daza, O., López-Arenas, T. **Predicting critical properties, density and viscosity of fatty acids, triacylglycerols and methyl esters by group contribution methods.** (2010) ESCAPE20.

Silva, C., Weschenfelder, T. A., Rovani, S., Corazza, F. C., Corazza, M. L., Dariva, C., Oliveira, J. V. **Continuous Production of Fatty Acid Ethyl Esters from Soybean Oil in Compressed Ethanol.** *Industrial & Engineering Chemistry Research*, 46(16) (2007) 5304. <https://doi.org/10.1021/ie070310r>

Song, C., Liu, Q., Ji, N., Deng, S., Zhao, J., Li, S., Kitamura, Y. **Evaluation of hydrolysis–esterification biodiesel production from wet microalgae,** *Bioresource Technology*. 214 (2016) 747-754. <https://doi.org/10.1016/j.biortech.2016.05.024>

Trading economics, accessed at <https://tradingeconomics.com/commodity/ethanol>, on 25<sup>th</sup>, January, 2018.

Turton, R., Bailie, R.C., Whiting, W.B., Shaeiwitz, J.A. **Analysis, Synthesis, and Design of Chemical Processes**, 2nd ed. Prentice Hall, Upper Saddle River, New Jersey, 2003.

West, A. H., Posarac, D., Ellis, N. **Assessment of four biodiesel production processes using HYSYS.Plant.** *Bioresource Technology*, 99 (2008) 6587–6601. <https://doi.org/10.1016/j.biortech.2007.11.046>

Zhang, Y., Dube, M. A., McLean, D. D. L., Kates, M. **Biodiesel production from waste cooking oil: 1. Process design and technological assessment.** *Bioresource technology*, 89(1) (2003a) 1-16. [https://doi.org/10.1016/S0960-8524\(03\)00040-3](https://doi.org/10.1016/S0960-8524(03)00040-3)

Zhang, Y., Dube, M. A., McLean, D. D., & Kates, M. **Biodiesel production from waste cooking oil: 2. Economic assessment and sensitivity analysis.** *Bioresource technology*, 90(3) (2003b). 229-240. [https://doi.org/10.1016/S0960-8524\(03\)00150-0](https://doi.org/10.1016/S0960-8524(03)00150-0)

---

## 5. CONCLUSIONS AND PERSPECTIVES

---

### 5.1. Main conclusions

The main findings of the project can be summarized as follows:

- For both catalysts tested in this work (niobic acid and niobium phosphate), higher calcination temperatures bring a decrease of the surface area, total acidity and, consequently, on the activity for the esterification reaction.
- Niobium phosphate showed higher thermal stability than niobic acid, once that niobic acid changes from amorphous to crystalline when calcined at 500 °C and niobium phosphate changed its structure only at calcination temperatures up to 700°C.
- The operational conditions of temperature, amount of catalyst and ethanol:FFA molar ratio positively affected the response of the process, for both catalysts.
- Yield of esters up to 70% could be obtained at optimized conditions, for niobic acid and niobium phosphate.
- Niobic acid and niobium phosphate catalysts are promising on continuous esterification reaction of oleic acid and ethanol.
- The hydroesterification process simulated proved feasible from the technical assessment, producing biodiesel in a flowrate of 770 kg/h (6736 ton/year) with high purity (97%), in accordance to European standard (EN 14214:2008) for purity of biodiesel product.
- The economic assessment of the hydroesterification process was not economically reasonable. The cost of the utilities employed in the process was, in general, the factor that most affected the economic viability. Thus, suitable government subsidies may be required to produce positive rates of return.

## 5.2. Perspectives

- To investigate ways to decrease the high temperatures required in the continuous hydrolysis and esterification reactions, maintaining the values of conversions and yields of esters.
- To perform sensitivity analyses for the hydroesterification process, aiming to evaluate the effect of parameters on the profitability criterion of interest at the economic assessment.
- To optimize the hydroesterification plant, based on the results obtained in the sensitivity analyses.

---

## 6. APPENDIX I

---

### COPYRIGHT CLEARANCE

“Authors who publish in Elsevier journals can share their research by posting a free draft copy of their article to a repository or website. Theses and dissertations which contain embedded PJAs as part of the formal submission can be posted publicly by the awarding institution with DOI links back to the formal publications on ScienceDirect.” For more information:

<https://www.elsevier.com/about/our-business/policies/sharing>



#### Journal author rights

In order for Elsevier to publish and disseminate research articles, we need publishing rights. This is determined by a publishing agreement between the author and Elsevier. This agreement deals with the transfer or license of the copyright to Elsevier and authors retain significant rights to use and share their own published articles. Elsevier supports the need for authors to share, disseminate and maximize the impact of their research and these rights, in Elsevier proprietary journals\* are defined below:

##### For subscription articles

Authors transfer copyright to the publisher as part of a journal publishing agreement, but have the right to:

- \* Share their article for [Personal Use](#), [Internal Institutional Use](#) and [Scholarly Sharing](#) purposes, with a DOI link to the version of record on ScienceDirect (and with the Creative Commons [CC-BY-NC-ND license](#) for author manuscript versions)
- \* Retain patent, trademark and other intellectual property rights (including research data)
- \* Proper attribution and credit for the published work.

#### Article Sharing

Authors who publish in Elsevier journals can share their research by posting a free draft copy of their article to a repository or website. Researchers who have subscribed access to articles published by Elsevier can share too. There are some simple guidelines to follow, which vary depending on the article version you wish to share. Elsevier is a signatory to the [STM Voluntary Principles](#) for article sharing on Scholarly Collaboration Networks and a member of the [Coalition for Responsible Sharing](#)®.

---

## 7. APPENDIX II

---

This appendix gives the slide-show presentation used in the Doctorate defense.



## Table of contents

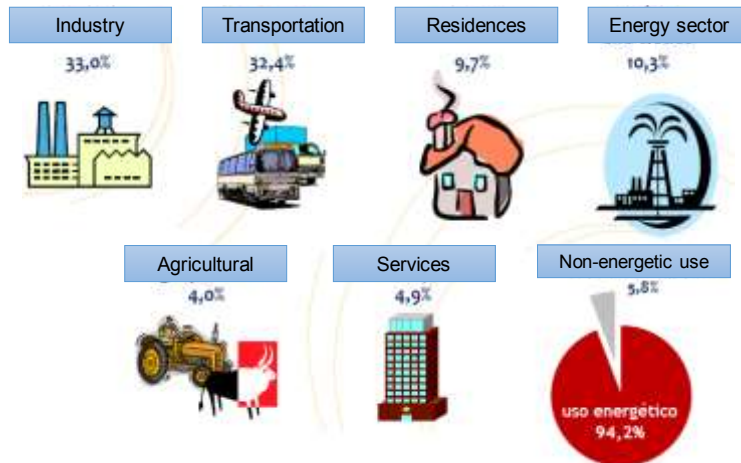
2

- ▶ Introduction
- ▶ Goals
- ▶ Materials and Methods Step 1
- ▶ Results and Discussion Step 1
- ▶ Materials and Methods Step 2
- ▶ Results and Discussion Step 2
- ▶ Conclusions

## Introduction

## Introduction

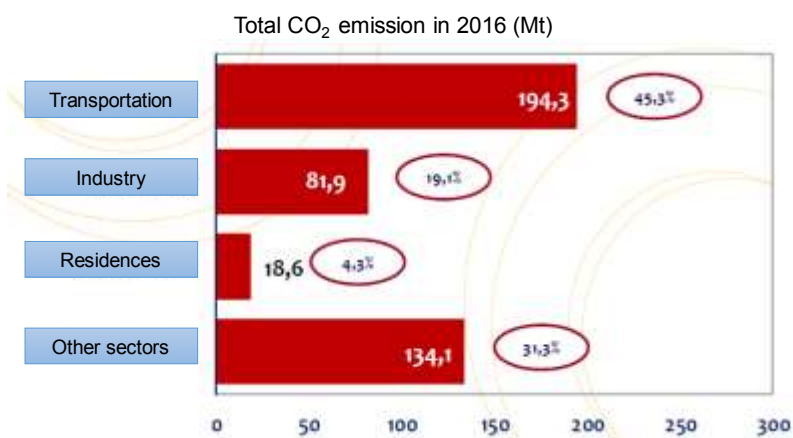
4



Source: Balanço Energético Nacional 2017

## Introduction

5



Source: Balanço Energético Nacional 2017

## Introduction

6



Source: Balanço Energético Nacional 2017

### Drawbacks

- Significant impact on the quality of the environment
- The worldwide demand for energy is increasing continuously and the known reserves of these fuels are limited

## Introduction

7

### Alternative

### BIODIESEL (VEGETABLE OILS OR ANIMAL FATS)



About 15% of the diesel used in Brazil was imported, in 2016 (ANP)



- Non-toxic,
- Biodegradable,
- Renewable,
- High flash point,
- Lower emissions of pollutants,
- Technically feasible,
- Economically competitive,
- Properties similar to petrodiesel,
- Miscible with petroleum-based diesel in all proportions,
- It contributes to the generation of jobs in agriculture.



## Introduction

8

### Esterification reaction:

The alcohol in contact with the free fatty acid (FFA) generates esters as a main product (biodiesel) and water as a byproduct.



Any source of FFA  
or  
Hydroesterification → hydrolysis + esterification

Conventionally →  
catalyzed by mineral  
liquid acids



- Contamination problems
- Corrosion of equipment
- High amounts of waste and effluents
- Separation problems

## Introduction

9

Heterogeneous  
catalysts

- Amberlyst 15
- Zeolites
- ZrO<sub>2</sub>

Loss of acidic active sites in polar medium

Low thermal stability

Mass transfer resistance

Niobia based  
catalyst



High concentration of acid sites

Little or no sensitivity to water

High porosity

Insolubility

## Introduction

10

Aranda et al. (2008)

**Goal:** to study the influence of the parameters alcohol:fatty acid molar ratio, temperature, catalyst amount and presence of water, on the yield of esters at the esterification of palm fatty acids, using heterogeneous catalysts.

Catalysts used: PSA, niobic acid ( $\text{Nb}_2\text{O}_5$ ) and four zeolites: Hbeta ( $\text{H}\beta$ ), HMordenite (HMOR), HZSM-5 and HY (CBV-760)

Niobic acid calcined at 300 °C.

Batch reactor.

## Introduction

11

Aranda et al. (2008)

### Results:

1. The zeolites showed higher surface areas compared to the other catalysts (HY).
2. PSA and niobium oxide presented the best catalytic performance, even with smaller surface areas than zeolites.
3. Calcined niobium oxides exhibit better reaction yields, showing that calcination is an important step for the activation of catalytic acid sites.

## Introduction

12

Bassan et al. (2013)

**Goal:** evaluation of niobium catalysts (niobic acid and niobium phosphate) in the esterification reactions of fatty acids (C12–C18) with alcohols (methanol, ethanol, butanol).

Catalysts calcined at 300 °C.

Characterizations: Nitrogen adsorption, X-ray powder diffraction and FTIR of adsorbed pyridine.

Batch reactor.

## Introduction

13

Bassan et al. (2013)

### Results:

1. Both catalysts are amorphous at the calcination temperature of 300 °C.
2. Niobium phosphate showed a slightly higher surface area than niobic acid.
3. In the reaction of butanol and lauric acid (10:1), at 120 °C and 4 hours of reaction: niobic acid had a conversion of 41%. Niobium phosphate had a conversion of 81%.
4. The superior catalytic activity of niobium phosphate is due to the presence of POH groups in the amorphous niobium phosphate, which provides a slightly stronger Brønsted acidity than niobic acid.



## Goals

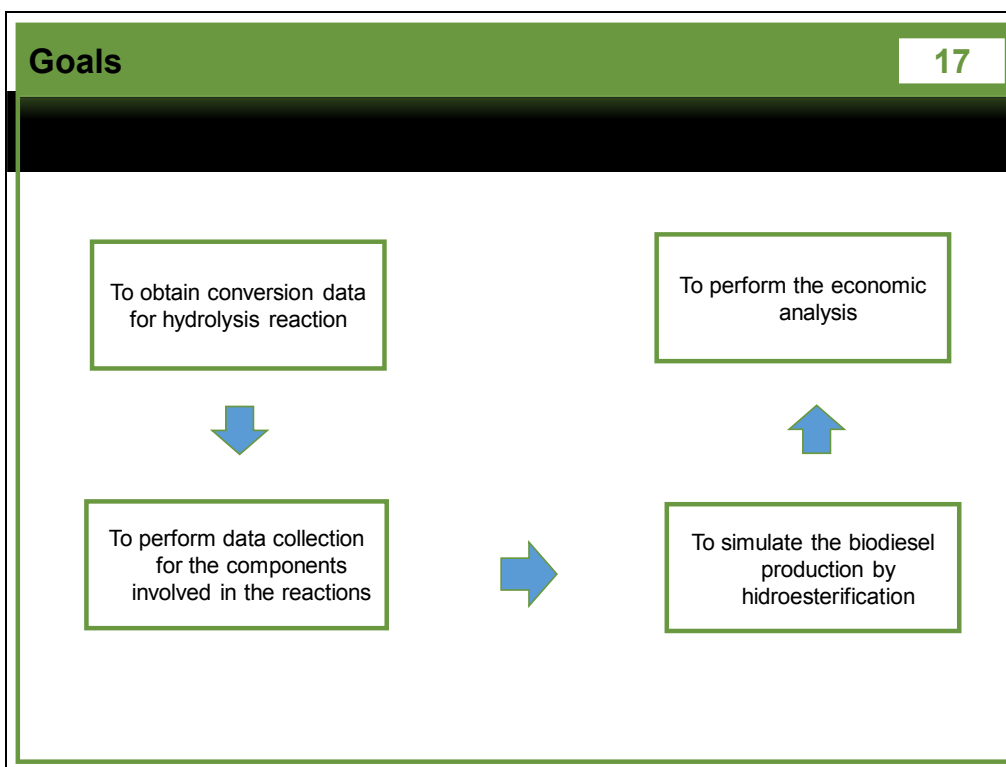
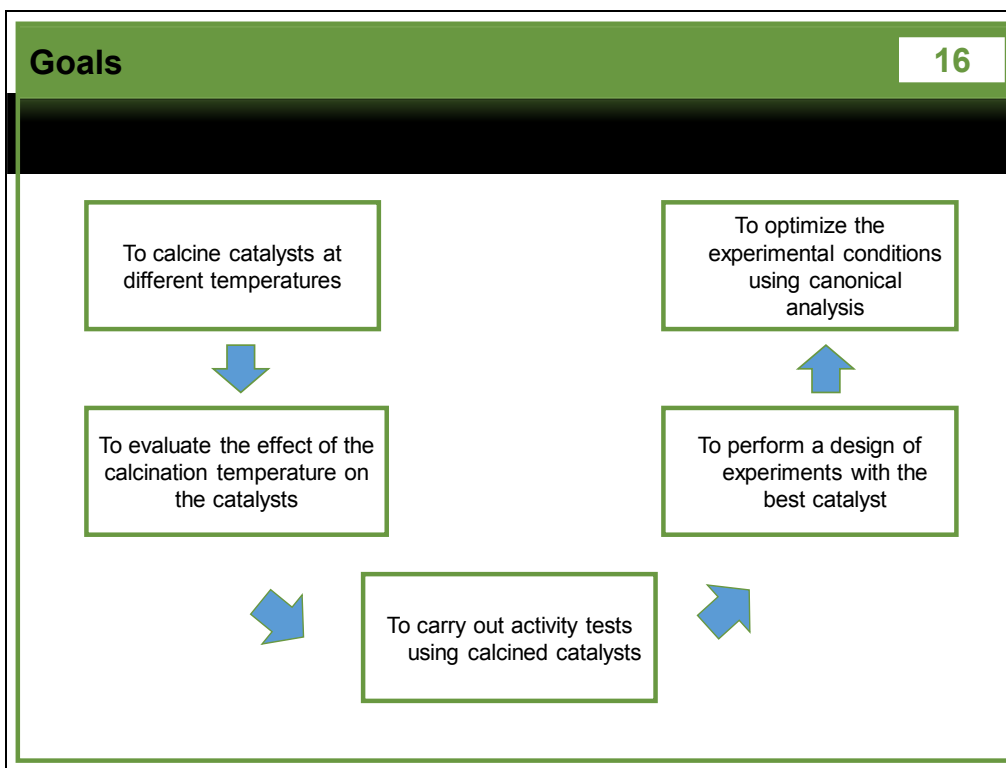
## Goals

15

### GOALS

**Step 1:** To evaluate niobium-based materials as catalysts in the continuous esterification reaction

**Step 2:** To simulate the biodiesel production plant through the hydroesterification route, using UniSim software and to perform the economic analysis of the process.



## Step 1

Evaluation of niobium-based materials in the esterification reaction

## Material and Methods

## Catalysts

Niobic acid  
 $\text{Nb}_2\text{O}_5 \cdot n\text{H}_2\text{O}$  (HY-340)

Niobium phosphate  
(AD-5970)



Calcined in air 20 mL/min for 2h

300 °C

350 °C

400 °C

450 °C

500 °C

600 °C

- Nitrogen adsorption
- X-ray powder diffraction
- Temperature-programmed desorption of ammonia ( $\text{NH}_3$ -TPD)

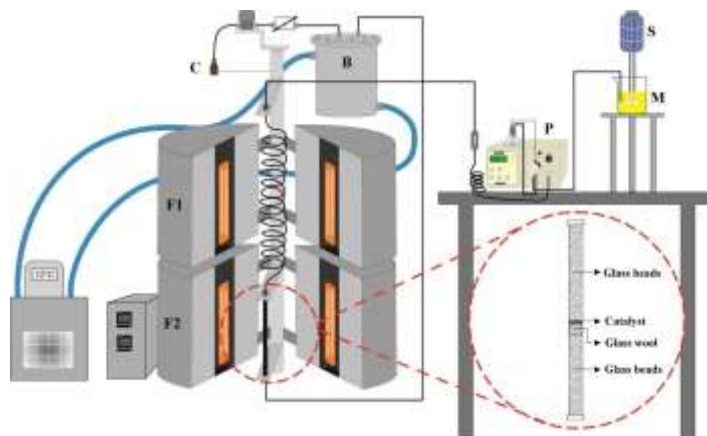


Figure 1- Schematic diagram of the experimental apparatus. S- stirrer, M- substrate mixture, P- high-pressure liquid pump, F1- pre-heating zone furnace, F2- furnace of the fixed bed reactor, B- water bath, C- product collector.

## Material and Methods

22

Conversion: AOCS Method, Ca 5a-40 (AOCS, 1978)

Esters content: Gas chromatography (methyl heptadecanoate as internal standard)



## Material and Methods

23

Response: Yield of esters (y)

Parameters: Temperature ( $X_T$ ) - 220 a 290 °C

Mass of catalyst ( $X_{MC}$ ) - 0 a 0.8 g

Ethanol:oleic acid molar ratio ( $X_{MR}$ ) - 2:1 a 14:1

The coded variables were defined as follow:

$\alpha = 1,414$ .

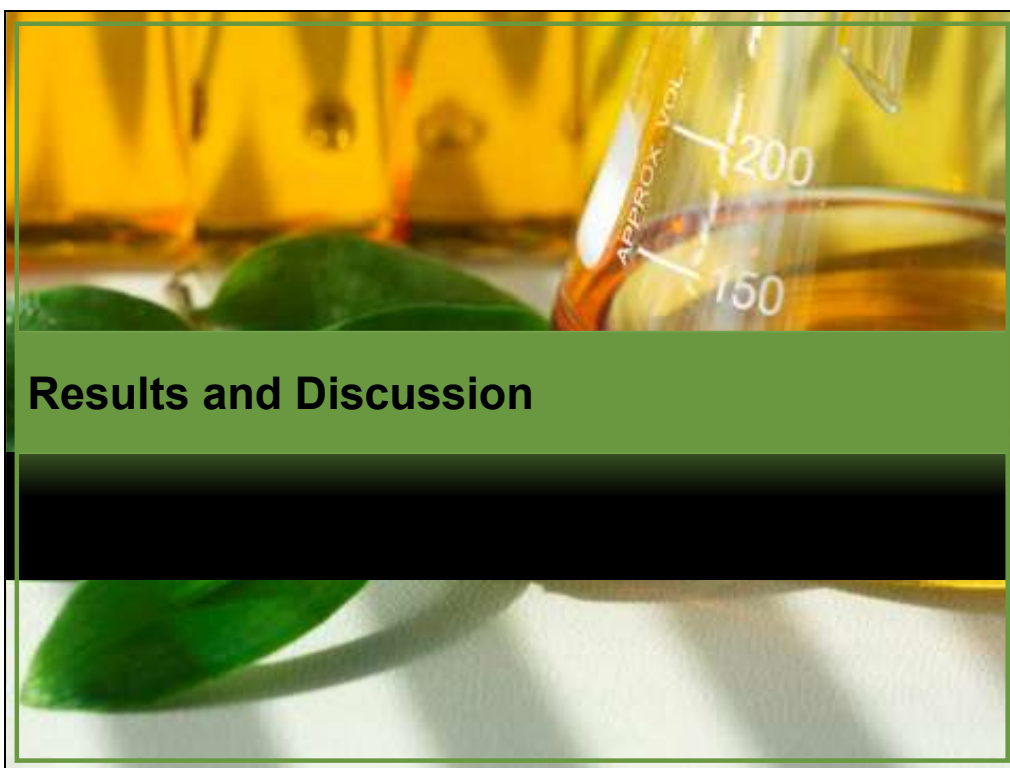
$$X_T = \frac{T(^{\circ}\text{C}) - 255}{25}$$

$$X_{MC} = \frac{AC(g) - 0.4}{0.3}$$

$$X_{MR} = \frac{MR - 8}{4}$$

Optimization: Canonical analysis technique





## Results and Discussion

## Results and Discussion

25

### Nitrogen adsorption

Table 1- Textural properties of niobic acid and niobium phosphate calcined between 300 and 600 °C

Calcination temperature	Surface area (m <sup>2</sup> /g)	
	Niobic acid	Niobium phosphate
300 °C	111	166
350 °C	95	165
400 °C	86	170
450 °C	66	161
500 °C	34	157
600 °C	15	113

Table 2- Total acidity of niobic acid and niobium phosphate calcined at different temperatures

Calcination temperature	Total acidity (mmol NH <sub>3</sub> /g)	
	Niobic acid	Niobium phosphate
300 °C	0.101	0.253
350 °C	0.082	0.275
400 °C	0.074	0.222
450 °C	0.061	0.214
500 °C	0.035	0.228
600 °C	-*	0.129

\* Total acidity present in the sample was at the noise level

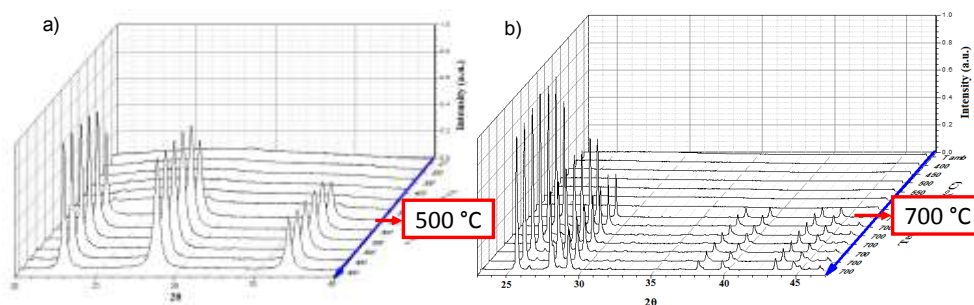


Figure 2- In-situ XRD pattern of a)niobic acid calcined from room temperature to 500 °C and b) niobium phosphate calcined from room temperature to 700 °C

## Results and Discussion

28

W/F tests



Experimental conditions:  
250 °C, 6:1 ethanol:oleic acid molar ratio, flow rate of 0,3 mL/min. Amount of catalysts: 0 a 0.8 g.

Catalytic activity



Experimental conditions:  
250 °C, 6:1 ethanol:oleic acid molar ratio, flow rate of 0,3 mL/min, 0.3 g of catalyst.

Table 3- Conversion obtained for niobic acid and niobium phosphate calcined at different temperatures

Calcination temperature	Conversion (%)	
	Niobic acid	Niobium phosphate
300 °C	44	61
350 °C	50	55
400 °C	48	54
450 °C	24	53
500 °C	16	53
600 °C	7	50

## Results and Discussion

29

Run	Temperature (°C)	Amount of catalyst (g)	Ethanol:oleic acid molar ratio
1	230	0.1	4:1
2	280	0.1	4:1
3	230	0.7	4:1
4	280	0.7	4:1
5	230	0.1	12:1
6	280	0.1	12:1
7	230	0.7	12:1
8	280	0.7	12:1
9	220	0.4	8:1
10	290	0.4	8:1
11	255	0	8:1
12	255	0.8	8:1
13	255	0.4	2:1
14	255	0.4	14:1
15	255	0.4	8:1
16	255	0.4	8:1
17	255	0.4	8:1
18	255	0.4	8:1

## Results and Discussion

30

Niobic acid:

$$y (\%) = 40.14 + 6.78X_T + 17.30X_{MC} + 7.70X_{MR} - 4.58X_{MC}^2 \quad (1)$$

Niobium phosphate:

$$y (\%) = 51.73 + 5.17X_T + 15.83X_{MC} + 7.33X_{MR} - 9.37X_{MC}^2 - 4.92X_{MR}^2 \quad (2)$$

Where:  $y$  = Yield of esters,  $X_T$  = coded temperature,  $X_{MC}$  = coded mass of catalyst,  $X_{MR}$  = coded ethanol:oleic acid molar ratio

## Results and Discussion

31

### Niobic acid:

Reaction temperature of 249 °C, ethanol:oleic acid molar ratio of 10.8:1 and 0.7 g of niobic acid

Yield of esters predicted: 72%

Yield of esters obtained: 71%

### Niobium phosphate:

Reaction temperature of 279 °C, ethanol:oleic acid molar ratio of 11:1 and 0.62 g of niobium phosphate

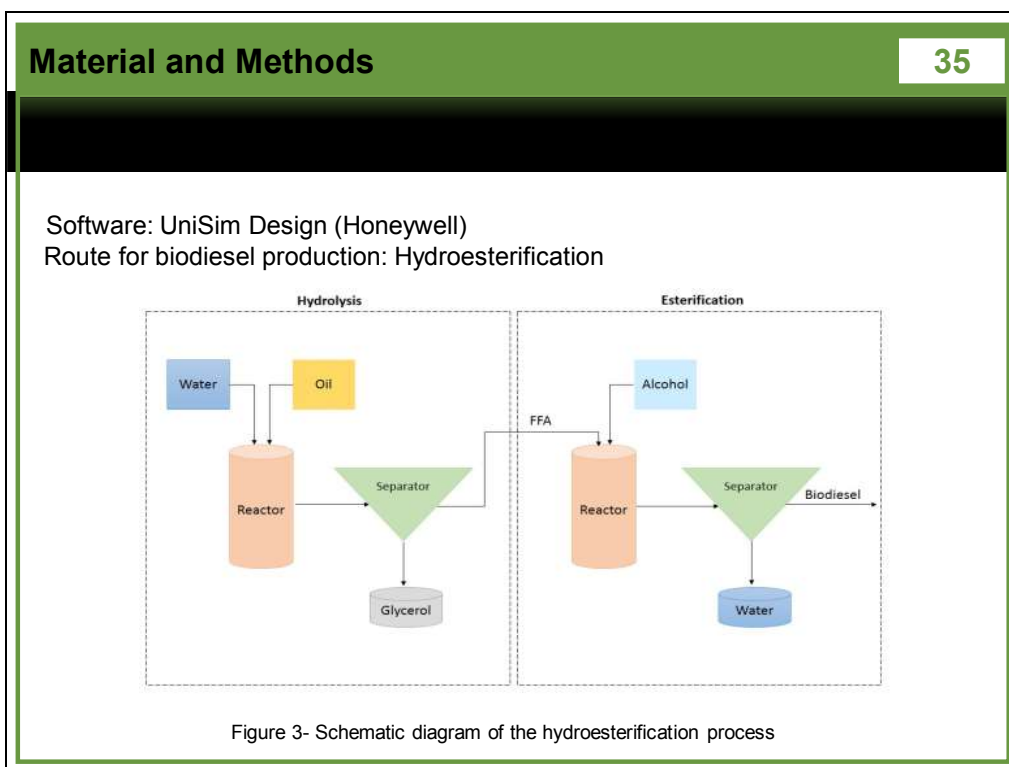
Yield of esters predicted: 71%

Yield of esters obtained: 69%



## Step 2

Simulation of the biodiesel production by hydroesterification route



Procedure for the simulation:

- I. Definition of the chemical components,
- II. Thermodynamic models selection,
- III. Specification of the plant capacity,
- IV. Selection of the main operations,
- V. Data input, such as: conversion, temperature, pressure, flow rate, among others.

“Study estimate” with estimates accurate in the range of + 40% to – 25%, using CAPCOST program (CAPCOST\_2008.xls).

Process evaluated based on fixed capital investment and cost of manufacturing.

**Capital cost:** takes into consideration the direct and indirect costs, contingencies and fees and costs of auxiliary facilities (equipment costs, materials required for installation, labor to install materials and equipment, freight, insurance, taxes, construction overhead, engineering expenses, contingency, auxiliary buildings, among others).

**Cost of manufacturing:** costs associated with the day-to-day operation of a chemical plant. It includes raw material prices, operating labor, utilities, maintenance and repairs, operating supplies, laboratory charges, expenses for patents and royalties, research and development, administrations costs, local taxes and insurance, among others.

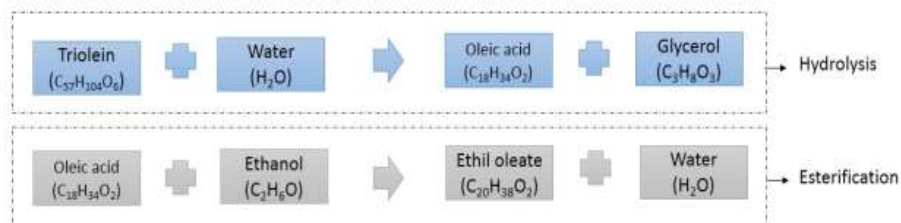


## Results and Discussion

## Results and Discussion

39

Components selected to describe the reactions:



Information for the components ethanol, glycerol and water was available at UniSim library.

Components that were not available: triolein, ethyl oleate and oleic acid. Hypothetical components using the "Hypo Manager" tool.



## Results and Discussion

40

Thermodynamic/activity model: NRTL for the description of the liquid phase  
SRK for the description of the vapor phase

Plant capacity: 925 kg/h vegetable oil  
1111 kg/h water  
770 kg/h biodiesel

Main operations: reactors, pumps, heat exchangers, distillation columns and process vessels.

Input data: hydrolysis conversion of 86% and esterification conversion of 92%.  
400 °C, water:oil 52:1, flow rate 0.2 ml/min, 1.1 g niobic acid  
250 °C, ethanol:oleic acid 11:1, flow rate 0.3 ml/min, 0.7 g niobic acid

The ANP (National Agency of Petroleum, Natural Gas and Biofuels) standard for purity of biodiesel product was applied (i.e., 96.5 wt.%)

## Results and Discussion

41

Table 4- Input properties of oleic acid, triolein and ethyl oleate

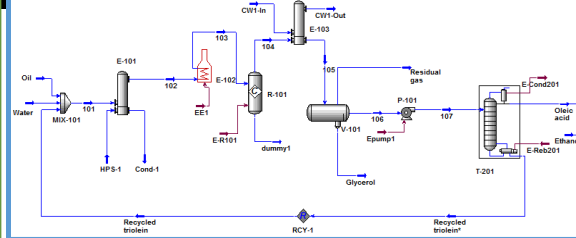
Component	T <sub>c</sub> [°C]	P <sub>c</sub> [kPa]	ω	Boiling point [°C]	Density [kg/m <sup>3</sup> ]	Molecular weight
Oleic acid <sup>1</sup>	522.1	1220	1.214	358.9	893.4	282.5
Triolein <sup>2</sup>	704.8	730	1.594	416.2	900.0	885.4
Ethyl oleate <sup>2</sup>	523.1	1050	1.3282	217.0	870.0	310.5

Sales-Cruz et al. (2010)<sup>1</sup>  
Arvelos et al. (2014)<sup>2</sup> – For oleic acid: T<sub>c</sub> by Constantinou and Gani, P<sub>c</sub> by Marrero and Gani and ω by KLM.  
For ethyl oleate: T<sub>c</sub> and P<sub>c</sub> by Marrero and Gani and Joback-Reid, respectively and ω by Ptizer.

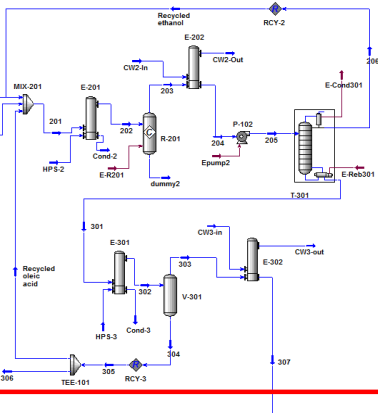
## Results and Discussion

42

### Hydrolysis



### Esterification



### FAEE purification

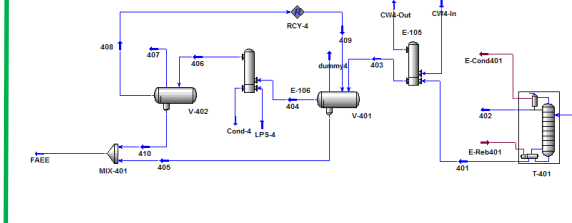
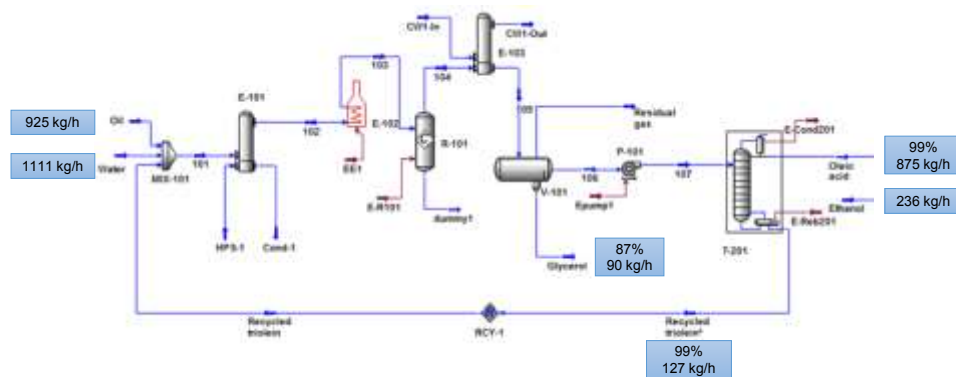


Figure 4- Process flow sheet to produce biodiesel from waste oils by hydroesterification route

## Results and Discussion

43

### Hydrolysis

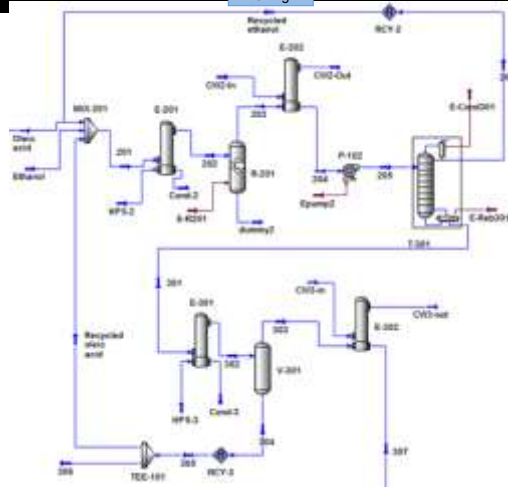


## Results and Discussion

44

### Esterification

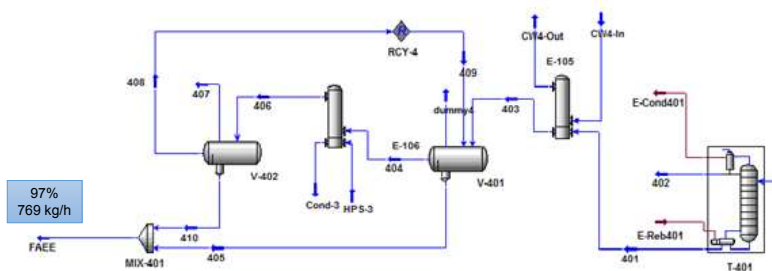
72%  
2131 kg/h



## Results and Discussion

45

### FAEE purification



## Results and Discussion

46

2) Esterification: volume = 5 m<sup>3</sup>

Heat exchangers: Heat transfer area = 60.3 m<sup>2</sup>

Column distillation: 1) Diameter = 1.2 m, height = 10.5 m, 17 theoretical stages

2) Diameter = 1.2 m, height = 9.5 m, 15 theoretical stages

3) Diameter = 1.2 m, height = 7 m, 10 theoretical stages

Vessels: 1) Diameter = 0.91 m, height = 3.20 m

2) Diameter = 0.46 m, height = 2.50 m

3) Diameter = 0.41 m, height = 1.23 m

4) Diameter = 0.61 m, height = 2.10 m

The material of construction of all equipment was carbon steel

## Results and Discussion

47

CEPCI: 541,7 (2016)

Plant construction: 2 years

Plant life: 10 years

Annual interest rate: 10%

Pump and furnace efficiencies: 70% and 90%, respectively

Table 5- Basic conditions for the economic assessment

Materials	Cost
Waste cooking oil <sup>a</sup>	200 \$/ton
Ethanol <sup>b</sup>	430 \$/ton
Biodiesel <sup>c</sup>	920 \$/ton
Glycerol <sup>a</sup>	750 \$/ton

<sup>a</sup> Zhang et al., 2003, <sup>b</sup>Trading Economics, <sup>c</sup>Neste

## Results and Discussion

48

Table 6- Equipment costs and fixed capital costs

Type	Description	Purchased cost	Total Module Cost	Grass Roots Cost
<b>Reactors</b>	Hydrolysis	\$9810	\$46300	\$51200
	Esterification	\$9810	\$46300	\$51200
<b>Towers</b>	T-201	\$41600	\$118000	\$165000
	T-301	\$37600	\$138000	\$181000
	T-401	\$27500	\$93000	\$127000
<b>Fired Heater</b>	E-102	\$54100	\$138000	\$197000
<b>Others</b>	Separators	\$20900	\$74600	\$103800
	Heat exchangers	\$563900	\$2195000	\$3125000
	Pumps	\$26800	\$125600	\$170000
<b>Total</b>		\$792020	\$2970000	\$4170000
<b>Fixed Capital Investment (FCI)</b>			\$4170000	
<b>Working Capital (WC)</b>			\$670000	

## Results and Discussion

49

Table 7- Total manufacturing cost of the hydroesterification process

<b>Raw material</b>	\$2.39	
Waste cooking oil	\$1.54	
Ethanol	\$0.85	
<b>Operating labor</b>	\$0.16	
<b>Utilities</b>	\$2.48	→ 52% Distillation columns
Low-Pressure steam	\$1.26	
High-Pressure steam	\$1.07	
Electricity	\$0.00	
Cooling water	\$0.05	
<b>Total manufacturing cost</b>	\$7.17	
Revenue from sales	\$6.27	

Costs reported as \$ million

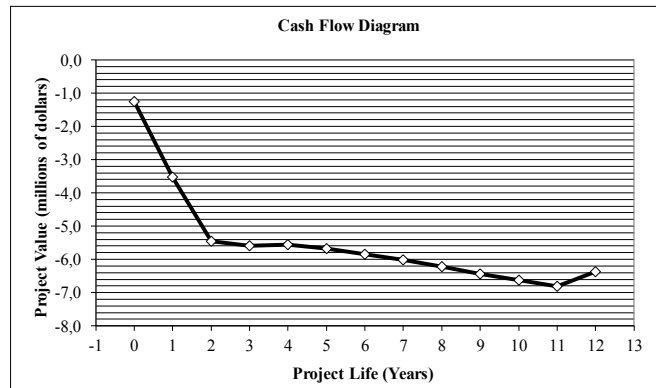


Figure 5- Cash flow diagram obtained for the hydroesterification process, for biodiesel cost of \$0.92/kg

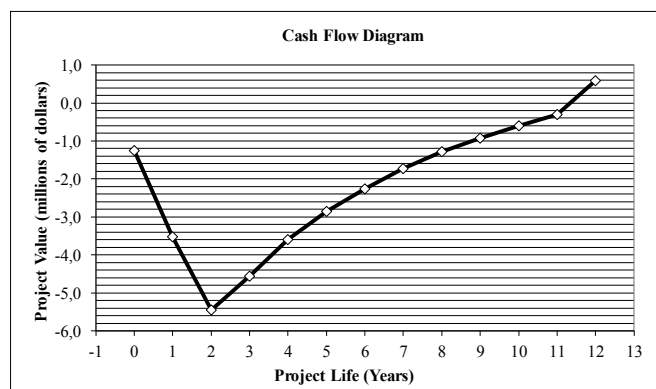


Figure 6- Cash flow diagram obtained for the hydroesterification process, for biodiesel cost of \$1.3/kg



## Conclusions

## Conclusions

53

1. For both catalysts tested in this work (niobic acid and niobium phosphate), higher calcination temperatures bring a decrease on the activity for the esterification reaction.
2. Niobium phosphate showed higher thermal stability than niobic acid.
3. The operational conditions of temperature, amount of catalyst and ethanol:FFA molar ratio positively affected the response of the process, for both catalysts.

4. Niobic acid and niobium phosphate catalysts are promising on continuous esterification reaction of oleic acid and ethanol.
5. The hydroesterification process proposed proved feasible from the technical assessment, producing biodiesel in a flow rate of 770 kg/h (6736 ton/year) with high purity (97%).
6. The economic assessment of the hydroesterification process was not economically reasonable. The cost of the utilities employed in the process was, in general, the factor that most affected the economic viability.